

# **SOLUTION TO OPTIMAL POWER FLOW INCORPORATING MULTI-TYPE FACTS DEVICES USING EVOLUTIONARY TECHNIQUES**

## **A DISSERTATION**

*Submitted in partial fulfilment of the  
requirements for the award of the degree  
of*

**MASTER OF TECHNOLOGY**

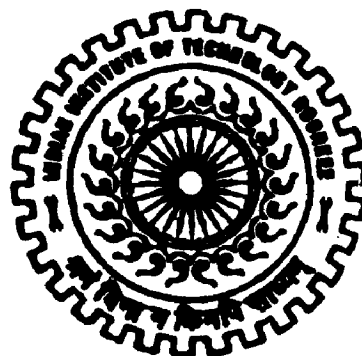
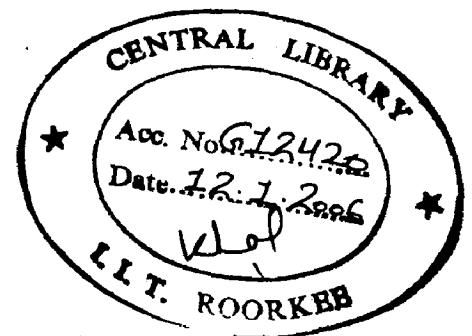
*in*

**ELECTRICAL ENGINEERING**

**(With Specialization in Power System Engineering)**

*By*

**ANAND R.**



*LR*

**DEPARTMENT OF ELECTRICAL ENGINEERING  
INDIAN INSTITUTE OF TECHNOLOGY ROORKEE  
ROORKEE - 247 667 (INDIA)**

**JUNE, 2004**

**CANDIDATE'S DECLARATION**

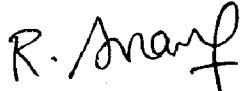
---

I hereby certify that the work which is being presented in the thesis entitled **"SOLUTION TO OPTIMAL POWER FLOW INCORPORATING MULTI TYPE FACTS DEVICES USING EVOLUTIONARY TECHNIQUES"** submitted in partial fulfillment of the requirement for the award of the Degree of Master of Technology in Electrical Engineering, with the specialization in **Power System Engineering**, in the **Department of Electrical Engineering, Indian Institute of Technology, Roorkee**, is an authentic record of my own work, carried out effect from July 2003 to June 2004, under the guidance of **Dr. N.P.Padhy**, Assistant Professor, Department of Electrical Engineering, Indian Institute of Technology, Roorkee and **Dr. E.Fernandez**, Assistant Professor, Department of Electrical Engineering, Indian Institute of Technology, Roorkee.

The matter embodied in this thesis has not been submitted for the award of any other degree.

Date: 30-6-04

Place: ROORKEE

  
(Anand.R)

---

**CERTIFICATE**

This is to certify that the above statement made by the candidate is correct to the best of my knowledge and belief.

  
(Dr.N.P.Padhy)

Assistant Professor,  
Department of Electrical Engineering  
Indian Institute of Technology, Roorkee.  
Roorkee -247667, INDIA

  
(Dr.E.Fernandez)

Assistant Professor,  
Department of Electrical Engineering  
Indian Institute of Technology, Roorkee.  
Roorkee -247667, INDIA

## ACKNOWLEDGEMENTS

---

It is my proud privilege to express my deep sense of gratitude and indebtedness towards my thesis supervisor **Dr.N.P.Padhy**, Assistant Professor, Department of Electrical Engineering, for his invaluable guidance and criticism, and kind and continuous encouragement, which were vital factors in successful completion of the present work. I am heartily thankful to him for his deep concern towards my academics and personal welfare.

His painstaking support and exhaustive involvement in preparation of manuscript, conduction of simulation studies is gratefully acknowledged. I sincerely appreciate his pronounced individualities, humanistic and warm personal approach, which has given me strength to carry out this research work on steady and smooth course. I humbly acknowledge a lifetime's gratitude to him.

I am greatly indebted to my Co-guide **Dr.E.Fernandez**, for extending moral support and guidance during my work. His co-operation have made my work possible.

I am also thankful to **Dr.H.O.Gupta**, Head of the Department and **Dr.J.D.Sharma**, Group Leader, Power System Engineering Group, and **Sri Bharat Gupta**, O.C.Power System Simulation Lab, for providing me the best of facilities, which enabled my work to roll faster.

Special and sincere thanks to **Sumit**, **Saravanan**, **Balan**, **Upendra**, **Isabell**, **Zarena**, **Muthu**, **Mohan** and all my friends at IIT,Roorkee whose support and encouragement has been a constant source of assurance, guidance strength, inspection and upliftment to me.

Thanks are also due to all those who helped me directly and indirectly for the completion of the work.

My special, sincere, heartfelt gratitude and indebtedness are due to my father, mother and family members for their sincere prayers, constant encouragement and blessings. They have undergone to bring me up to this stage. To them all I bow in the deepest reverence.

# CONTENTS

---

	PAGE No.
<b>ABSTRACT</b>	<b>i</b>
<b>ACKNOWLEDGEMENT</b>	<b>ii</b>
<b>CONTENTS</b>	<b>iii</b>
<b>LIST OF FIGURES</b>	<b>vi</b>
<b>LIST OF TABLES</b>	<b>vii</b>
<b>LIST OF ABBREVIATIONS</b>	<b>viii</b>
<b>Chapter-1 INTRODUCTION</b>	<b>1</b>
1.1 General	1
1.2 Optimal Power Flows	1
1.3 Flexible Ac Transmission Systems	2
1.4 Optimal Location Of Facts Devices	3
1.5 Literature Review	4
1.6 Objective Of The Thesis	7
1.7 Organization Of The Thesis	7
<b>Chapter – 2 FLEXIBLE AC TRANSMISSION SYSTEMS</b>	<b>9</b>
2.1 Introduction	9
2.2 Thyristor Controlled Series Capacitor (TCSC) As Series Controller	9
2.2.1 Operating Principle Of TCSC	10
2.2.2 Modeling Of TCSC For Power Flow Studies	12
2.3 Static Var Compensator (SVC) as a Shunt Controller	13
2.3.1 Operating principle of SVC	13
2.3.2 Modeling of SVC for Power flow studies	16

2.4 Unified Power Flow Controller (UPFC) As A Combined Series-Shunt Controller	19
2.4.1 Operating principle of UPFC	20
2.4.2 Modeling of UPFC for Power flow studies	21
2.4.3 Modified non-linear power flow equation for UPFC	23
<b>Chapter-3 LOAD FLOWS</b>	<b>27</b>
3.1 Introduction	27
3.2 Bus Classification	27
3.3 Step By Step Procedure Of Newton-Raphson Algorithm For Load Flow Solution	29
3.4 Load Flow Results Obtained For IEEE 30 BUS Test Case	32
3.5 Conclusion	34
<b>Chapter-4 OPTIMAL POWER FLOW</b>	<b>35</b>
4.1 Introduction	35
4.2 Optimal Power Flow Problem Formulation	36
4.3 Steepest Descent Method	37
4.3.1. Inequality Constraints on control variables	38
4.3.2 Inequality Constraints on the Dependent Variables	38
4.3.3. Step by Step Procedure for SD –OPF method	39
4.3.4 Simulation Results	40
4.4 Conclusion	43
<b>Chapter-5 EVOLUTIONARY PROGRAMMING BASED OPTIMAL POWER FLOW</b>	<b>44</b>
5.1 Introduction	44
5.1.1 Difference Between Evolutionary Programming And Other Traditional Methods	44
5.1.2 Difference Between Evolutionary Programming And Genetic Algorithm	45

5.1.3 Evolutionary Programming Operation	45
5.2 Step By Step Algorithm of Evolutionary Programming based OPF	48
5.3 Simulation Results	51
5.4 Comparison Of Results	54
5.5 Conclusion	55

**Chapter-6 EVOLUTIONARY PROGRAMMING BASED OPTIMAL  
POWERFLOW INCORPORATING MULTI TYPE  
FACTS DEVICES 56**

6.1 Basic Outline	56
6.2 Step By Step Algorithm of Evolutionary Programming Based OPF	56
6.3 Observed Results.	58
6.3 Conclusion	93

<b>CONCLUSIONS AND FUTURE SCOPE OF WORK</b>	<b>94</b>
<b>REFERENCES</b>	<b>96</b>
<b>APPENDIX A</b>	<b>99</b>

## LIST OF FIGURES

---

	PAGE No.
Figure 2.1 TCSC equivalent reactance as a function of firing angle	10
Figure 2.2 Schematic of TCSC	11
Figure 2.3 Structure of SVC	14
Figure 2.4: SVC equivalent reactance as a function of firing angle	15
Figure 2.5: SVC equivalent susceptance as a function of firing angle	16
Figure 2.6 SVC models using conventional power flow PV buses	17
Figure 2.7 - A simplified block diagram of power system and SVC.	18
Figure 2.8 - Characteristic of SVC and connected Power system	19
Figure 2.9 Schematic of UPFC	20
Figure 2.10 Vector Diagram of UPFC	21
Figure 2.11 - Equivalent circuit of UPFC	22
Figure 2.12 Injection Model of UPFC	23
Figure: 3.1. Flowchart for Newton-Raphson method for load flow solution	31
Figure 5.1 Schematic diagram of EP	47
Figure 5.2 Flowchart of EP-OPF	49
Figure 5.3 Convergence of EP-OPF (Cost of Generation)	54

## LIST OF TABLES

---

	PAGE No.
Table: 3.1 Load flow Result for IEEE 30 Bus Data	32
Table 4.1 Simulation results of SD-OPF	40
Table 4.2: Load flow Results of SD-OPF	41
Table 5.1 EP parameters	51
Table 5.2 Simulation results of EP based OPF	51
Table 5.3: Load flow results for EP-OPF	52
Table 5.4 Comparison of OPF methods	54
Table 6.1 – Index for the cases done in this work.	59
Table 6.2 – The Minimum cost of Generation obtained for different cases.	60
Table 6.3: Load Flow Results for Case I	62
Table 6.4: Load Flow Results for Case II	64
Table 6.5: Load Flow Results for Case III	67
Table 6.6: Load Flow Results for Case IV	70
Table 6.7: Load Flow Results for Case V	72
Table 6.8: Load Flow Results for Case VI	75
Table 6.9: Load Flow Results for Case VII	78
Table 6.10 Load Flow for Case VIII	81
Table 6.11 Load Flow Results for Case IX	84
Table 6.12: Load Flow Results for Case X	87
Table 6.13: Load Flow Results for Case XI	91
Table A.1. Generator Power Data	99
Table A.2 Reactor / Capacitor data	99
Table A.3 Load bus data	100
Table A.4 Transformer data	100
Table A.5 Line Data	101
Table A.6 Generator Cost Characteristics	102



## LIST OF ABBREVIATIONS

---

FACTS	Flexible AC Transmission Systems
ISO	Independent System Operator
OPF	Optimal Power Flow
GA	Genetic Algorithm
EP	Evolutionary Programming
HVDC	High Voltage Direct Current
IEEE	Institute of Electrical and Electronics Engineering
KWh	Kilo Watt Hour
MVA	Mega Volt Ampere
MW	Mega Watt
MVAR	Mega Volt Ampere Reactive
TCSC	Thyristor Controlled Series Capacitor
SVC	Static VAR Compensator
UPFC	Unified Power Flow Controller
VSC	Voltage Source Converter
N-R	Newton -Raphson

# Chapter-1

## INTRODUCTION

---

### 1.1 GENERAL

The demand for electric power is ever increasing due to rapid industrialization and population growth. Perhaps on India, the total power generation requirement has been tremendously increased during the past decades. And hence power systems became more complex and have grown very large. It is now important to design and operate systems with high degree of practical efficiency, security and reliability. In recent years, active power optimization has gained more importance due to exploitation of power generating sources at remote places and inclusion of long EHVAC as well as long DC transmission networks in the system. The optimal power flow (OPF) problem can be formulated as a constrained non-linear optimization problem. The solution of an OPF problem determines the optimal settings for control variables in a power network observing various constraints. In the last few year development, many different solution approaches have been proposed to solve the OPF problems. AC transmission systems could not be controlled practically and fast when traditional controllers are used. Traditional controllers that used before, like series and shunt compensators, voltage regulators, phase shifting and tap changing transformers could not realize the required level of control of these transmission systems. Recent developments in power electronics have opened a new world in power systems control. Several control devices are being developed under this new concept, known as FACTS (Flexible AC Transmission System). FACTS devices are integrated in power system to control power flow, increase transmission line stability limit and improve the security of transmission systems. FACTS controllers are used to enhance system flexibility and increase system loadability. In addition to controlling the power flow in specific lines, it is also used to minimize the total generator fuel cost in optimal power flow (OPF) problem.

### 1.2 OPTIMAL POWER FLOWS

Conventionally, the optimal operations of the power system networks have been based on economic criterion. However, recent concerns about power quality has forced

the system engineers to incorporate other criteria such as improving system voltage, transmission loss minimization etc.

The optimal power flow optimizes a power system operating objective function (such as the operating cost of thermal resources) while satisfying a set of system operating constraints. OPF has been widely used in power system operation and planning. The OPF problem can be formulated as a static constrained nonlinear optimization problem. The solution of an OPF problem determines the optimal settings for control variables in a power network observing various constraints.

### **1.3 FLEXIBLE AC TRANSMISSION SYSTEMS**

It is attractive for electrical utilities to have a way of permitting a more efficient use of the transmission lines by controlling the power flows. Such a means could be also interesting for the independent system operator (ISO) in a deregulated system, in order to assure a maximum level of competition among producers. Until a few years ago, the only means of carrying out this function were electromechanical devices such as switched inductors or capacitors banks and phase-shifting transformers. However, specific problems related to these devices make them not very efficient on some situations. They are not only relatively slow, but they also cannot be switched frequently, because they tend to wear quickly.

In recent years, the fast progress in the field of power electronics and microelectronics has resulted into new opportunity for more flexible operation of power systems suppressing these drawbacks. The FACTS program was launched by EPRI to develop a number of controllers for this purpose. These new devices have made the present transmission and distribution of electricity more reliable, more controllable and more efficient. Power system, around the world, has been forced to operate in almost their full capacities due to the environmental and/or economical constraints to build new generation centers and transmission lines. Due to these problems it is necessary to change in the traditional concepts and practices of power system and which also provides the needed correction on transmission line parameters so that the existing transmission system be fully utilized within the thermal limit of the line. Hence for the better utilization of transmission line the concept of FACTS were introduced. It opens new

opportunities for controlling power and enhancing the usable capacity of existing transmission line.

FACTS is a technology states that how the parameter of line should change to improve the performance of line by using the series and shunt compensation principle. A FACTS technology development has been an area of interest for many research organizations. These organizations recognized the potential benefits of inverter-based FACTS devices to allow utilities to operate their transmission system at higher capacities, more efficiently, and with improved reliability.

#### **1.4 OPTIMAL LOCATION OF FACTS DEVICES**

High speed switching capability of FACTS devices provides a mechanism for controlling line power flows, which permits increased loading of existing transmission lines, and allows for rapid readjustment of line power flow in response to various contingencies. The FACTS also can regulate steady-state power flow within its rating limits. The fast acting FACTS can provide a means of rapidly increasing power transfer upon detection of the critical contingencies, a resulting in increased transient stability.

FACTS devices having the ability to simultaneously control all three parameters of power flow: voltage, line impedance and phase angle, there by controlling two quantities such as active and reactive power flows of lines. Power system planers design their system, so that they can operate securely in the case of unexpected line or transformer outage. A secure system is defined as one where none of the system's operating constraints is violated under any of the considered line. FACTS devices can be used effectively in maintaining system's security by eliminating or alleviating overloads along the selected transmission line. Again after getting power flow solution of transmission network incorporating FACTS, question arises that in which line the FACTS should be placed i.e. optimal solution of FACTS devices in a given transmission network. Placement of FACTS devices is decided based on different factors such as generation cost reduction, loss reduction, improvement in stability margin etc. due to high cost of these FACTS devices, it is important to decide their optimal placement to meet the desired objective.

## 1.5 LITERATURE REVIEW

In 1999, Jason Yuryevich et al [1] presented evolutionary programming algorithm to solve OPF. The objective of this algorithm is to minimize the total generation cost. Authors have developed EP-based load flow incorporates a Jacobian acceleration stage. Steepest descent method was also used to improve the speed of convergence of the EP-OPF algorithm. This method was tested on IEEE 30 bus system. Three sets generator cost cover were used to illustrate the robustness of this technique, these are quadratic cost curves, piecewise quadratic curves, quadratic curve with sine curve.

In 2002, A. G. Bakirtzis et al. [2] presented a simple genetic algorithm and enhanced genetic algorithm to solve OPF. The objective of this algorithm is to optimize the operating cost of thermal resources. GA is based on the mechanics of natural selection and genetics. Advanced and problem-specific operators are introduced in order to enhance the genetic algorithm's efficiency and accuracy. Numerical results on IEEE 30 bus system and IEEE 3-AREA RTS 96 systems are presented and compared with results of other approach.

In 1999, James.A.Momoh et al. [3] offered a survey of literature on optimal power flow upto 1993. That part treats Newton-Based, Linear Programming and Interior Point Methods of solution. In that review, Papers were selected to emphasize the diversity of formulation and the breadth of the scope of problems considered. Authors have concluded that Linear Programming has fast speed and reasonable accuracy, suitable for large systems. An interior point method features good starting point and fast convergence.

In 2000, H.C.Leung et al [4] presented Genetic Algorithm method to solve OPF incorporating Flexible AC Transmission System (FACTS). A powerful and versatile FACTS device, UPFC (unified power flow controller) is considered in this paper. The proposed method was tested on IEEE-14 bus system. Author concluded that the FACTS device cannot reduce the generation cost compared with normal system OPF. However, it can provide wider operating margin and higher voltage stability with higher reserve capacity.

In 2001, T.S.Chung et al [5] presented a hybrid genetic algorithm (GA) method to solve optimal power flow (OPF) in a power system incorporating Flexible AC Transmission System (FACTS). In the solution process GA is integrated with conventional OPF to select the best control parameters to minimize the total generation fuel cost and keep the power flows within the security limits. The optimal control parameter selection of two types of FACTS devices, namely TCPS (Thyristor control phase shifter) and TCSC (Thyristor control series capacitor), using the integrated GA approach are demonstrated on IEEE 14-bus system.

In 2002, P.Bhasaputra and W.Ongsakul [6] proposed hybrid tabu search and simulated annealing (TS/SA) approach to minimize the generator fuel cost in OPF control with multi-type of Flexible AC Transmission System (FACTS) devices. Four types of FACTS devices are used in this work; they are TCSC, TCPS, UPFC and SVC. Algorithm is tested on the modified IEEE 30 bus system. Author concluded that proposed hybrid TS/SA approach can obtain better solutions and require less CPU times than genetic algorithm, SA, or TS alone and also multi type of FACTS devices results in less total generator fuel cost than using individual FACTS device.

In 2000, H.Ambriz-Perez et al [7] presented advanced load flow models incorporating existing load flow (LF) and optimal power flow (OPF) Newton algorithm for the static VAR compensator (SVC). Comprehensive SVC models suitable for conventional and optimal power flow analysis have been presented in this paper, namely SVC total susceptance model and SVC firing angle model. A Newton-Raphson load flow and a Newton's OPF algorithm have been upgraded to incorporate the new SVC models. Author obtained conventional and optimal solutions in less than 6 iterations.

In 2001, Stephane Gerbex et al [8] presented genetic algorithm to seek the optimal location of multi-type FACTS devices in a power system. The optimizations are based on branch loading and voltage levels. The FACTS devices are used in order to maximize the power transmitted by the network by controlling the power flows.

In 1997, C.R.Fuerte-Esquiavel and E.Acha [9] have discussed the steady state response of FACTS devices on the network wide basis. They have proposed the Newton-Raphson load flow program incorporating the variable series capacitor.

In 1998, Y.H.Song et al. [10] Presented an optimal multiplier based Newton-Raphson power flow algorithm for realize efficiently handling power systems with embedded FACTS devices. A steady state UPFC models has been proposed and its power injection transformation has been described in rectangular form. The optimal multiplier power flow method has been applied to implement the UPFC model. The proposed UPFC model of power flow algorithm has been tested, which illustrate the effectiveness of the proposed algorithm.

In 1995, L.Gyugi et al [11] proposed UPFC for real time control and dynamic compensation of as transmission systems. It has been shown that UPFC is able to control both the transmitted real power and independently, the reactive power flows at the sending and receiving of transmission line. Author also compared UPFC to other power flow controllers such as TCSC and TCPAR.

In 2002, Ying Xiao et al [12] developed an approach to steady state power flow control of FACTS device equipped power systems. A novel versatile power flow control approach has been formulated based on a power injection model of FACTS devices and an optimal power flow model. Numerical results on a practical system with various FACTS device have been presented to illustrate the vigourness of the proposed approach.

In 2003, M.H.Haque et al [13] proposed a simple method to solve the load flow problem of a power system in the presence of UPFC. Author has proposed a new static model of the UPFC to control the power flow. This static model of UPFC can be easily incorporated into any standard flow program, without modifying Jacobian matrix. This proposed method converged successfully for all cases, but required a few more iterations to converge.

In 1995, L.L.Lai et al [14] presented the use of an EP to solve OPF problems in FACTS. UPFC has been used to regulate both angle and magnitude of branch voltages. Author concluded that, when EP coupled with power flow, selects the best regulation to minimize the real power loss and keep the power flows in their secure limits.

In 1968, Dommel.H.W et al [16] proposed a practical method to solve power flow problem with control variables such as real and reactive power to minimize cost or losses. This proposed method is based on power flow solution by Newton's method, a gradient

adjustment algorithm for obtaining the minimum and penalty function to account for dependent constraints.

The book written by D.E.Goldberg [22] explains genetic algorithm. It also explains about the operators used in the genetic algorithm along with some examples.

## **1.6 OBJECTIVE OF THE THESIS**

As reviewed from the background information, FACTS is a concept covering a widespread of application of power electronics technology by which loading limit of existing power system can be increased. It can also give flexible and effective power flow control in power system. Their modeling and incorporation in load flow and optimal power flow is very much required. In this dissertation work following points has been analyzed using FACTS devices on optimal power flow.

From the literature it is found that N-R method is used for AC power flow calculation in system with FACTS devices. Therefore, in the existing FACTS Newton-Raphson load flow algorithm UPFC model has been incorporated. Based on the injection model of UPFC to control active and reactive powers and voltage magnitude in any combination, the modified Jacobian matrix and power mismatch equations are derived

A steady state model of FACTS devices has been used and introduced in the optimal power flow algorithm. Optimization has been performed with the system operating constraints such as power balance constraints, real and reactive power generation limits and FACTS devices parameters limit.

Evolutionary programming has been proposed to solve the OPF with FACTS devices. Optimal generation schedule and optimal setting of their parameters has been obtained. Performance of the proposed algorithm has been validated on test systems.

## **1.7 ORGANIZATION OF THE THESIS**

The present Chapter 1 introduces some problems of power systems, presents the importance of FACTS devices and sets motivations behind the work carried out in this thesis

In Chapter 2, a detail review of various FACTS controllers, which exist around the world, discusses along with their model structure and operating mechanism. It also



presents the development of suitable static model of FACTS devices such as TCSC, SVC and UPFC. Based on the location of UPFC, the power flow equations are solved using modified N-R method.

Chapter 3 presents the algorithm of Load flow analysis using Newton-Raphson method.

Chapter 4 presents the algorithm of steepest descent method to Optimal Power flow.

Chapter 5 presents the algorithm of proposed Evolutionary Programming to Optimal Power flow and its results has been compared with classical technique.

Chapter 6 presents proposed Evolutionary Programming to OPF incorporating Multi type FACTS devices.

Chapter 7 highlights the main finding and significant contributions of the thesis and identifies the scope for future research in the area of FACTS devices.

**FLEXIBLE AC TRANSMISSION SYSTEMS (FACTS)**

---

**2.1 INTRODUCTION**

The FACTS is a concept based on power electronic controllers, which enhance the value of transmission networks by increasing the use of their capacity. As these controllers operate very fast, they enlarge the safe operating limits of a transmission system without risking stability. Today, it is expected that within the operating constraints of the current-carrying thermal limits of conductors, the voltage limits of electrical insulating devices, and the structural limits of the supporting infrastructure, an operator should be able to control power flows on lines to secure the highest safety margin as well as transmit electrical power at a minimum of operating cost.

In this work, three types of FACTS controllers have been considered:

- Series controller
- Shunt controller
- Combined series-shunt controller

**2.2 THYRISTOR CONTROLLED SERIES CAPACITOR (TCSC) AS SERIES CONTROLLER**

Series capacitors are used to partially offset the effects of the series inductances of lines. Series compensation results in the improvement of the maximum power-transmission capacity of the line. The net effect is a lower load angle for given power transmission level and, therefore, a higher stability margin. The reactive power absorption of a line depends on the transmission current, so when series capacitors are employed, automatically the resulting reactive power compensation is adjusted proportionately. Also, because the series compensation effectively reduces the overall line reactance, it is expected that the net line voltage drop would become less susceptible to the loading conditions.

### 2.2.1 Operating principle of TCSC

TCSC consist of the series compensating capacitor shunted by a Thyristor controlled reactor. The basic idea behind the TCSC scheme is to provide a continuously variable capacitor by means of partially canceling the effective compensating capacitance by the TCR. TCR at the fundamental system frequency is continuously variable reactive impedance, controllable by delay angle  $\alpha$ , the steady state impedance of the TCSC is that of a parallel LC circuit, consisting of a fixed capacitive impedance,  $X_C$ , and a variable inductive impedance,  $X_L(\alpha)$ . Let consider TCSC as shown in Figure 2.1.

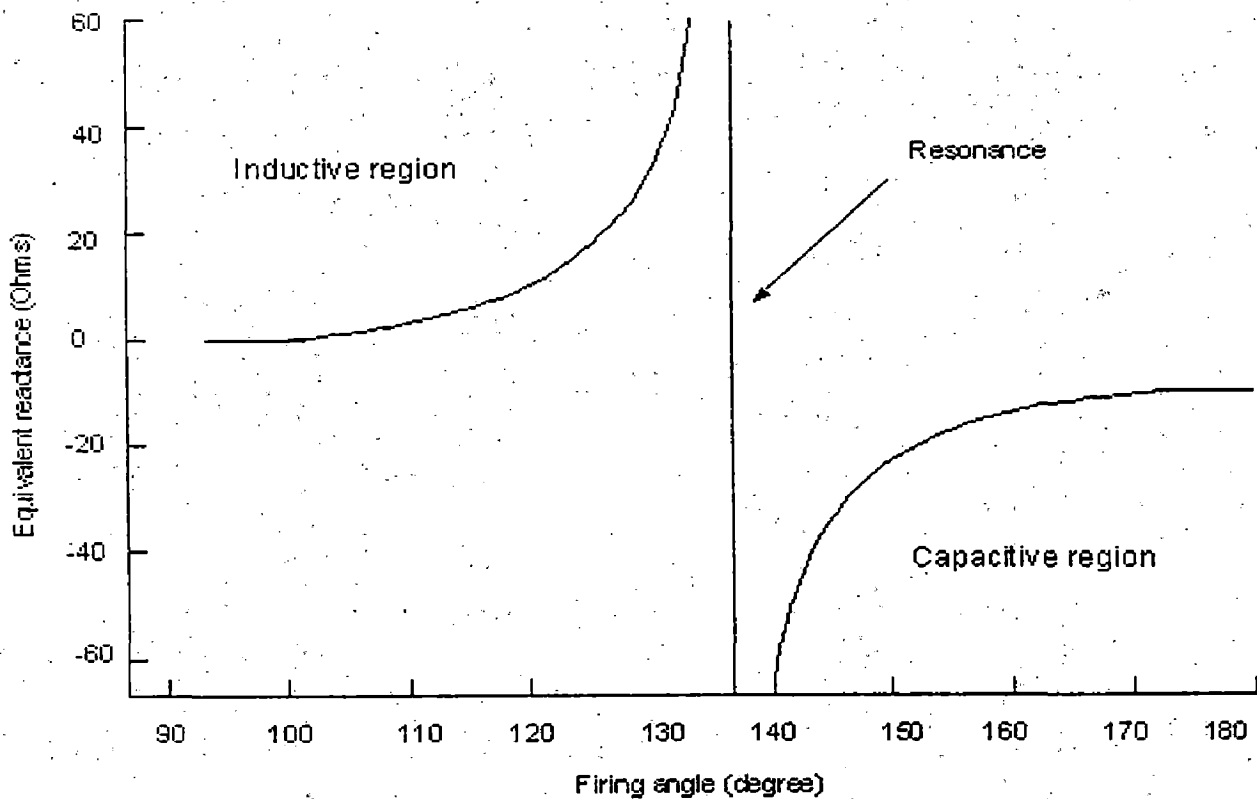
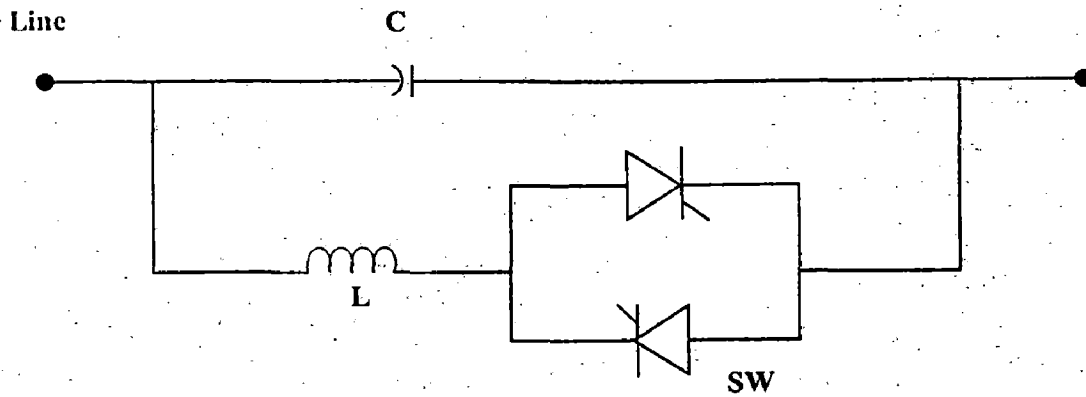


Figure 2.1 TCSC equivalent reactance as a function of firing angle



**Figure 2.2 Schematic of TCSC**

Let the capacitive reactance of capacitor bank

$$X_c = \frac{1}{\omega_n C} \quad (2.1)$$

And reactance of Thyristor controlled shunt arm is given by

$$X_L = \omega_n L \quad (2.2)$$

$$X_L(\alpha) = \frac{\pi X_L}{\pi - 2\alpha - \sin(\alpha)} \quad (2.3)$$

$$X_{TCSC} = -j \frac{X_c X_L(\alpha)}{X_L(\alpha) - X_c} \quad (2.4)$$

Where

$X_L$  = reactance of the inductor

$\alpha$  = firing angle of Thyristor

$X_L(\alpha)$  = reactance of the Thyristor controlled inductor arm

$\omega_n$  = supply frequency of power

From eqn 2.4, we see that

If  $X_L(\alpha) > X_C$  then TCSC shows capacitive characteristics

If  $X_L(\alpha) < X_C$  then TCSC shows inductive characteristics

If  $X_L(\alpha) = X_C$  then the impedance of the TCSC will be infinite and this is the condition of resonance in parallel inductive and capacitive circuit. Therefore in this region operation of TCSC is not allowed. The TCSC must operate either in capacitive region or in inductive region. Normally it operates in capacitive region.

### 2.2.2 Modeling of TCSC for Power flow studies

The effect of FACTS devices like TCSC on the network can be seen as a controllable reactance inserted in the related transmission line. The model of the network with TCSC is shown in figure 2.2. During steady state the TCSC can be considered as a static capacitor/reactor offering impedance  $jX_{TCSC}$ . The controllable reactance  $X_{TCSC}$  is directly used as a control variable to be implemented in the power flow equations. The real power and reactive power flow equations of the branch K flowing from bus i to j can be expressed as,

$$P_{ij} = V_i^2 G_{ij} - V_i V_j (G_{ij} \cos \delta_{ij} + B_{ij} \sin \delta_{ij}) \quad (2.5)$$

$$Q_{ij} = -V_i^2 (B_{ij} + B_{sh}) + V_i V_j (B_{ij} \cos \delta_{ij} - G_{ij} \sin \delta_{ij}) \quad (2.6)$$

$$\text{Where } G_{ij} = \frac{R_{ij}}{R_{ij}^2 + (X_{ij} - X_{TCSC})^2}, \quad B_{ij} = \frac{X_{ij} - X_{TCSC}}{R_{ij}^2 + (X_{ij} - X_{TCSC})^2} \quad (2.7)$$

Similarly, the real power and reactive power flow from bus j to bus i can be expressed as,

$$P_{ji} = V_j^2 G_{ij} - V_i V_j (G_{ij} \cos \delta_{ij} - B_{ij} \sin \delta_{ij}) \quad (2.8)$$

$$Q_{ji} = -V_i^2 (B_{ij} + B_{sh}) + V_i V_j (B_{ij} \cos \delta_{ij} + G_{ij} \sin \delta_{ij}) \quad (2.9)$$

Here the only difference between normal line power flow equation and the TCSC line power flow equation is the controllable reactance  $X_{TCSC}$ .

The TCSC may have one of the two possible characteristic capacitive or inductive, respectively to decrease or increase the reactance of the line. It is modeled with two ideal switched elements in parallel: a capacitance and an inductance. The capacitance and the inductance are variable and their values are function of the reactance of the line in which the device is located. In order to avoid resonance, the  $\alpha$  value must be properly adjusted.

## **2.3 STATIC VAR COMPENSATOR (SVC) AS A SHUNT CONTROLLER**

Steady state transmittable power can be increased and the voltage profile along the line controlled by appropriate reactive shunt compensation. The purpose of this reactive compensation is to change the natural electrical characteristics of the transmission line to make it more compatible with the prevailing load demand. Thus, shunt connected reactors are applied to minimize line overvoltages under light load conditions, and shunt connected capacitors are applied to maintain voltage levels under heavy load conditions. The ultimate objective of applying reactive shunt compensation in a transmission system is to increase the transmittable power.

### **2.3.1 Operating principle of SVC**

The SVC consists of a group of shunt connected capacitors and reactors banks with fast control action by means of Thyristor switching. From the operational point of view, the SVC can be seen as a variable shunt reactance that adjusts automatically in response to changing system operative conditions. Depending on the nature of the equivalent SVC's reactance, i.e, capacitive or inductive, the SVC draws either capacitive or inductive current from the network. Suitable control of this equivalent reactance allows voltage magnitude regulation at the SVC point of connection.

SVC's normally include a combination of mechanically controlled and Thyristor controlled shunt capacitors and reactors. The most popular configuration for continuously controlled SVC's is the combination of either fix capacitor and Thyristor controlled reactor. The SVC structure shown in Figure 2.3 is used to derive a SVC model that considers the TCR firing angle  $\alpha$  as state variable.

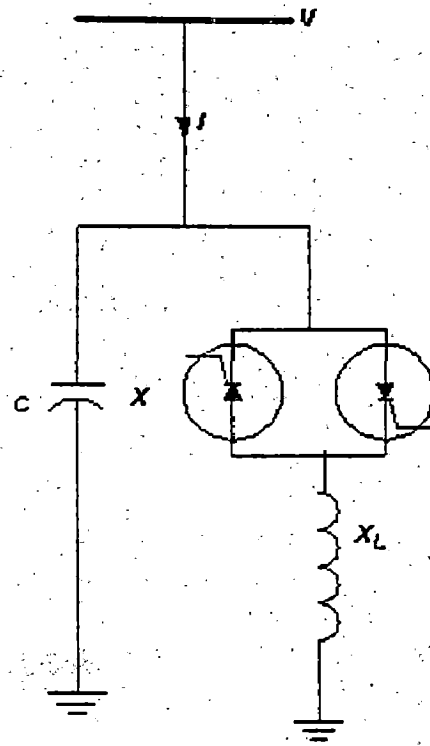


Figure 2.3 Structure of SVC

The variable TCR equivalent reactance at fundamental frequency is given by,

$$X_{Leq} = X_L \frac{\pi}{2(\pi - \alpha) + \sin(2\alpha)} \quad (2.10)$$

Where  $\alpha$  is the thyristor's firing angle.

The SVC effective reactance  $X_{eq}$  is determined by the parallel combination of  $X_C$  and  $X_{Leq}$ ,

$$X_{eq} = \frac{X_C X_L}{\frac{X_C}{\pi} (2(\pi - \alpha) + \sin(2\alpha)) - X_L} \quad (2.11)$$

Depending on the ratio  $X_C/X_L$ , there is a value of firing angle that causes a steady state resonance to occur. Figure 2.4 depicts the SVC equivalent impedance at the fundamental

frequency as function of firing angle, corresponding to a capacitive reactance of 15 ohm and a variable inductive reactance of 2.56 ohm.

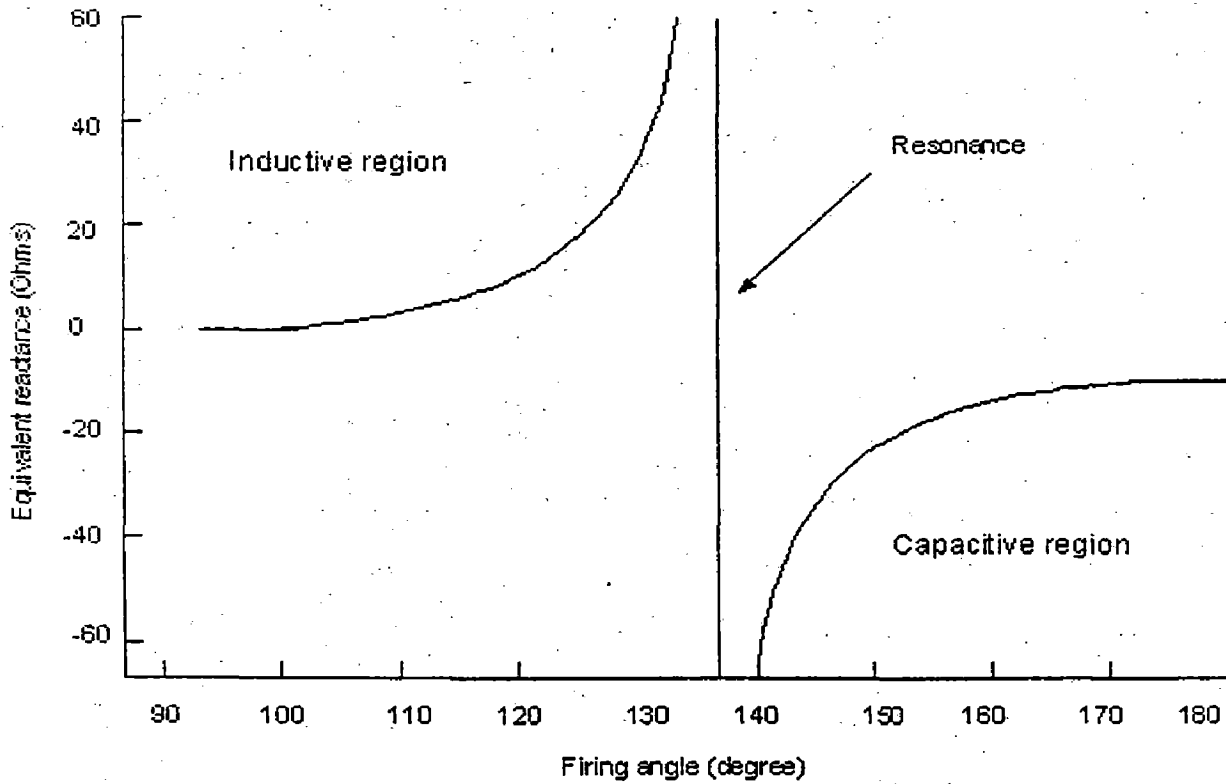


**Figure 2.4: SVC equivalent reactance as a function of firing angle**

The SVC equivalent susceptance is given by its profile, as function of firing angle, is given in Figure 2.5

$$B_{eq} = [X_L - X_C * (2(\pi - \alpha) + \sin(2\alpha)) / \pi] / (X_C * X_L) \quad (2.12)$$

It is shown in Figure 2.5 that the SVC equivalent susceptance profile, as function of firing angles, does not present discontinuities, i.e.,  $B_{eq}$  varies in a continuous, smooth fashion in both operative regions. Hence, linearization of the SVC power flow equations, based on  $B_{eq}$  with respect to firing angle, will exhibit a better numerical behavior than the linearized model based on  $X_{eq}$ .



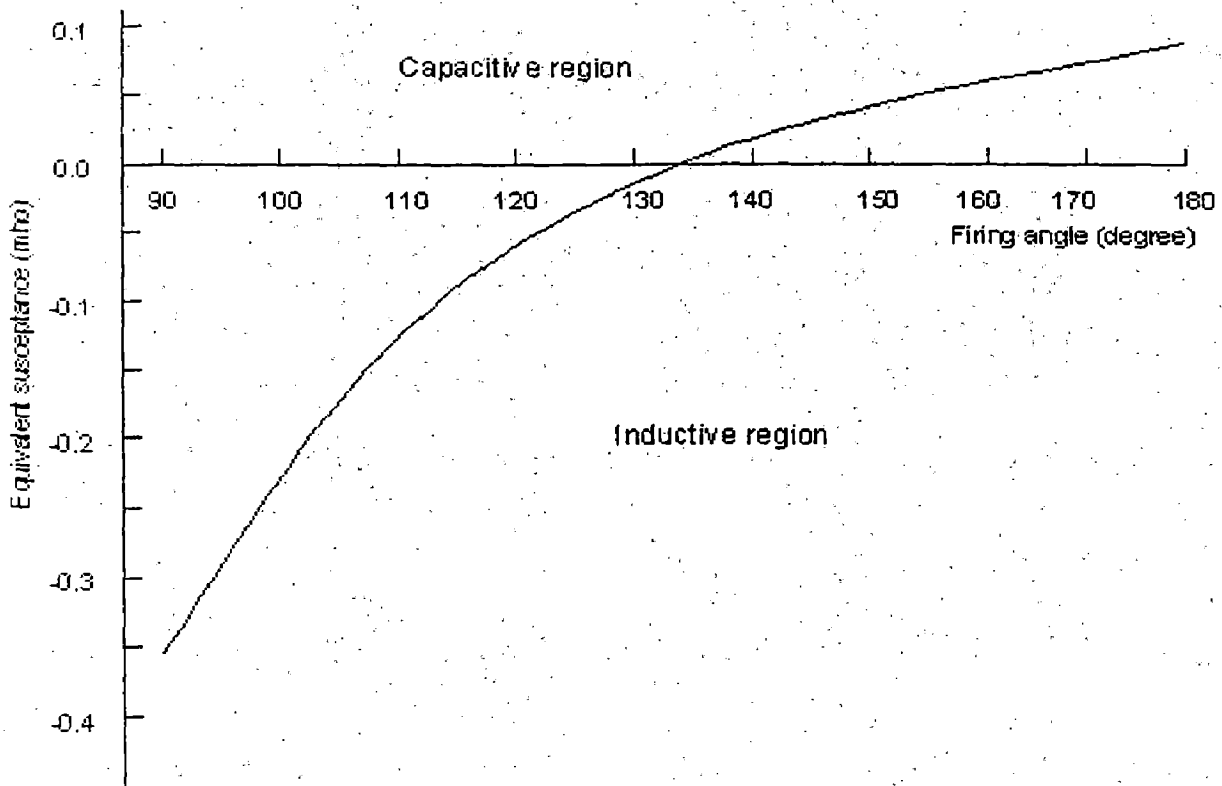


**Figure 2.5: SVC equivalent susceptance as a function of firing angle**

### 2.3.2 Modeling of SVC for Power flow studies

The SVC models in these studies should represent the fundamental frequency, steady state, and balanced performance of the SVC. It may be necessary to model the SVC in terms of its three individual phases when an unbalanced operation of the SVC is considered, such as during load compensation or voltage balancing. The features of conventional load flow programs are described as follows.

If the slope of the SVC is neglected, then the SVC is modeled as a PV bus, with  $P=0$  and  $V=V_{ref}$ . However, if the slope is considered (as in the analysis of weak ac systems), the same is modeled by connecting the high voltage side of the SVC bus to a fictitious auxiliary bus by means of a reactance equal to the slope expressed in per units on the SVC base. Such a model is shown in Figure 2.6.

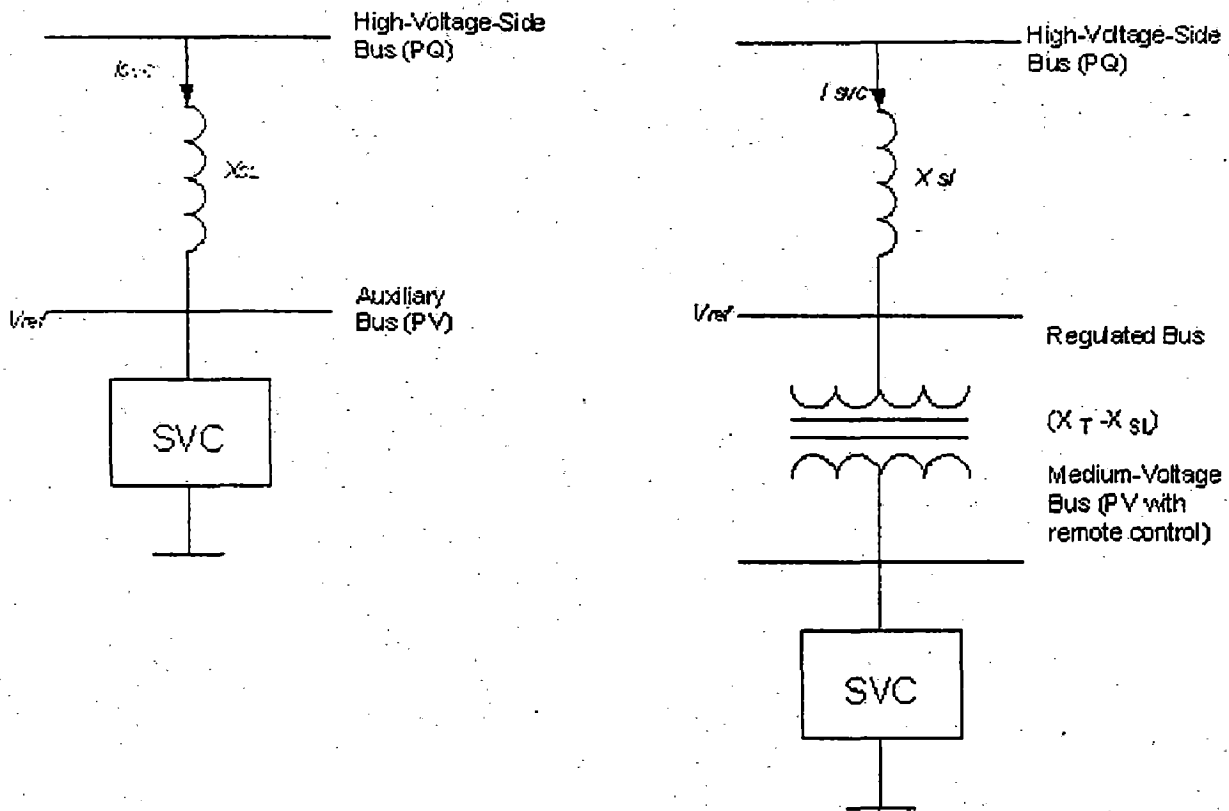


**Figure 2.6 SVC models using conventional power flow PV buses**

It may become necessary to model the coupling transformer should the SVC be connected to the tertiary winding. When the transformer is represented explicitly, the susceptance range of the SVC must be appropriately adjusted to represent the correct reactive power rating as seen at the high voltage bus. The corresponding load flow model is illustrated in Figure 2.6.

The voltage control action of the SVC can be explained through a simplified block representation of the SVC and the power system.

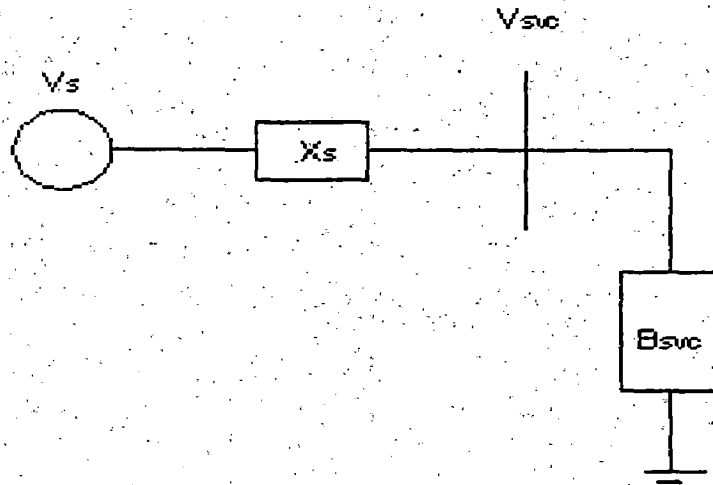


**Figure 2.7 - A simplified block diagram of power system and SVC.**

The power system is modeled as an equivalent voltage source  $V_s$ , behind equivalent system impedance  $X_s$ , as viewed from the SVC terminal is illustrated in Figure 2.7. The system impedance  $X_s$  indeed corresponds to the short circuit MVA at the SVC bus and is obtained as

$$X_s = (V_b \cdot V_b) \cdot \text{MVA}_b / S_c \text{ p.u} \quad (2.13)$$

Where  $S_c$  = the 3 phase short circuit MVA at the SVC Bus

$V_b$  = the base line to line voltage

$\text{MVA}_b$  = the base MVA of the system

If the SVC draws a reactive current  $I_{svc}$ , then in the absence of the SVC regulator, the SVC bus voltage is given by,

$$V_s = V_{svc} + I_{svc} \cdot X_s \quad (2.14)$$

The SVC current thus results in a voltage drop of  $I_{svc} \cdot X_s$  in phase with the system voltage  $V_s$ . The SVC bus voltage decreases with the inductive SVC current and increases with the capacitive current. The equation  $V_s = V_{svc} + I_{svc} \cdot X_s$  represents the power system characteristics or system load line. An implication of this equation is that the SVC is more effective in controlling the voltage in weak ac system (high  $X_s$ ) and less effective in strong ac system (low  $X_s$ ).

The Dynamic characteristics of the SVC describe the reactive power compensation provided by the svc in response to a variation in the SVC terminal voltage.

The intersection of the SVCD dynamic characteristics and the system load line provides the quiescent operating point of the SVC as shown in the Figure 2.8.

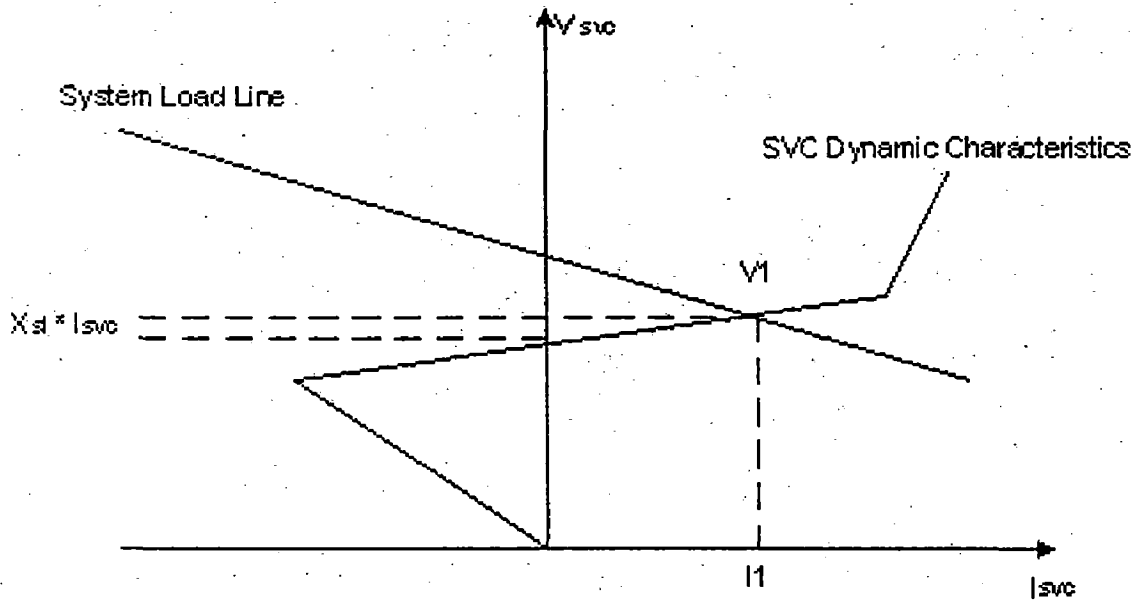


**Figure 2.8 - Characteristic of SVC and connected Power system.**

The voltage control action in the linear range is described below

$$V_{svc} = V_{ref} + X_{sl} * I_{svc} \quad (2.15)$$

Where  $I_{svc}$  is positive if inductive, negative if capacitive.

#### **2.4 UNIFIED POWER FLOW CONTROLLER (UPFC) AS A COMBINED SERIES-SHUNT CONTROLLER**

Series or shunt controllers are either reactive compensators (i.e., SVC and TCSC) which are unable to exchange real power with the AC system or regulators (i.e., TCVR and TCPAR) which can exchange real and reactive power, but are unable to generate reactive power and thus cannot provide reactive compensation. Combined series-shunt controller has the inherent capability, like a synchronous machine, to exchange both real and reactive power with the AC system. Furthermore this controller automatically generates or absorbs the reactive power exchanged and thus provides compensation

without AC capacitors or reactors. However, the real power exchanged must be supplied to them or absorbed from them by the AC system.

#### 2.4.1 Operating principle of UPFC

The UPFC is the most versatile FACTS controller developed so far, with all encompassing capabilities of voltage regulation, series compensation, and phase shifting. It can independently and very rapidly control both real and reactive power flows in a transmission line. It is configured as shown in Figure 2.9 and comprises two VSCs coupled through a common dc terminal. One VSC-converter 1-is connected in shunt with the line through a coupling transformer: the other VSC-converter 2- is inserted in series with the transmission line through a interface transformer. The dc voltage for both converters is provided by a common capacitor bank. The series converter is controlled to inject a voltage phasor,  $V_{pq}$  in series with the line, which can be varied from 0 to  $V_{pq, \text{max}}$ . Moreover, the phase angle of  $V_{pq}$  can be independently varied from 0 to 360. In this process, the series converter exchanges both real and reactive power with the transmission line. Although the reactive power is internally generated /absorbed by the series converter, the real power generation/absorption is made feasible by the dc-energy-storage device-that is, the capacitor.

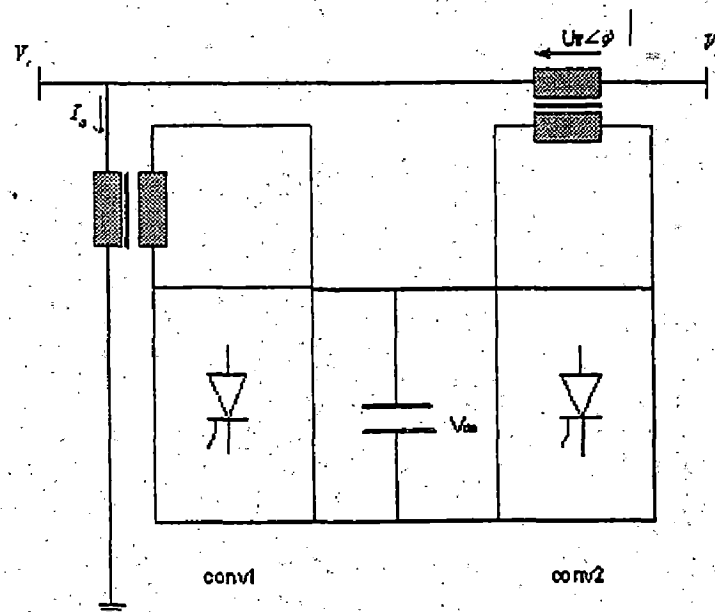


Figure 2.9 Schematic of UPFC

The shunt-connected converter 1 is used mainly to supply the real power demand of converter 2, which it derives from the transmission line itself. The shunt converter maintains constant voltage of the dc bus. Thus the net real power drawn from the ac system is equal to the losses of the two converters and their coupling transformers. In addition, the shunt converter independently regulates the terminal voltage of the interconnected bus by generating/absorbing a requisite amount of reactive power (refer Figure 2.10).

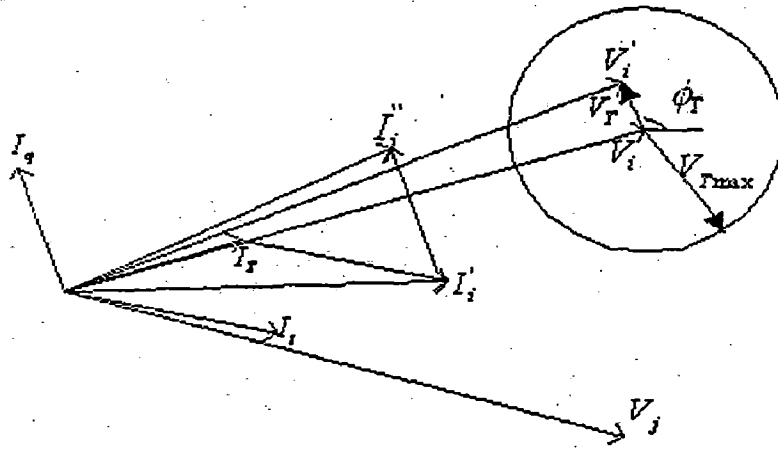


Figure 2.10 Vector Diagram of UPFC

### 2.4.2 Modeling of UPFC for Power flow studies

The equivalent circuit of UPFC placed in line connected between bus -  $i$  and bus -  $j$  is shown in Figure 2.11. UPFC has three controllable parameters, namely the magnitude and the angle of inserted voltage ( $V_T, \phi_T$ ) and the magnitude of the current ( $I_q$ ).

Based on the principle of UPFC and the vector diagram, the basic mathematical relations can be given as

$$V_i' = V_i + V_T,$$

$$\text{Arg}(l_q) = \text{Arg}(V_i) \pm \pi / 2,$$

$$\text{Arg}(l_T) = \text{Arg}(V_i) \text{ and}$$

$$l_T = \frac{\text{Re}[V_T l_i']}{V_i} \quad (2.16)$$

The power flow equations from bus  $-i$  to bus  $-j$  and from bus  $-j$  to bus  $-i$  can be written as

$$S_{ij} = P_{ij} + jQ_{ij} = V_i l_{ij}' = V_i (jV_i b_{sh} / 2 + l_T + l_q + l_i') \quad (2.17)$$

$$S_{ji} = p_{ji} + jQ_{ji} = V_j l_{ji}' = V_j (jV_j b_{sh} / 2 - l_i') \quad (2.18)$$

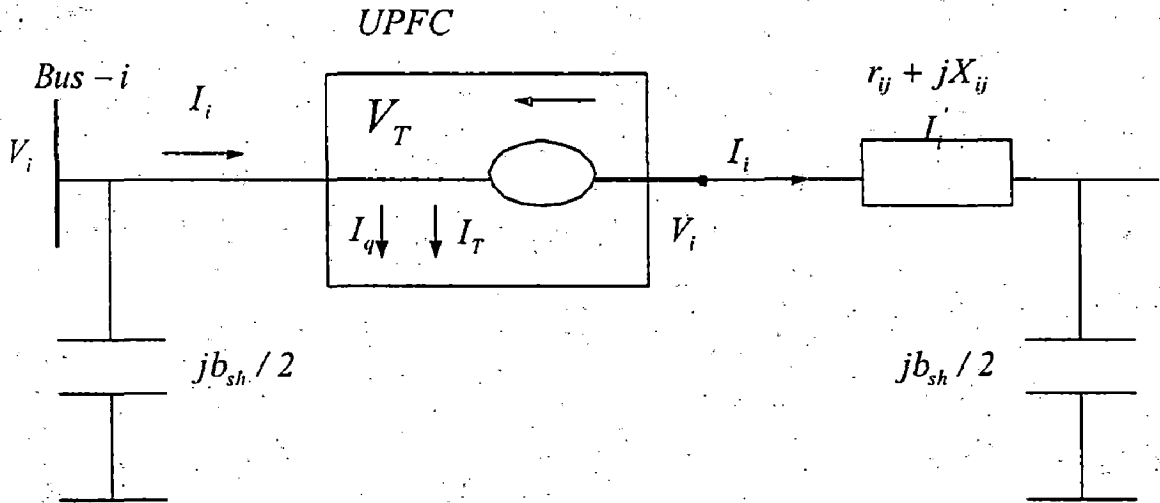


Figure 2.11 - Equivalent circuit of UPFC

Active and reactive power flows in the line having UPFC can be written, with above equations (2.16) –(2.18), as

$$P_{ij} = (V_i^2 + V_T^2)g_{ij} + 2V_i V_T g_{ij} \cos(\phi_T - \delta_j) - V_j V_T [g_{ij} \cos(\phi_T - \delta_j) + b_{ij} \sin(\phi_T - \delta_j)] \\ V_i V_j (g_{ij} \cos \delta_{ij} + b_{ij} \sin \delta_{ij}) \quad (2.19)$$

$$p_{ji} = V_j^2 g_{ij} - V_j V_T [g_{ij} \cos(\phi_T - \delta_j) - b_{ij} \sin(\phi_T - \delta_j)] - V_i V_j (g_{ij} \cos \delta_{ij} - b_{ij} \sin \delta_{ij}) \\ Q_{ij} = -V_i l_q - V_i^2 (b_{ij} + b_{sh} / 2) - V_i V_T [g_{ij} \sin(\phi_T - \delta_j) + b_{ij} \cos(\phi_T - \delta_j)] \quad (2.20)$$

$$-V_i V_j (g_{ij} \sin \delta_{ij} - b_{ij} \cos \delta_{ij})$$

$$Q_{ii} = -V_i^2 (b_{ij} + b_{sh} / 2) - V_j V_T (g_{ij} \sin(\phi_T - \delta_j) - b_{ij} \cos(\phi_T - \delta_j)) + V_i V_j (g_{ij} \sin \delta_{ij} + b_{ij} \cos \delta_{ij}) \quad (2.21)$$

From basic circuit theory, the injected equivalent circuit of Figure 2.12 can be obtained. The injected active power at bus- $i$  ( $P_{is}$ ) and bus- $j$  ( $P_{js}$ ), and reactive powers ( $Q_{is}$  and  $Q_{js}$ ) of a line having a UPFC are

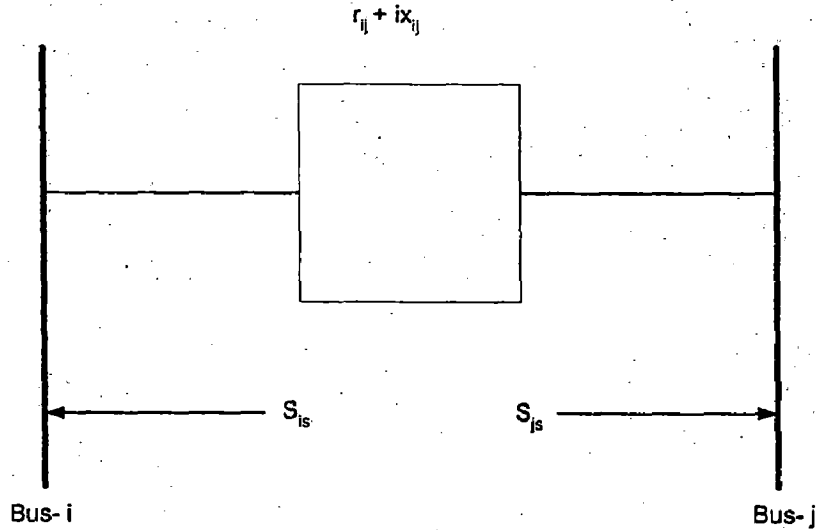


Figure 2.12 Injection Model of UPFC

$$P_{is} = -V_T^2 g_{ij} - 2V_i V_T g_{ij} \cos(\phi_T - \delta_i) + V_j V_T [g_{ij} \cos(\phi_T - \delta_j) + b_{ij} \sin(\phi_T - \delta_j)] \quad (2.22)$$

$$P_{js} = V_j V_T [g_{ij} \cos(\phi_T - \delta_j) - b_{ij} \sin(\phi_T - \delta_j)] \quad (2.23)$$

$$Q_{is} = V_i l_q + V_i V_T [g_{ij} \sin(\phi_T - \delta_i) + b_{ij} \cos(\phi_T - \delta_i)] \quad (2.24)$$

$$Q_{js} = -V_j V_T [g_{ij} \sin(\phi_T - \delta_j) - b_{ij} \cos(\phi_T - \delta_j)] \quad (2.25)$$

### 2.4.3 Modified non-linear power flow equation for UPFC

The effect of UPFC on power system can be modeled by injected real and reactive power flows at two related buses as shown in fig,2.12 thus they have no effect on the



admittance matrix. The load flow equation at bus  $i$  for having  $n$  buses in the system and without UPFC, can be expressed as below

$$P_{Gi} - P_u = \sum_{j=1}^n V_i V_j (g_{ij} \cos \delta_{ij} + b_{ij} \sin \delta_{ij}) \quad (2.26)$$

$$Q_{Gi} - Q_u = \sum_{j=1}^n V_i V_j (g_{ij} \sin \delta_{ij} - b_{ij} \cos \delta_{ij}) \quad (2.27)$$

$$j = 1, 2, \dots, n$$

Where  $n$  is the total numbers of buses in the power system.  $P_{Gi}$  and  $Q_{Gi}$  are the active and reactive power injected to bus  $i$  by generator respectively.  $V_i$  is the magnitude of voltage of bus  $i$ .  $P_{Li}$  and  $Q_{Li}$  is the active and reactive power extracted from bus  $i$  by load respectively.  $V_j$  is the magnitude of voltage of bus  $j$ .  $\delta_{ij} = \delta_i - \delta_j$ , is the phase angle difference between bus  $i$  and  $j$ .  $g_{ij} + jb_{ij}$  Denotes the element  $Y_{ij}$  of admittance matrix of system network.

The load flow equations with UPFC, can then be obtained and referred directly as for a generic case, it is assumed that UPFC is embedded in a transmission line with connected between node  $-l$  and node- $m$ . Therefore, for the UPFC embedded transmission line, the load flow power mismatch equations can be expressed as below.

$$P_{Gi} - P_u = \sum_{j=1}^n V_i V_j (g_{ij} \cos \delta_{ij} + b_{ij} \sin \delta_{ij}) \quad (2.28)$$

$$Q_{Gi} - Q_u = \sum_{j=1}^n V_i V_j (g_{ij} \sin \delta_{ij} - b_{ij} \cos \delta_{ij}) \quad \text{For } i = 1, 2, \dots, n; \text{ but } i \neq l, m$$

Thus four mismatch equations are:

$$P_{Gi} - P_{Li} = \sum_{j=1}^n V_i V_j (g_{ij} \cos \delta_{ij} + b_{ij} \sin \delta_{ij}) + P_{Is} \quad (2.29)$$

$$Q_{Gi} - Q_{Li} = \sum_{j=1}^n V_i V_j (g_{ij} \sin \delta_{ij} - b_{ij} \cos \delta_{ij}) + Q_{Is} \quad (2.30)$$

$$P_{Gim} - P_{Lim} = \sum_{i=1}^n V_m V_i (g_{mi} \cos \delta_{mi} + b_{mi} \sin \delta_{mi}) + P_{ms} \quad (2.31)$$

$$Q_{Gim} - Q_{Lim} = \sum_{i=1}^n V_m V_i (g_{mi} \sin \delta_{mi} - b_{mi} \cos \delta_{mi}) + Q_{ms} \quad (2.32)$$

Where  $n$  is the total number of buses.  $P_{Gi}$ ,  $Q_{Gi}$ ,  $P_{Li}$ , and  $Q_{Li}$  are the respective real and reactive power of generator and load of node  $-i$  and the values of,  $P_{is}$ ,  $Q_{is}$ ,  $P_{ms}$ , &  $Q_{ms}$  for UPFC will be

$$\begin{aligned} P_{is} &= -V_T^2 g_{im} - 2V_l V_T g_{lm} \cos(\phi_T - \delta_m) + V_m V_T [g_{lm} \cos(\phi_T - \delta_m) + b_{lm} \sin(\phi_T - \delta_m)] \\ P_{ms} &= V_m V_T [g_{im} \cos(\phi_T - \delta_m) - b_{im} \sin(\phi_T - \delta_m)] \\ Q_{is} &= V_l I_q + V_l V_T [g_{lm} \sin(\phi_T - \delta_l) + b_{lm} \cos(\phi_T - \delta_l)] \\ Q_{ms} &= -V_m V_T [g_{lm} \sin(\phi_T - \delta_m) + b_{lm} \cos(\phi_T - \delta_m)] \end{aligned} \quad (2.33)$$

Thus, the relationship are obtained for small variations in  $V$  and  $\delta$ , by forming the total differentials,

$$\begin{aligned} \begin{bmatrix} \Delta P \\ \Delta Q \end{bmatrix} &= J_1 \begin{bmatrix} \Delta \delta \\ \Delta V \end{bmatrix} + J_2 \begin{bmatrix} \Delta \delta \\ \Delta V \end{bmatrix} \\ J &= J_1 + J_2 \end{aligned} \quad (2.34)$$

Where  $J_1$ , the normal N-R power is flow Jacobian matrix and  $J_2$  is the partial derivative matrixes of injected power with respect to the variables. When bus- $l$  and bus- $m$  are PQ buses, the matrix  $J_1$  may have 10 nonzero elements as if bus- $l$  is a PV corresponding elements of row and column will not exist. When more than one UPFC are installed in the network their effects are added to matrix  $J_2$ . In this situation the non-zero elements may be more than 10. Now we can see that the power flow can be solved by N-R method in the normal way except the small differences in  $J$  matrix and power mismatch equations.

The elements of  $J_2$  FOR UPFC are given below

$$\frac{\partial P_{is}}{\partial \delta_l} = -2V_l V_T g_{lm} \sin(\phi_T - \delta_l) \quad (2.35)$$

$$\frac{\partial P_{ls}}{\partial \delta_m} = V_m V_T [g_{lm} \sin(\phi_T - \delta_m) - b_{lm} \cos(\phi_T - \delta_m)] \quad (2.36)$$

$$\frac{\partial P_{ms}}{\partial \delta_m} = V_m V_T [g_{lm} \sin(\phi_T - \delta_m) + b_{lm} \cos(\phi_T - \delta_m)] \quad (2.37)$$

$$\frac{\partial Q_{ls}}{\partial \delta_l} = -V_l V_T [-g_{lm} \cos(\phi_T - \delta_l) + b_{lm} \sin(\phi_T - \delta_l)] \quad (2.38)$$

$$\frac{\partial P_{ls}}{\partial V_l} = -2V_T g_{lm} \cos(\phi_T - \delta_l) \quad (2.39)$$

$$\frac{\partial P_{ls}}{\partial V_m} = V_T [g_{lm} \cos(\phi_T - \delta_m) + b_{lm} \sin(\phi_T - \delta_m)] \quad (2.40)$$

$$\frac{\partial P_{ms}}{\partial V_m} = V_T [g_{lm} \cos(\phi_T - \delta_m) + b_{lm} \sin(\phi_T - \delta_l)] \quad (2.41)$$

$$\frac{\partial Q_{ms}}{\partial \delta_m} = -V_m V_T [-g_{lm} \cos(\phi_T - \delta_m) + b_{lm} \sin(\phi_T - \delta_m)] \quad (2.42)$$

$$\frac{\partial Q_{ls}}{\partial V_l} = I_q + V_T [g_{lm} \sin(\phi_T - \delta_l) + b_{lm} \cos(\phi_T - \delta_l)] \quad (2.43)$$

$$\frac{\partial Q_{ms}}{\partial V_m} = -V_T [g_{lm} \sin(\phi_T - \delta_m) + b_{lm} \cos(\phi_T - \delta_m)] \quad (2.44)$$

$$\frac{\partial P_{ms}}{\partial \delta_l} = 0; \frac{\partial P_{ls}}{\partial V_l} = 0 \quad (2.45)$$

$$\frac{\partial Q_{ls}}{\partial V_m} = 0; \frac{\partial Q_{ms}}{\partial \delta_l} = 0; \frac{\partial Q_{ls}}{\partial \delta_m} = 0; \frac{\partial Q_{ms}}{\partial V_l} = 0 \quad (2.46)$$

With help of equations (2.35-2.46) the power flow Jacobian matrix is modifies and we can see that the power flow solution is obtained by N-R method in the normal ways except the small differences in  $J_2$  matrix and power mismatch.

## Chapter-3

### LOAD FLOWS

---

#### 3.1 INTRODUCTION

Load flow solution is solution of the network under steady state condition subject to certain inequality constraints under which the system operates. These constraints can be in the form of load nodal voltages, reactive power generation of the generators, the tap settings of a tap changing under load transformer etc.

The load flow solution gives the nodal voltages and phase angles and hence the power injection at all the buses and power flows through inter-connecting power channels (transmission lines). Load flow solution is essential for designing a new power system and for planning extension of the existing one for increased load demand. These analyses require the calculation of numerous load flows under both normal and abnormal (outage of transmission lines, or outage of some generating source) operating conditions. Load flow solution also gives the initial conditions of the system when the transient behaviour of the system is to be studied.

#### 3.2 BUS CLASSIFICATION

In a power system each bus or node is associated with four quantities, real and reactive powers, bus voltage magnitude and its phase angle. In a load flow solution two out of the four quantities are specified and the remaining two are required to be obtained through the solution of the equations. Depending upon which quantities have been specified, the buses are classified in the following three categories:

1. *Load bus:* At this bus the real and reactive components of power are specified. It is desired to find out the voltage magnitude and phase angles through the load flow solution. It is required to specify only  $P_D$  and  $Q_D$  at such a bus at a load bus voltage can be allowed to vary within the permissible values. Also phase angle of the voltage is not very important for the load.
2. *Generator Bus:* Here the voltage magnitude corresponding to the generation voltage and real power  $P_G$  corresponding to its ratings are specified. It is required to find out the

reactive power generations  $Q_G$  and the phase angle of the bus voltage.

3. *Slack bus*: In a power system there are mainly two types of buses: load and generator buses. For these buses we have specified the real power  $P$  injections. Now  $\sum_{i=1}^n P_i = \text{real power loss } P_l$  where  $P_i$  is the power injection at the buses, which is taken as positive for generator buses and is negative for load buses. The losses remain unknown until the load flow solution is complete. It is for this reason that generally one of the generator buses is made to take the additional real and reactive power to supply transmission losses. That is why this type of bus is also known as the slack or swing bus. At this bus, the voltage magnitude  $V$  and phase angle  $\delta$  are specified whereas real and reactive powers  $P_G$  and  $Q_G$  are obtained through the load flow solution. The following table summarizes the above discussion:

Bus Type	Quantities specified	Quantities to be obtained
Load bus	$P, Q$	$ V , \delta$
Generator Bus	$P,  V $	$Q, \delta$
Slack Bus	$ V , \delta$	$P, Q$

The phase angle of the voltage at the slack bus is usually taken as the reference.

### 3.3 STEP BY STEP PROCEDURE OF NEWTON-RAPHSON ALGORITHM FOR LOAD FLOW SOLUTION

1. Read Bus and Line Data and Form  $Y_{bus}$
2. Assume initial values of bus voltages  $|V_i|^0$  and phase angles  $\delta_i^0$  for  $i = 2, 3, \dots, n$  for load buses and phase angles for PV buses. Normally we set the assumed bus voltage magnitude and its phase angle equal to slack bus quantities  $|V_i| = 1.0, \delta_i = 0^\circ$ .

3. Compute  $P_i$  and  $Q_i$  for each load bus from the following equations:

$$P_i = \sum_{k=1}^n V_i V_k Y_{ik} \cos(\delta_i - \delta_k - \theta_{ik}) \quad (3.1)$$

$$Q_i = \sum_{k=1}^n V_i V_k Y_{ik} \sin(\delta_i - \delta_k - \theta_{ik}) \quad (3.2)$$

4. Compute the scheduled errors  $\Delta P_i$  and  $\Delta Q_i$  for each load from the following relations

$$\Delta P_i^{(r)} = P_{isp} - P_{i(cal)}^{(r)} \quad i = 2, 3, \dots, n \quad (3.3)$$

$$\Delta Q_i^{(r)} = Q_{isp} - Q_{i(cal)}^{(r)} \quad i = 2, 3, \dots, n \quad (3.4)$$

For PV buses, the exact value of  $Q_i$  is not specified, but its limits are known. If the calculated value of  $Q_i$  is within limits, only  $\Delta P_i$  is calculated. If the calculated value of  $Q_i$  is beyond the limits, then an appropriate limit is imposed and  $\Delta Q_i$  is also calculated by subtracting the calculated value of  $Q_i$  from the appropriate limit. The bus under consideration is now treated as a load (PQ) bus.

5. Compute the elements of the Jacobian matrix

$$\begin{bmatrix} \frac{\partial P}{\partial \delta} & \frac{\partial P}{\partial |v|} \\ \frac{\partial Q}{\partial \delta} & \frac{\partial Q}{\partial |v|} \end{bmatrix}$$

Using the estimated  $|V_i|$  and  $\delta_i$  from step 2.

$$6. \quad \begin{bmatrix} \Delta P \\ \Delta Q \end{bmatrix} = \begin{bmatrix} \frac{\partial P}{\partial \delta} & \frac{\partial P}{\partial |v|} \\ \frac{\partial Q}{\partial \delta} & \frac{\partial Q}{\partial |v|} \end{bmatrix} \begin{bmatrix} \Delta \delta \\ \Delta V \end{bmatrix}$$

(3.5)

7. Using the values of  $\Delta \delta_i$  and  $\Delta |V_i|$  calculated in step 6, modify the voltage magnitude and phase angle at all load buses by the equations.

$$|V_i^{(r+1)}| = |V_i^{(r)}| + \Delta |V_i^{(r)}| \quad (3.6)$$

$$\delta_i^{(r+1)} = \delta_i^{(r)} + \Delta \delta_i^{(r)} \quad (3.7)$$

8. Start the next iteration cycle at step 2 with these modified  $|V_i|$  and  $\delta_i$ .
9. Continue until scheduled errors  $\Delta P_i^{(r)}$  and  $\Delta Q_i^{(r)}$  for all load buses are within a specified tolerance, that is,

$$\Delta P_i^{(r)} < \varepsilon, \Delta Q_i^{(r)} < \varepsilon$$

10. where  $\varepsilon$  denotes the tolerance level for load buses.
11. Calculate line flows and power at the slack bus exactly in the same manner as in the GS method.

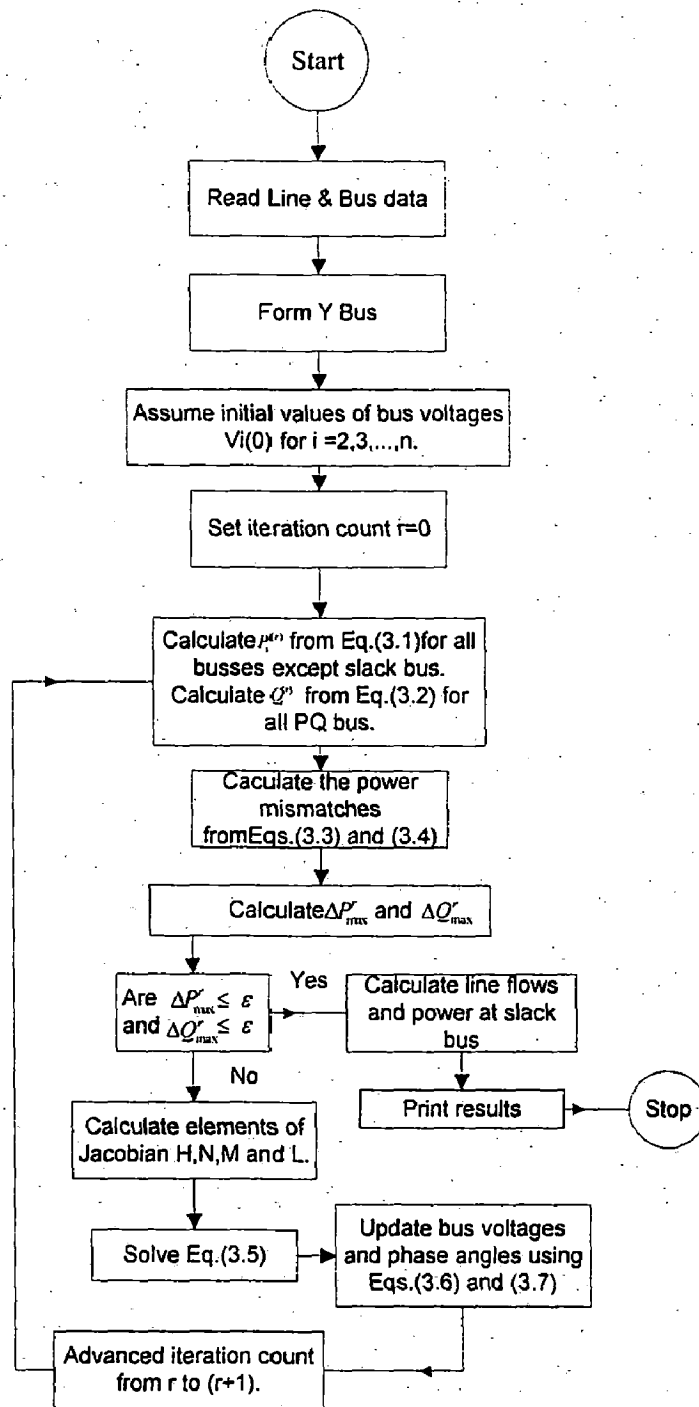


Figure: 3.1. Flowchart for Newton-Raphson method for load flow solution



### 3.4 LOAD FLOW RESULTS OBTAINED FOR IEEE 30 BUS TEST CASES

**Table: 3.1 Load flow Result for IEEE 30 Bus Data**

Bus. No	Bus Voltage (pu)	Bus phase angle (deg)	$P(P_G - P_L)$ (pu)	$Q(Q_G - Q_L)$ (pu)
1	1.0600	0.0	2.6099	-0.1711
2	1.0430	-5.4965	0.1830	0.3587
3	1.0217	-8.0054	-0.0240	-0.0120
4	1.0131	-9.6630	-0.0760	-0.0160
5	1.0100	-14.3799	-0.9420	0.1686
6	1.0123	-11.4010	-0.0000	0.0000
7	1.0036	-13.1506	-0.2280	-0.1090
8	1.0100	-12.1144	-0.3000	0.0019
9	1.0520	-14.4412	0.0000	0.0000
10	1.0464	-16.0310	-0.0580	-0.0200
11	1.0820	-14.4412	0.0000	0.1558
12	1.0580	-15.2876	-0.1120	-0.0750
13	1.0710	-15.2876	0.0000	0.0995
14	1.0433	-16.1765	-0.0620	-0.0160
15	1.0388	-16.2684	-0.0820	-0.0250
16	1.0459	-15.8752	-0.0350	-0.0180
17	1.0409	-16.1912	-0.0900	-0.0580
18	1.0293	-16.8778	-0.0320	-0.0090
19	1.0268	-17.0490	-0.0950	-0.0340
20	1.0309	-16.8518	-0.0220	-0.0070
21	1.0341	-16.4738	-0.1750	-0.1120
22	1.0346	-16.4600	-0.0000	-0.0000
23	1.0285	-16.6578	-0.0320	-0.0160
24	1.0233	-16.8332	-0.0870	-0.0670
25	1.0201	-16.4187	0.0000	0.0000
26	1.0024	-16.8361	-0.0350	-0.0230
27	1.0266	-15.9033	0.0000	0.0000
28	1.0110	-12.0597	-0.0000	-0.0000
29	1.0068	-17.1251	-0.0240	-0.0090
30	0.9954	-18.0018	-0.1060	-0.0190

Line No	From Bus	To Bus	Line flow from $i^{th}$ to $j^{th}$ Bus	Line flow from $j^{th}$ to $i^{th}$ Bus
1	1	2	1.7777 - 0.2066i	-1.7230 + 0.3410i
2	1	3	0.8322 + 0.0618i	-0.8042 + 0.0312i
3	2	4	0.4570 + 0.0359i	-0.4460 - 0.0216i
4	3	4	0.7802 - 0.0303i	-0.7725 + 0.0481i
5	2	5	0.8298 + 0.0284i	-0.7999 + 0.0754i
6	2	6	0.6192 - 0.0007i	-0.5987 + 0.0430i
7	4	6	0.7021 - 0.1733i	-0.6961 + 0.1897i
8	5	7	-0.1421 + 0.1091i	0.1436 - 0.1157i
9	6	7	0.3753 - 0.0134i	-0.3716 + 0.0161i
10	6	8	0.2952 - 0.0301i	-0.2941 + 0.0291i
11	6	9	0.2715 - 0.1864i	-0.2715 + 0.2084i
12	6	10	0.1538 - 0.0559i	-0.1538 + 0.0704i
13	9	11	-0.0000 - 0.1515i	0.0000 + 0.1558i
14	9	10	0.2777 + 0.0582i	-0.2777 - 0.0502i
15	4	12	0.4104 - 0.1577i	-0.4104 + 0.2059i
16	12	13	0.0000 - 0.0983i	-0.0000 + 0.0995i
17	12	14	0.0784 + 0.0238i	-0.0776 - 0.0222i
18	12	15	0.1782 + 0.0669i	-0.1761 - 0.0627i
19	12	16	0.0717 + 0.0307i	-0.0712 - 0.0296i
20	14	15	0.0156 + 0.0062i	-0.0156 - 0.0062i
21	16	17	0.0362 + 0.0116i	-0.0361 - 0.0114i
22	15	18	0.0598 + 0.0159i	-0.0594 - 0.0151i
23	18	19	0.0274 + 0.0061i	-0.0274 - 0.0060i
24	19	20	-0.0676 - 0.0280i	0.0678 + 0.0284i
25	10	20	0.0906 + 0.0372i	-0.0898 - 0.0354i
26	10	17	0.0541 + 0.0470i	-0.0539 - 0.0466i
27	10	21	0.1577 + 0.0990i	-0.1566 - 0.0967i
28	10	22	0.0760 + 0.0453i	-0.0755 - 0.0442i
29	21	22	-0.0184 - 0.0153i	0.0185 + 0.0153i
30	15	23	0.0498 + 0.0280i	-0.0495 - 0.0274i
31	22	24	0.0571 + 0.0289i	-0.0566 - 0.0282i
32	23	24	0.0175 + 0.0114i	-0.0175 - 0.0113i
33	24	25	-0.0129 + 0.0175i	0.0130 - 0.0174i
34	25	26	0.0354 + 0.0237i	-0.0350 - 0.0230i
35	25	27	-0.0484 - 0.0063i	0.0487 + 0.0068i
36	28	27	0.1757 - 0.0340i	-0.1757 + 0.0464i
37	27	29	0.0619 + 0.0167i	-0.0610 - 0.0151i
38	27	30	0.0709 + 0.0166i	-0.0693 - 0.0136i
39	29	30	0.0370 + 0.0061i	-0.0367 - 0.0054i
40	8	28	-0.0059 - 0.0140i	0.0059 - 0.0079i
41	6	28	0.1879 - 0.0634i	-0.1873 - 0.0010i

### **3.5 CONCLUSION**

In this chapter, need for the load flow has been discussed. A Newton-Raphson based algorithm has been applied to solve the load flow equations. Step by Step procedure for the above method has been given. It has been validated on IEEE 30 bus test case system and the results are displayed.

## Chapter-4

### OPTIMAL POWER FLOW

---

#### 4.1 INTRODUCTION

Optimal power flow (OPF) has been widely used in power system operation and planning. In deregulated environment of power sector, it is of increasing importance, for determination of electricity prices and also for congestion management. The OPF optimizes a power system operating objective function, while satisfying a set of system constraints:

Today any problem that involves the determination of the instantaneous optimal steady state of a power system is a OPF problem. The optimal steady state is obtained by adjusting the available controls to minimize an objective function subject to specified linear or nonlinear operating constraints. Many different solution approaches have been developed to solve the problem. Based on the optimization techniques applied, the classical OPF method may be classified into the following two main categories

- (i) Linear programming (LP) based methods
- (ii) Non-linear programming (NLP) based methods

*Linear programming* has been recognized for many years as a reliable and robust technique for solving a large subset of OPF problems with linearized relationship. LP based OPF methods have been widely used in solving active and reactive power OPF problems.

*Non-linear programming* methods based OPF methods are a class of methods with very wide range, which include the steepest descent method, Newton's method and quadratic programming methods.

In this chapter, well known basic classical technique gradient steepest descent method has been validated for the proposed approach. This method has been applied to IEEE-30 bus system and their results are displayed.

## 4.2 OPTIMAL POWER FLOW PROBLEM FORMULATION

Let the objective function to be minimized, is given below.

$$f = \sum_i F_i(Pg_i) \quad (4.1)$$

This is the sum of operating cost over all controllable power sources.

$F_i(Pg_i)$  = Generation cost function for  $Pg_i$  generation at bus i

The cost is optimized with the following constraints

The inequality constraint on real power generation at bus i

$$Pg_i^{\min} \leq Pg_i \leq Pg_i^{\max} \quad (4.2)$$

Where

$Pg_i^{\min}$  and  $Pg_i^{\max}$  are respectively minimum and maximum values of real power generation allowed at generator bus i.

The power flow equation of the power network

$$g(V, \phi) = 0 \quad (4.3)$$

Where

$$g(V, \phi) = \begin{cases} P_i(V, \phi) - P_i^{net} \\ Q_i(V, \phi) - Q_i^{net} \end{cases} \left. \vphantom{\begin{matrix} P_i(V, \phi) - P_i^{net} \\ Q_i(V, \phi) - Q_i^{net} \end{matrix}} \right\} \begin{array}{l} \text{For each PQ bus } i \\ \text{For each PV bus } m, \text{ not} \\ \text{including the ref. bus,} \end{array} \quad (4.4)$$

Where;

$P_i$  and  $Q_i$  are respectively calculated real and reactive power for PQ bus i.

$P_i^{net}$  and  $Q_i^{net}$  are respectively specified real and reactive power for PQ bus i.

$P_m$  and  $P_m^{net}$  are respectively calculated and specified real power for PV bus m.

$V$  and  $\phi$  are voltage magnitude and phase angles at different buses.

The inequality constraint on reactive power generation  $Qg_i$  at each PV bus

$$Qg_i^{\min} \leq Qg_i \leq Qg_i^{\max} \quad (4.5)$$

where  $Qg_i^{\min}$  and  $Qg_i^{\max}$  are respectively minimum and maximum value of reactive power at PV bus  $i$ .

### 4.3 STEEPEST DESCENT METHOD

This is the most basic classical optimization method. The main features of this method are gradient procedure for finding the optimum and use of penalty functions to handle functional inequality constraints. This method provides bus increment cost directly, which is quite useful for cost analysis of power system under deregulated environment.

Let the objective be

$$\text{Min } f(x, u) \quad (4.6)$$

Subject to equality constraints corresponding to power flow equations

$$[g(x, u, p)] = 0 \quad (4.7)$$

where

$x$  = unknown or state vector (such as voltage magnitude and its angle at load bus, voltage angle at PV bus).

$u$  = constant parameters or independent variables (such as generator output and generator bus voltage).

$p$  = fixed parameters (such as real and reactive power at load buses).

This is equivalent to minimization of unconstrained Lagrangian function

$$L(x, u, p) = f(x, u) + [\lambda]^T \cdot [g(x, u, p)] \quad (4.8)$$

The  $\lambda$ , in  $[\lambda]$  are called Lagrangian multipliers

From above equation (4.8) follows the set of necessary conditions for a minimum:

$$\left[ \frac{\partial L}{\partial x} \right] = \left[ \frac{\partial f}{\partial x} \right] + \left[ \frac{\partial g}{\partial x} \right]^T [\lambda] = 0 \quad (4.9)$$

$$\left[ \frac{\partial L}{\partial u} \right] = \left[ \frac{\partial f}{\partial u} \right] + \left[ \frac{\partial g}{\partial u} \right]^T [\lambda] = 0 \quad (4.10)$$

$$\left[ \frac{\partial L}{\partial \lambda} \right] = [g(x, u, p)] = 0 \quad (4.11)$$

Equations (4.9) (4.10) and (4.11) are non-linear algebraic equations and can only be solved by iterations. A simple yet efficient iteration scheme that can be employed is the steepest descent method. The basic technique is to adjust the control vector  $u$ , so as to move from one feasible solution point, in the direction of steepest descent (negative gradient) to a new feasible solution point with a lower value of objective function. By repeating these moves in the direction of negative gradient, the minimum will finally be reached.

#### 4.3.1. Inequality Constraints on control variables

Let the control variable  $u$  (such as  $Pg_i$ , voltage magnitude at PV buses, tap ratio for the tap setting transformers) has its minimum and maximum constraints.

$$u_{\min} \leq u \leq u_{\max} \quad (4.12)$$

If during optimization the correction  $\Delta u_i$  causes  $u_i$  to exceed one of limits,  $u_i$  is set equal to the corresponding limit.

$$u_{i \text{ new}} = \begin{cases} u_{i \text{ max}} & \text{if } u_{i \text{ old}} + \Delta u_i > u_{i \text{ max}} \\ u_{i \text{ min}} & \text{if } u_{i \text{ old}} + \Delta u_i < u_{i \text{ min}} \\ u_{i \text{ old}} + \Delta u_i & \text{otherwise} \end{cases} \quad (4.13)$$

In accordance with Kuhn-Tucker theorem, the necessary conditions for minimization of  $L$  under constraint are:

$$\left. \begin{cases} \frac{\partial L}{\partial u_i} = 0 & \text{if } u_{i \text{ min}} < u_i < u_{i \text{ max}} \\ \frac{\partial L}{\partial u_i} \leq 0 & \text{if } u_i = u_{i \text{ max}} \\ \frac{\partial L}{\partial u_i} \geq 0 & \text{if } u_i = u_{i \text{ min}} \end{cases} \right\} \quad (4.14)$$

#### 4.3.2 Inequality Constraints on the Dependent Variables

The upper and lower limit on dependent variables such as voltage  $V$  at P-Q buses, MVA limit on transmission lines.

$$x_{\min} \leq x \leq x_{\max} \quad (4.15)$$

Such inequality constraints are handled by the penalty function method.

The penalty method calls for augmentation of the objective function so that the new objective function becomes

$$f' = f(x, u) + \sum_j W_j \quad (4.16)$$

Where the penalty  $W_j$  is introduced for each violated inequality constraint. A suitable penalty function is defined as

$$W_j = \eta_j (x_j - x_{j,\max})^2 \quad \text{whenever } x_j > x_{j,\max} \quad (4.17)$$

$$W_j = \eta_j (x_j - x_{j,\min})^2 \quad \text{whenever } x_j < x_{j,\min}$$

Where  $\eta_j$  is penalty factor for violated inequality constraint  $j$ .

The necessary conditions (2.12) and (2.13) would now be modified as given below, while the condition (2.14), i.e. power flow equation, remain unchanged.

$$\left[ \frac{\partial L}{\partial x} \right] = \left[ \frac{\partial f}{\partial x} \right] + \left[ \sum_j \frac{\partial W_j}{\partial x} \right] + \left[ \frac{\partial g}{\partial x} \right]^T [\lambda] = 0 \quad (4.18)$$

$$\left[ \frac{\partial L}{\partial u} \right] = \left[ \frac{\partial f}{\partial u} \right] + \left[ \sum_j \frac{\partial W_j}{\partial u} \right] + \left[ \frac{\partial g}{\partial u} \right]^T [\lambda] = 0 \quad (4.19)$$

This section has shown that Newton- Raphson method of power flow can be extended to yield the optimal load flow solution that is feasible with respect to all relevant inequality constraints.

#### 4.3.3. Step by Step Procedure for SD –OPF method

The computational procedure for the steepest descent based optimal power flow (SD-OPF) method with relevant details is given below:

Step 1. Make an initial guess for  $u$ , the control variables.

Step 2. Find a feasible power flow solution by Newton-Raphson method. This yields the Jacobian matrix  $J$  for the solution point of  $x$ .

Step 3. Solve (4.9) for  $[\lambda]$  after replacing function  $f$  by  $f'$  as per equation (4.16), in order to include inequality constraints on dependent variables.

$$[\lambda] = - \left( \left[ \frac{\partial g}{\partial x} \right]^T \right)^{-1} * \left[ \frac{\partial f'}{\partial x} \right] \quad (4.20)$$



Step 4. Insert  $[\lambda]$  form (4.20) into (4.10) after replacing  $f$  by  $f'$  as per equation (4.16) and compute the gradient

$$[\nabla L] = \left[ \frac{\partial f'}{\partial u} \right] + \left[ \frac{\partial g}{\partial u} \right]^T * [\lambda] \quad (4.21)$$

Step 5. If  $\nabla L$  is within prescribed tolerance as per equation (4.14), the minimum has been reached, otherwise go to next step.

Step 6. Find a new set of control variables

$$u_{new} = u_{old} + \Delta u \quad (4.22)$$

$$\text{where } \Delta u = -\delta * [\nabla L] \quad (4.23)$$

Return to step. 2

Here  $\Delta u$  is a step in the negative direction of the gradient. The step size is adjusted by the positive scalar  $\delta$ .

#### 4.3.4 Simulation Results

The above explained algorithm for OPF is applied to IEEE-30 bus test system whose data has been given in Appendix-A. For this analysis the quadratic cost characteristic of generators has been taken as per following equation.

$$F_i(Pg_i) = a + b * Pg_i + c * Pg_i^2 \quad (4.24)$$

Where the values of cost coefficients has been given in Appendix-A. the simulation results are given in table 4.1

**Table 4.1 Simulation results of SD-OPF**

Generator	Bus Number	Power Generation (MW)
G1	1(Reference)	176.3177
G2	2	48.7980
G3	5	21.5015
G4	8	22.3196
G5	11	12.2708
G6	13	12.0000
Total Generation Cost		803.5495 \$/hr

**Table 4.2: Load flow Results of SD-OPF**

Bus. No	Bus Voltage (pu)	Bus phase angle (deg)	$P(P_G - P_L)$ (pu)	$Q(Q_G - Q_L)$ (pu)
1	1.0600	0	1.7632	-0.0137
2	1.0430	-3.5528	0.2710	0.1647
3	1.0256	-5.4981	-0.0240	-0.0120
4	1.0174	-6.6033	-0.0760	-0.0160
5	1.0100	-10.2494	-0.7270	0.0702
6	1.0150	-7.7388	0.0000	0.0000
7	1.0052	-9.2964	-0.2280	-0.1090
8	1.0100	-7.9103	-0.0768	-0.1416
9	1.0541	-9.7724	0.0000	0.0000
10	1.0489	-11.5361	-0.0580	-0.0200
11	1.0820	-8.4901	0.1227	0.1466
12	1.0606	-10.7465	-0.1120	-0.0750
13	1.0710	-9.8991	0.1200	0.0804
14	1.0459	-11.6454	-0.0620	-0.0160
15	1.0413	-11.7511	-0.0820	-0.0250
16	1.0484	-11.3520	-0.0350	-0.0180
17	1.0434	-11.6867	-0.0900	-0.0580
18	1.0319	-12.3650	-0.0320	-0.0090
19	1.0294	-12.5398	-0.0950	-0.0340
20	1.0335	-12.3459	-0.0220	-0.0070
21	1.0366	-11.9941	-0.1750	-0.1120
22	1.0371	-11.9859	-0.0000	0.0000
23	1.0310	-12.1888	-0.0320	-0.0160
24	1.0256	-12.4315	-0.0870	-0.0670
25	1.0217	-12.2376	-0.0000	0.0000
26	1.0041	-12.6536	-0.0350	-0.0230
27	1.0278	-11.8601	0.0000	0.0000
28	1.0131	-8.2451	-0.0000	0.0000
29	1.0080	-13.0789	-0.0240	-0.0090
30	0.9966	-13.9536	-0.1060	-0.0190

Line No	From Bus	To Bus	Line flow from $i^{\text{th}}$ to $j^{\text{th}}$ Bus	Line flow from $j^{\text{th}}$ to $i^{\text{th}}$ Bus
1	1	2	1.1772 - 0.0576i	-1.1535 + 0.0994i
2	1	3	0.5824 + 0.0701i	-0.5684 - 0.0353i
3	2	4	0.3416 + 0.0403i	-0.3354 - 0.0408i
4	3	4	0.5444 + 0.0363i	-0.5407 - 0.0299i
5	2	5	0.6335 + 0.0477i	-0.6160 + 0.0041i
6	2	6	0.4494 + 0.0233i	-0.4385 - 0.0102i
7	4	6	0.4733 - 0.0753i	-0.4707 + 0.0799i
8	5	7	-0.1110 + 0.0819i	0.1119 - 0.0900i
9	6	7	0.3430 + 0.0103i	-0.3399 - 0.0096i
10	6	8	0.0996 + 0.0907i	-0.0994 - 0.0946i
11	6	9	0.1825 - 0.1873i	-0.1825 + 0.2011i
12	6	10	0.1268 - 0.0576i	-0.1268 + 0.0681i
13	9	11	-0.1227 - 0.1401i	0.1227 + 0.1466i
14	9	10	0.3093 + 0.0546i	-0.3093 - 0.0449i
15	4	12	0.3045 - 0.1607i	-0.3045 + 0.1900i
16	12	13	-0.1200 - 0.0779i	0.1200 + 0.0804i
17	12	14	0.0793 + 0.0234i	-0.0785 - 0.0218i
18	12	15	0.1820 + 0.0660i	-0.1798 - 0.0616i
19	12	16	0.0735 + 0.0302i	-0.0730 - 0.0291i
20	14	15	0.0165 + 0.0058i	-0.0164 - 0.0058i
21	16	17	0.0380 + 0.0111i	-0.0379 - 0.0109i
22	15	18	0.0604 + 0.0156i	-0.0600 - 0.0148i
23	18	19	0.0280 + 0.0058i	-0.0279 - 0.0057i
24	19	20	-0.0671 - 0.0283i	0.0672 + 0.0286i
25	10	20	0.0901 + 0.0374i	-0.0892 - 0.0356i
26	10	17	0.0523 + 0.0475i	-0.0521 - 0.0471i
27	10	21	0.1614 + 0.0977i	-0.1603 - 0.0952i
28	10	22	0.0785 + 0.0444i	-0.0780 - 0.0433i
29	21	22	-0.0147 - 0.0168i	0.0147 + 0.0168i
30	15	23	0.0538 + 0.0268i	-0.0535 - 0.0261i
31	22	24	0.0632 + 0.0265i	-0.0627 - 0.0257i
32	23	24	0.0215 + 0.0101i	-0.0214 - 0.0099i
33	24	25	-0.0028 + 0.0139i	0.0029 - 0.0138i
34	25	26	0.0354 + 0.0237i	-0.0350 - 0.0230i
35	25	27	-0.0383 - 0.0099i	0.0385 + 0.0102i
36	28	27	0.1658 - 0.0323i	-0.1658 + 0.0433i
37	27	29	0.0619 + 0.0167i	-0.0610 - 0.0151i
38	27	30	0.0709 + 0.0166i	-0.0693 - 0.0136i
39	29	30	0.0370 + 0.0061i	-0.0367 - 0.0054i
40	8	28	0.0226 - 0.0338i	-0.0226 + 0.0121i
41	6	28	0.1491 - 0.0426i	-0.1487 - 0.0229i

#### **4.4 CONCLUSION**

In this chapter many classical methods to OPF have been given. A well known basic classical technique, Steepest Descent has been discussed. Steepest Descent Based OPF Algorithm has been developed and applied to IEEE-30 bus test system and their results are displayed.

## Chapter-5

# EVOLUTIONARY PROGRAMMING BASED OPTIMAL POWER FLOW

---

### 5.1 INTRODUCTION

In general, OPF problem is a large dimension non-linear, non-convex and highly constrained optimization problem. It is non-convex due to existence of nonlinear AC power flow equality constraints, non-convex unit operating cost functions and units with prohibited operating zones. This non-convexity is further increased when valve point loading effects of the thermal generators have to be included in the network.

Classical techniques suffer from the difficulty in handling inequality constraints. Moreover these techniques rely on convexity to obtain the global optimum solution and as such are forced to simplify relationships in order to ensure convexity. These techniques are not guaranteed to converge to the global optimum of the general non-convex OPF problem. These days, genetic algorithm (GA) and evolutionary programming techniques has been suggested to overcome the above mentioned difficulties of classical methods.

In this work, an evolutionary programming approach has been used to solve OPF for the proposed model. In this chapter, EP based OPF has been applied to IEEE-30 bus test system and the results are compared with steepest descent method based OPF.

Evolutionary programming, search for the optimal solution by evolving a population of candidate solutions, over a number of generations or iterations. The evolution of solution is carried out through mutation and competitive selection.

#### 5.1.1 Difference between Evolutionary programming and other traditional methods

In order for EPs to surpass the traditional methods in the quest for robustness, EPs must differ in some very fundamental ways. EPs are different from more normal optimization and research procedures in four ways:

(1) **EP search from a population of points, not a single point.** The population can move over hills and across valleys. EP can therefore discover a globally or near globally optimal point. Because each individual in the population is computed independently, EP has inherent parallel computation ability.

(2) **EP use payoff (fitness or objective functions) information** directly for the search direction, neither derivatives nor other auxiliary knowledge. EP therefore can deal with non smooth, non continuous and non differentiable functions that are the real-life optimization problem. This property also relieves EP is of the approximate assumptions for many practical optimization problems, which are quite often required in traditional optimization methods.

(3) **EP use probabilistic transition rules** to select generations, not deterministic rules, so they are a kind of stochastic optimization algorithm which can search a complicated and uncertain area to find the global optimum. EP is more flexible and robust than conventional methods.

These features make EP robust and parallel algorithm which can adaptively search the globally optimal point. EP offer new tools for the optimization of complex system problems.

### **5.1.2 Difference between Evolutionary programming and Genetic Algorithm**

EP is different from GA in the following respects:

(1) EP uses the control parameters, not their codings; the generation selection procedure of EP is mutation and competition, not reproduction, mutation and crossover.

(2) GA emphasis models of genetic operators, while EP emphasis mutational transformations that maintain behavioral linkage.

### **5.1.3 Evolutionary Programming Operation**

While applying a Evolutionary programming for any optimization problem, the following steps are usually followed:

### 1. *Initial population:*

The initial population of control variables is selected randomly from the set of uniformly distributed control variables ranging over their upper and lower limits. The fitness score  $f_i$  is obtained according to the objective function.

### 2. *Fitness function:*

The next step is to specify a function that can assign a score to any possible solution or structure. The score is a numerical value that indicates how well the particular solution solves the problem. Using a biological metaphor, the score is the fitness of the individual solution. It represents how well the individual adapts to the environment. In case of optimization, the environment is the search space. The task of the GA is to discover solutions that have fitness values among the set of all possible solutions

### 3. *Mutation:*

Each selected parent, for example  $P_i$ , is mutated and added to its population following the rule:

$$P_{i+m,j} = P_{i,j} + N(0, \sigma^2), \quad j=1, 2, \dots, n,$$

$N(\mu, \sigma^2)$  Represents a Gaussian random variable with mean  $\mu$  and variance  $\sigma^2$ .

If any mutated value exceeds its limit, it will be given the limit value. The mutation process allows an individual with larger fitness to produce more offspring for the next generation.

### 4. *Competition:*

Several individuals which have the best fitness are kept as the parents for the next generation. Other individual in the combined population have to compete with each other to get their chances for the next generation

### 5. *Convergence test:*

If the convergence condition is not met, the mutation and the competition processes will run again. The maximum generation number can be used for convergence

condition. If the convergence has reached a given accuracy, an optimal solution has been found for an optimization problem.

The schematic diagram is shown in figure 5.1. The major steps involved in the EP approach are explained as follows.

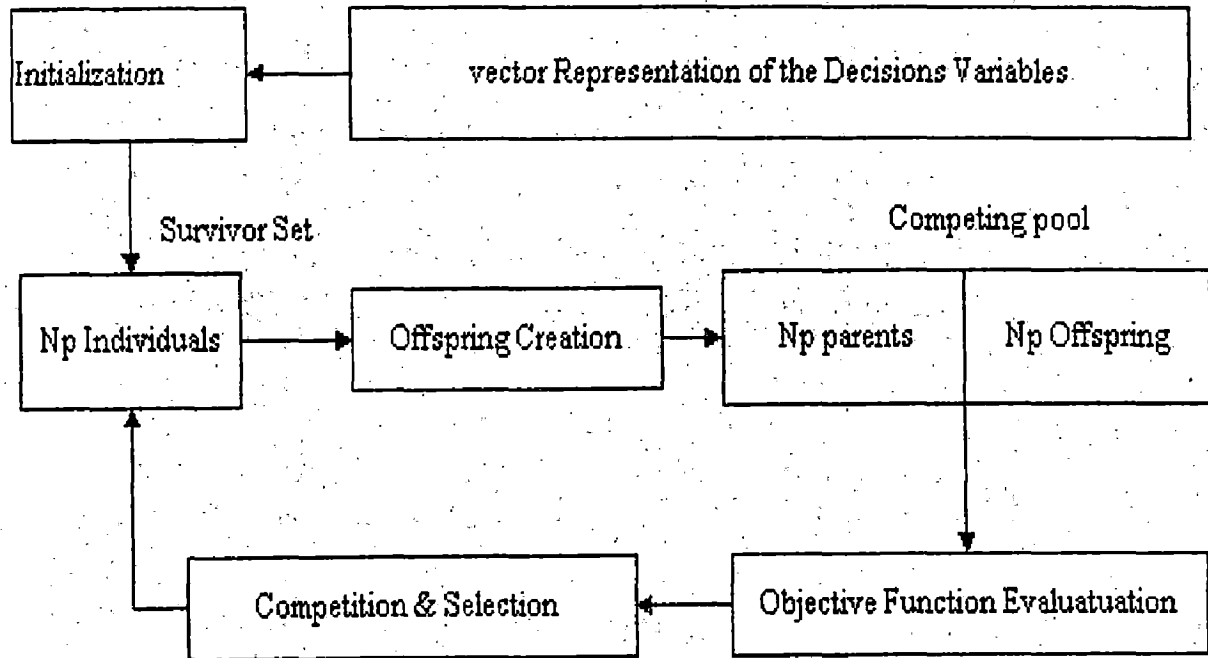


**Figure 5.1 Schematic diagram of EP**



## 5.2 STEP BY STEP ALGORITHM OF EVOLUTIONARY PROGRAMMING BASED OPF

1. Prepare the database for the system including line data, bus data, generator data and tap setting of the transformers. Line data includes the information of the lines such as resistance, reactance and shunt admittance. Bus data includes the information of the generators, loads connected at each and every bus.
2. Generate parent vector population for power generated by the generators.
3. Formation of Y bus using line resistance, reactance, shunt elements, tap changing ratio
4. Assume suitable values of voltage magnitude at all the buses excluding swing bus and its angle for all the buses, also set the error for calculated active and reactive power.
5. Calculate the real and reactive power using the formula for all buses.

$$P_i = \sum_{j \in N} |V_i| |V_j| Y_{ij} \cos(\theta_{ij} + \delta_j - \delta_i)$$

$$Q_i = \sum_{j \in N} |V_i| |V_j| Y_{ij} \sin(\theta_{ij} + \delta_j - \delta_i)$$

6. Calculate error for real and reactive power between specified and calculated for load buses and only real power for voltage control buses. If it is within tolerable limit go to step no: 10 else continue the next steps.
7. Calculate Jacobian matrix using the formula

$$J = \begin{pmatrix} \frac{\partial P}{\partial \delta} & \frac{\partial P}{\partial |V|} \\ \frac{\partial Q}{\partial \delta} & \frac{\partial Q}{\partial |V|} \end{pmatrix}$$

8. Calculate voltage magnitude and angle increment using formula (except reference bus)

$$\begin{pmatrix} \Delta \theta \\ \Delta |V| \end{pmatrix} = [J]^{-1} \begin{pmatrix} \Delta P \\ \Delta Q \end{pmatrix}$$

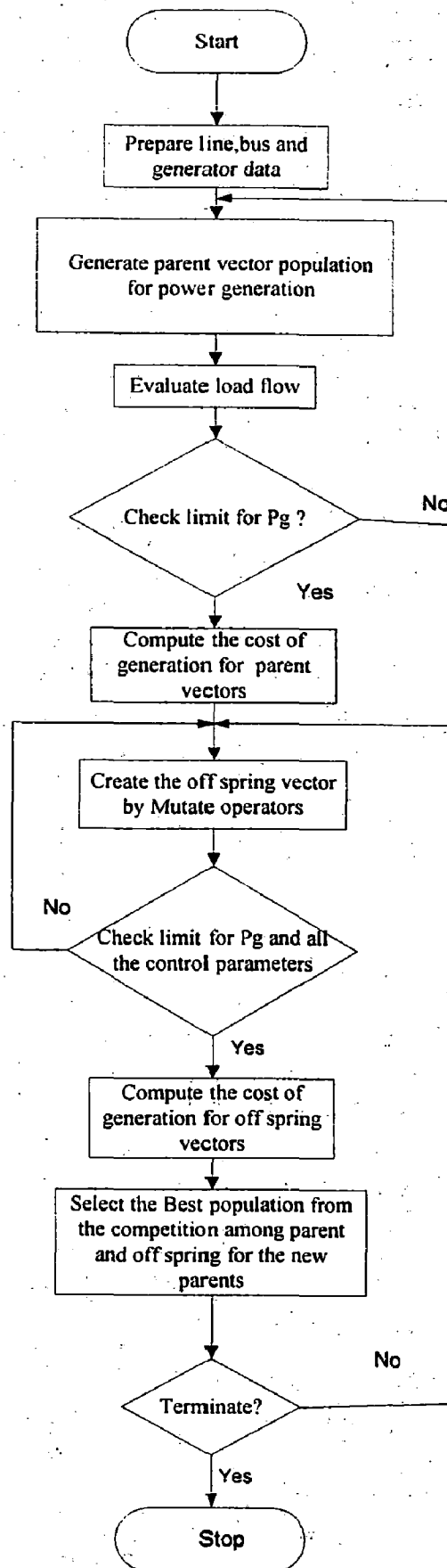


**Figure 5.2 Flowchart of EP-OPF**

9. Calculate new bus magnitude and its angle on all buses (except reference bus)

$$V_{new} = V_{old} + \Delta V$$

$$\theta_{new} = \theta_{old} + \Delta \theta$$

10. Go to step no: 5

11. Compute the total cost of generation for all the generators

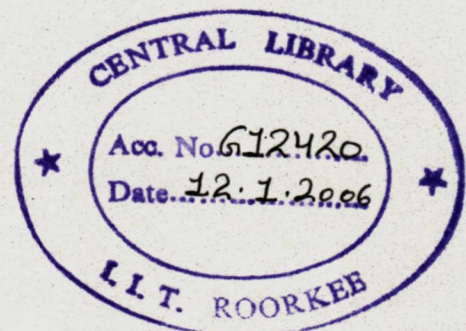
12. Create off spring vector for all the control variables by adding Gaussian random variable to it.

13. Check for the limits for the off spring vector. If it violates go to step 12

14. Compute the total cost of generations.

15. If the convergence condition satisfied go to next step else go to step:12

16. Find the optimal solution among all population groups.



### 5.3 SIMULATION RESULTS

This EP-OPF algorithm is applied to IEEE-30 bus test system whose data has been given in Appendix-A. EP parameters as shown in table 5.1 have been taken for this analysis. The convergence of this algorithm is shown in figure 5.3.

**Table 5.1 EP parameters**

S.No	EP Parameter	Value
1	Population Size	10
2	Maximum generation	30

The simulation results are given in the following table

**Table 5.2 Simulation results of EP based OPF**

Generator	Bus Number	Power Generation (MW)
G1	1(Reference)	166.6512
G2	2	49.5479
G3	5	23.0744
G4	8	27.6360
G5	11	10.5680
G6	13	14.6984
Total Generation Cost		803.8613\$/hr.

**Table 5.3: Load flow results for EP-OPF**

Bus. No	Bus Voltage (pu)	Bus phase angle (deg)	$P(P_G - P_L)$ (pu)	$Q(Q_G - Q_L)$ (pu)
1	1.0600	0	1.6665	0.0058
2	1.0430	-3.3443	0.2785	0.1483
3	1.0260	-5.2063	-0.0240	-0.0120
4	1.0178	-6.2475	-0.0760	-0.0160
5	1.0100	-9.8391	-0.7113	0.0637
6	1.0152	-7.3145	-0.0000	-0.0000
7	1.0053	-8.8778	-0.2280	-0.1090
8	1.0100	-7.3671	-0.0236	-0.1611
9	1.0541	-9.4145	0.0000	-0.0000
10	1.0487	-11.1162	-0.0580	-0.0200
11	1.0820	-8.3101	0.1057	0.1464
12	1.0610	-10.1844	-0.1120	-0.0750
13	1.0710	-9.1468	0.1470	0.0778
14	1.0463	-11.0997	-0.0620	-0.0160
15	1.0415	-11.2217	-0.0820	-0.0250
16	1.0486	-10.8491	-0.0350	-0.0180
17	1.0433	-11.2417	-0.0900	-0.0580
18	1.0319	-11.8739	-0.0320	-0.0090
19	1.0294	-12.0718	-0.0950	-0.0340
20	1.0334	-11.8900	-0.0220	-0.0070
21	1.0364	-11.5677	-0.1750	-0.1120
22	1.0370	-11.5575	0.0000	0.0000
23	1.0311	-11.6904	-0.0320	-0.0160
24	1.0256	-11.9752	-0.0870	-0.0670
25	1.0217	-11.7833	-0.0000	-0.0000
26	1.0041	-12.1993	-0.0350	-0.0230
27	1.0279	-11.4070	0.0000	0.0000
28	1.0132	-7.7934	0.0000	0.0000
29	1.0081	-12.6257	-0.0240	-0.0090
30	0.9967	-13.5002	-0.1060	-0.0190

Line No	From Bus	To Bus	Line flow from $i^{th}$ to $j^{th}$ Bus	Line flow from $j^{th}$ to $i^{th}$ Bus
1	1	2	1.1131 - 0.0404i	-1.0919 + 0.0746i
2	1	3	0.5533 + 0.0725i	-0.5407 - 0.0430i
3	2	4	0.3266 + 0.0420i	-0.3209 - 0.0441i
4	3	4	0.5167 + 0.0440i	-0.5134 - 0.0387i
5	2	5	0.6155 + 0.0498i	-0.5989 - 0.0021i
6	2	6	0.4283 + 0.0277i	-0.4184 - 0.0176i
7	4	6	0.4475 - 0.0623i	-0.4452 + 0.0658i
8	5	7	-0.1124 + 0.0817i	0.1133 - 0.0898i
9	6	7	0.3444 + 0.0106i	-0.3413 - 0.0098i
10	6	8	0.0537 + 0.1073i	-0.0536 - 0.1113i
11	6	9	0.1885 - 0.1863i	-0.1885 + 0.2005i
12	6	10	0.1270 - 0.0570i	-0.1270 + 0.0674i
13	9	11	-0.1057 - 0.1406i	0.1057 + 0.1464i
14	9	10	0.2984 + 0.0558i	-0.2984 - 0.0467i
15	4	12	-0.2896 - 0.1618i	-0.2896 + 0.1890i
16	12	13	-0.1470 - 0.0745i	0.1470 + 0.0778i
17	12	14	0.0804 + 0.0230i	-0.0796 - 0.0214i
18	12	15	0.1865 + 0.0652i	-0.1842 - 0.0606i
19	12	16	0.0789 + 0.0293i	-0.0783 - 0.0281i
20	14	15	0.0176 + 0.0054i	-0.0175 - 0.0053i
21	16	17	0.0433 + 0.0101i	-0.0431 - 0.0097i
22	15	18	0.0633 + 0.0149i	-0.0629 - 0.0141i
23	18	19	0.0309 + 0.0051i	-0.0309 - 0.0050i
24	19	20	-0.0641 - 0.0290i	0.0643 + 0.0294i
25	10	20	0.0871 + 0.0381i	-0.0863 - 0.0364i
26	10	17	0.0470 + 0.0486i	-0.0469 - 0.0483i
27	10	21	0.1599 + 0.0980i	-0.1588 - 0.0956i
28	10	22	0.0775 + 0.0446i	-0.0770 - 0.0435i
29	21	22	-0.0162 - 0.0164i	0.0162 + 0.0164i
30	15	23	0.0564 + 0.0260i	-0.0560 - 0.0253i
31	22	24	0.0607 + 0.0271i	-0.0603 - 0.0264i
32	23	24	0.0240 + 0.0093i	-0.0239 - 0.0092i
33	24	25	-0.0028 + 0.0137i	0.0028 - 0.0137i
34	25	26	0.0354 + 0.0237i	-0.0350 - 0.0230i
35	25	27	-0.0383 - 0.0100i	0.0384 + 0.0103i
36	28	27	0.1658 - 0.0322i	-0.1658 + 0.0432i
37	27	29	0.0619 + 0.0167i	-0.0610 - 0.0151i
38	27	30	0.0709 + 0.0166i	-0.0693 - 0.0136i
39	29	30	0.0370 + 0.0061i	-0.0367 - 0.0054i
40	8	28	0.0299 - 0.0365i	-0.0298 + 0.0150i
41	6	28	0.1417 - 0.0398i	-0.1414 - 0.0259i

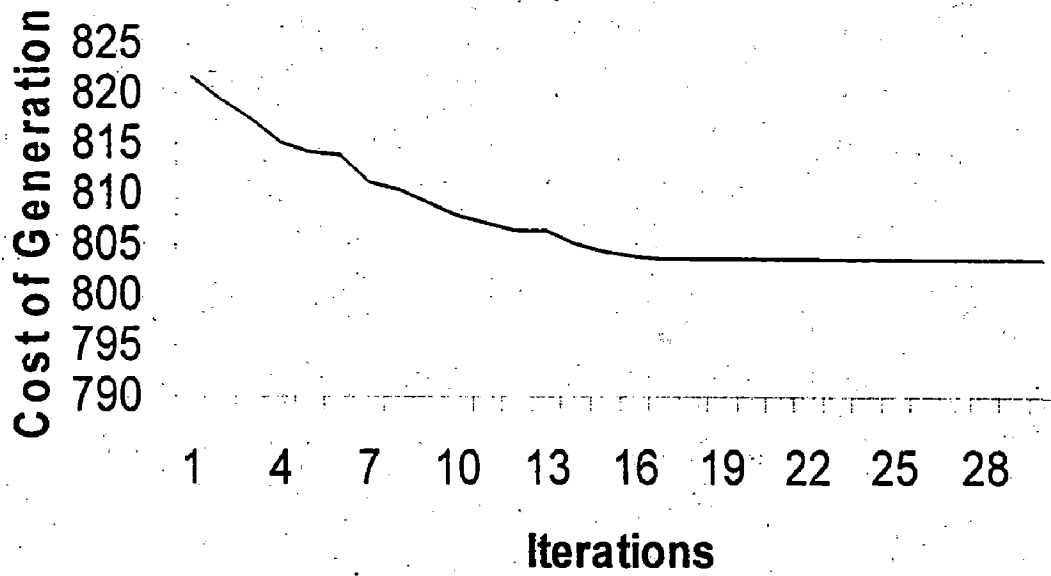


**Figure 5.3 Convergence of EP-OPF (Cost of Generation)**

#### 5.4 COMPARISON OF RESULTS

Comparison of the optimum solution for the above two methods has been given in the table 5.4. These methods are applied to same IEEE 30-bus test system.

**Table 5.4 Comparison of OPF methods**

S.No	Approach	Minimum generation cost
1	Steepest Descent-OPF	803.549568 \$/hr
2	EP-OPF	803.8613\$/hr

## 5.5 CONCLUSION

In this paper EP based OPF algorithm has been validated with classical gradient method. It has been observed that optimal solution obtained by EP-OPF is very close to that obtained by classical methods. The main advantage of the EP solution to the OPF problem is its modeling flexibility: nonconvex unit cost functions, prohibited unit operating zones and complex and non-linear constraints can be easily modeled. With a non-monotonic solution surface, classical methods are highly sensitive to starting points and frequently converge to local optimal solution or diverge altogether. EP based OPF algorithm has accurately and reliably converged to the global optimum solutions.

The developed EP-OPF algorithm provides a sound basis on which an EP-OPF algorithm with the power control functions of FACTS devices incorporated can be developed for the proposed model.



## Chapter-6

# EVOLUTIONARY PROGRAMMING BASED OPTIMAL POWERFLOW INCORPORATING MULTI TYPE FACTS DEVICES

---

### 6.1 BASIC OUTLINE

This work proposes an application of Evolutionary Programming to Optimal Power Flow incorporating Multi-Type FACTS Devices. EP is a search algorithm based on the simulated evolutionary process of natural selection and natural genetics. EAs are randomized search algorithms, which, however, do not necessarily mean directionless random walk.

Non-convexity of the nonlinear AC power flow equality constraints is increased when FACTS devices have to be included in the network. So, an evolutionary programming approach has been used to solve OPF incorporating Multi Type FACTS devices

The objective function is built in order to panelize the configuration of FACTS, leading to overloaded transmission lines and over or under voltages at busses. Only technical benefits of the FACTS controller are taken into account. Other criteria such as costs of installing and maintaining devices are not taken into consideration at this stage of work,

### 6.2 STEP BY STEP ALGORITHM OF EVOLUTIONARY PROGRAMMING BASED OPF

1. Prepare the database for the system including line data, bus data, generator data and tap setting of the transformers. Line data includes the information of the lines such as resistance, reactance and shunt admittance. Bus data includes the information of the generators, loads connected at each and every bus.
2. Generate parent vector population for power generated by the generators.

3. Formation of Y bus using line resistance, reactance, shunt elements, tap changing ratio
4. Assume suitable values of voltage magnitude at all the buses excluding swing bus and its angle for all the buses, also set the error for calculated active and reactive power.
5. Calculate the real and reactive power using the formula for all buses.

$$i. P_i = \sum_{j \in N} |V_i| |V_j| Y_{ij} \cos(\theta_j + \delta_j - \delta_i)$$

$$Q_i = \sum_{j \in N} |V_i| |V_j| Y_{ij} \sin(\theta_j + \delta_j - \delta_i)$$

6. Calculate error for real and reactive power between specified and calculated for load buses and only real power for voltage control buses. If it is within tolerable limit go to step no: 10 else continue the next steps.
7. Calculate Jacobian matrix using formula

$$J = \begin{pmatrix} \frac{\partial P}{\partial \delta} & \frac{\partial P}{\partial |V|} \\ \frac{\partial Q}{\partial \delta} & \frac{\partial Q}{\partial |V|} \end{pmatrix}$$

8. Calculate voltage magnitude and angle increment using formula (except reference bus)

$$\begin{pmatrix} \Delta \theta \\ \Delta |V| \end{pmatrix} = [J]^{-1} \begin{pmatrix} \Delta P \\ \Delta Q \end{pmatrix}$$

9. Calculate new bus magnitude and its angle on all buses (except reference bus)

$$V_{new} = V_{old} + \Delta V$$

$$\theta_{new} = \theta_{old} + \Delta \theta$$

10. Go to step no: 5

11. Compute the total cost of generation for all the generators

12. Create off spring vector for all the control variables by adding Gaussian random variable to it.
13. Check for the limits for the off spring vector. If it violates go to step 12
14. Compute the total cost of generations.
15. If the convergence condition satisfied go to next step else go to step:12
16. Find the optimal solution among all population groups.
17. Input the location for the FACTS devices such as TCSC, SVC and UPFC.
18. Set the firing angle for TCSC to increase the real power flow in the line
19. Set the voltage profile foe SVC to increase the voltage profile of the bus.
20. Set the series injected voltage and angle and shunt reactive current to increase the real and reactive power in the line independently and voltage profile.
21. Run the NR power flow for the optimal solution obtained using EP, incorporating FACTS devices.
22. Print the results.

### **6.3 OBSERVED RESULTS.**

The proposed model as explained in section 6.2 has been implemented on IEEE 30 bus system. The results obtained have been found satisfactory. The IEEE 30 bus test case system data was given in appendix A. the index of different cases done in this work is listed in table 6.1. A Newton – Raphson load flow solution of IEEE 30 bus system are tabulated in table 3.1.

EP based OPF without FACTS devices as also been solved and optimal solutions are tabulated in table 5.2 to compare with results obtained from EP based OPF with FACTS devices.

Objective function taken from equation 4.1 is solved by locating multi type multiple FACTS devices in the line. In this approach EP based OPF incorporating FACTS devices such as TCSC, SVC, and UPFC as shown in figure 6.1 is implemented.

Here we can observe that EP based OPF with multi type multiple FACTS devices give better power flow and voltage control over the EP based OPF without FACTS devices.

It has been observed in table 6.2 that objective attained (to minimize the Cost of generation) by EP-OPF incorporating Multi type FACTS devices is very Close to that obtained by EP-OPF and it has better control over the power flow.

**Table 6.1 – Index for the cases done in this work.**

EP-OPF with One TCSC	Case I
EP-OPF with One SVC	Case II
EP-OPF with One UPFC	Case III
EP-OPF with Two TCSC	Case IV
EP-OPF with Two SVC	Case V
EP-OPF with Two UPFC	Case VI
EP-OPF with TCSC and SVC	Case VII
EP-OPF with TCSC and UPFC	Case VIII
EP-OPF with SVC and UPFC	Case IX
EP-OPF with One TCSC,SVC and UPFC	Case X
EP-OPF with Two TCSC,SVC and UPFC	Case XI

**Table 6.2 – The Minimum cost of Generation obtained for different cases.**

	Minimum Cost of Generation
Case I	803.9708 \$/hr
Case II	804.9847 \$/hr
Case III	806.7000 \$/hr
Case IV	803.9766 \$/hr
Case V	804.9861 \$/hr
Case VI	806.7380 \$/hr
Case VII	805.3837 \$/hr
Case VIII	807.0539 \$/hr
Case IX	806.5719 \$/hr
Case X	806.9269 \$/hr
Case XI	807.1614 \$/hr

### Case Study No.1

The objective of *TCSC* is to control the active power flow between the two buses. From Table 5.3, it was found that the line 2-4 is less loaded. It shows that 32.66 MW of real power flows. It is desired to increase the real power in line 2-4 by 20% of its initial value. *TCSC* used had capacitive impedance and inductive impedance equal to 6.3662ohm and 0.0314ohm.

It has been shown in Table 6.3 that real power flow in the line 2-4 has been increased to 39.37 MW from 32.6 MW which is 20% increase after incorporating *TCSC*. *TCSC* reduces line reactance there by increasing real power flow. Line reactance is reduced from 0.1737pu to 0.12366pu. The above results were obtained with no variation or practically very less variation of bus voltages. The firing angle of *TCSC* obtained is **2.12 radian (121.53 degree)**. The reactance offered by *TCSC* is -j0.0501. *TCSC* is operating in the capacitive region in this case.

### Case Study No.2

The primary objective of connecting *SVC* is to regulate bus voltage, with all other system parameters under practical limits. When *SVC* connected to PQ bus, it is operated to improve voltage profile of bus under light and heavy load conditions.

From Table 5.3, it was found that bus no.12 voltage shoots up. It shows that voltage magnitude of bus 12 is 1.061pu. It is desired to regulate voltage of bus 12 at 1.00pu under all conditions.

It has been shown in Table 6.4, that voltage of bus 12 is reduced from 1.061pu to 1.0pu, which is 5.6% drop after incorporating *SVC*. *SVC* absorbs reactive power of 49.69 Mvar, there by maintaining the voltage profile.

**Table 6.3: Load Flow Results for Case I**

Bus. No	Bus Voltage (pu)	Bus phase angle (deg)	$P(P_G - P_L)$ (pu)	$Q(Q_G - Q_L)$ (pu)
1	1.0600	0	1.6675	0.0014
2	1.0430	-3.4289	0.2785	0.1520
3	1.0262	-4.9543	-0.0240	-0.0120
4	1.0180	-5.9403	-0.0760	-0.0160
5	1.0100	-9.7789	-0.7113	0.0636
6	1.0153	-7.0998	0.0000	0.0000
7	1.0054	-8.7259	-0.2280	-0.1090
8	1.0100	-7.1499	-0.0236	-0.1649
9	1.0541	-9.1837	0.0000	-0.0000
10	1.0487	-10.8771	-0.0580	-0.0200
11	1.0820	-8.0793	0.1057	0.1461
12	1.0611	-9.9106	-0.1120	-0.0750
13	1.0710	-8.8731	0.1470	0.0768
14	1.0464	-10.8301	-0.0620	-0.0160
15	1.0416	-10.9565	-0.0820	-0.0250
16	1.0486	-10.5896	-0.0350	-0.0180
17	1.0434	-10.9964	-0.0900	-0.0580
18	1.0320	-11.6178	-0.0320	-0.0090
19	1.0294	-11.8211	-0.0950	-0.0340
20	1.0335	-11.6423	-0.0220	-0.0070
21	1.0365	-11.3279	-0.1750	-0.1120
22	1.0370	-11.3173	0.0000	-0.0000
23	1.0312	-11.4345	-0.0320	-0.0160
24	1.0256	-11.7320	-0.0870	-0.0670
25	1.0217	-11.5502	0.0000	-0.0000
26	1.0041	-11.9662	-0.0350	-0.0230
27	1.0279	-11.1803	0.0000	0.0000
28	1.0133	-7.5768	0.0000	-0.0000
29	1.0082	-12.3989	-0.0240	-0.0090
30	0.9967	-13.2734	-0.1060	-0.0190

Line No	From Bus	To Bus	Line flow from $i^{th}$ to $j^{th}$ Bus	Line flow from $j^{th}$ to $i^{th}$ Bus
1	1	2	1.1391 - 0.0474i	-1.1169 + 0.0847i
2	1	3	0.5284 + 0.0751i	-0.5168 - 0.0501i
3	2	4	0.3937 + 0.0274i	-0.3855 - 0.0292i
4	3	4	0.4928 + 0.0510i	-0.4897 - 0.0466i
5	2	5	0.6025 + 0.0514i	-0.5866 - 0.0065i
6	2	6	0.3993 + 0.0344i	-0.3906 - 0.0281i
7	4	6	0.4857 - 0.0700i	-0.4830 + 0.0750i
8	5	7	-0.1247 + 0.0860i	0.1258 - 0.0937i
9	6	7	0.3571 + 0.0074i	-0.3538 - 0.0059i
10	6	8	0.0536 + 0.1107i	-0.0535 - 0.1147i
11	6	9	0.1871 - 0.1860i	-0.1871 + 0.2000i
12	6	10	0.1262 - 0.0569i	-0.1262 + 0.0672i
13	9	11	-0.1057 - 0.1403i	0.1057 + 0.1461i
14	9	10	0.2970 + 0.0560i	-0.2970 - 0.0469i
15	4	12	0.2922 - 0.1613i	-0.2922 + 0.1888i
16	12	13	-0.1470 - 0.0735i	0.1470 + 0.0768i
17	12	14	0.0806 + 0.0229i	-0.0799 - 0.0213i
18	12	15	0.1877 + 0.0649i	-0.1853 - 0.0603i
19	12	16	0.0802 + 0.0290i	-0.0796 - 0.0277i
20	14	15	0.0179 + 0.0053i	-0.0178 - 0.0052i
21	16	17	0.0446 + 0.0097i	-0.0444 - 0.0094i
22	15	18	0.0640 + 0.0147i	-0.0636 - 0.0139i
23	18	19	0.0316 + 0.0049i	-0.0315 - 0.0047i
24	19	20	-0.0635 - 0.0293i	0.0636 + 0.0296i
25	10	20	0.0864 + 0.0383i	-0.0856 - 0.0366i
26	10	17	0.0457 + 0.0490i	-0.0456 - 0.0486i
27	10	21	0.1597 + 0.0980i	-0.1586 - 0.0956i
28	10	22	0.0774 + 0.0446i	-0.0769 - 0.0435i
29	21	22	-0.0164 - 0.0164i	0.0164 + 0.0164i
30	15	23	0.0571 + 0.0258i	-0.0568 - 0.0251i
31	22	24	0.0604 + 0.0271i	-0.0600 - 0.0264i
32	23	24	0.0248 + 0.0091i	-0.0247 - 0.0089i
33	24	25	-0.0024 + 0.0135i	0.0024 - 0.0135i
34	25	26	0.0354 + 0.0237i	-0.0350 - 0.0230i
35	25	27	-0.0378 - 0.0102i	0.0380 + 0.0105i
36	28	27	0.1653 - 0.0321i	-0.1653 + 0.0430i
37	27	29	0.0619 + 0.0167i	-0.0610 - 0.0151i
38	27	30	0.0709 + 0.0166i	-0.0693 - 0.0136i
39	29	30	0.0370 + 0.0061i	-0.0367 - 0.0054i
40	8	28	0.0298 - 0.0370i	-0.0297 + 0.0155i
41	6	28	0.1414 - 0.0392i	-0.1411 - 0.0265i



**Table 6.4: Load Flow Results for Case II**

Bus. No	Bus Voltage (pu)	Bus phase angle (deg)	$P(P_G - P_L)$ (pu)	$Q(Q_G - Q_L)$ (pu)
1	1.0600	0	1.6706	0.0498
2	1.0430	-3.3731	0.2785	0.2408
3	1.0179	-5.0900	-0.0240	-0.0120
4	1.0080	-6.1061	-0.0760	-0.0160
5	1.0100	-9.9219	-0.7113	0.0928
6	1.0096	-7.3187	-0.0000	-0.0000
7	1.0019	-8.9161	-0.2280	-0.1090
8	1.0100	-7.4696	-0.0236	0.0026
9	1.0399	-9.6225	-0.0000	-0.0000
10	1.0228	-11.4783	-0.0580	-0.0200
11	1.0820	-8.5032	0.1057	0.2198
12	1.0000	-9.8990	-0.1120	-0.5719
13	1.0324	-8.7569	0.1470	0.2400
14	0.9892	-10.9400	-0.0620	-0.0160
15	0.9887	-11.1994	-0.0820	-0.0250
16	1.0019	-10.8974	-0.0350	-0.0180
17	1.0110	-11.5344	-0.0900	-0.0580
18	0.9881	-12.0524	-0.0320	-0.0090
19	0.9910	-12.3480	-0.0950	-0.0340
20	0.9981	-12.1955	-0.0220	-0.0070
21	1.0093	-11.9347	-0.1750	-0.1120
22	1.0096	-11.9174	0.0000	-0.0000
23	0.9872	-11.8135	-0.0320	-0.0160
24	0.9941	-12.2473	-0.0870	-0.0670
25	0.9997	-12.1084	0.0000	0.0000
26	0.9817	-12.5433	-0.0350	-0.0230
27	1.0119	-11.7438	-0.0000	-0.0000
28	1.0075	-7.8289	0.0000	-0.0000
29	0.9919	-13.0019	-0.0240	-0.0090
30	0.9802	-13.9057	-0.1060	-0.0190

Line No	From Bus	To Bus	Line flow from $i^{th}$ to $j^{th}$ Bus	Line flow from $j^{th}$ to $i^{th}$ Bus
1	1	2	1.1220 - 0.0428i	-1.1004 + 0.0780i
2	1	3	0.5487 + 0.1188i	-0.5359 - 0.0884i
3	2	4	0.3249 + 0.1006i	-0.3187 - 0.1011i
4	3	4	0.5119 + 0.0892i	-0.5084 - 0.0836i
5	2	5	0.6203 + 0.0492i	-0.6034 - 0.0004i
6	2	6	0.4337 + 0.0589i	-0.4234 - 0.0473i
7	4	6	0.4717 - 0.1711i	-0.4687 + 0.1768i
8	5	7	-0.1078 + 0.1091i	0.1089 - 0.1166i
9	6	7	0.3400 - 0.0163i	-0.3369 + 0.0170i
10	6	8	0.0564 - 0.0288i	-0.0563 + 0.0243i
11	6	9	0.2029 - 0.1434i	-0.2029 + 0.1559i
12	6	10	0.1347 - 0.0192i	-0.1347 + 0.0293i
13	9	11	-0.1057 - 0.2093i	0.1057 + 0.2198i
14	9	10	0.3131 + 0.1668i	-0.3131 - 0.1540i
15	4	12	0.2605 + 0.0400i	-0.2605 - 0.0225i
16	12	13	-0.1470 - 0.2296i	0.1470 + 0.2400i
17	12	14	0.0738 + 0.0074i	-0.0731 - 0.0060i
18	12	15	0.1725 + 0.0009i	-0.1705 + 0.0030i
19	12	16	0.0681 - 0.0414i	-0.0675 + 0.0427i
20	14	15	0.0111 - 0.0100i	-0.0111 + 0.0100i
21	16	17	0.0325 - 0.0607i	-0.0322 + 0.0616i
22	15	18	0.0550 - 0.0236i	-0.0546 + 0.0244i
23	18	19	0.0226 - 0.0334i	-0.0225 + 0.0336i
24	19	20	-0.0725 - 0.0676i	0.0728 + 0.0682i
25	10	20	0.0962 + 0.0783i	-0.0948 - 0.0752i
26	10	17	0.0584 + 0.1211i	-0.0578 - 0.1196i
27	10	21	0.1612 + 0.1105i	-0.1599 - 0.1078i
28	10	22	0.0784 + 0.0528i	-0.0778 - 0.0515i
29	21	22	-0.0151 - 0.0042i	0.0151 + 0.0042i
30	15	23	0.0446 - 0.0145i	-0.0444 + 0.0150i
31	22	24	0.0626 + 0.0473i	-0.0620 - 0.0462i
32	23	24	0.0124 - 0.0310i	-0.0122 + 0.0313i
33	24	25	-0.0128 - 0.0096i	0.0129 + 0.0097i
34	25	26	0.0355 + 0.0237i	-0.0350 - 0.0230i
35	25	27	-0.0483 - 0.0334i	0.0487 + 0.0341i
36	28	27	0.1758 - 0.0053i	-0.1758 + 0.0174i
37	27	29	0.0619 + 0.0167i	-0.0610 - 0.0151i
38	27	30	0.0710 + 0.0167i	-0.0693 - 0.0136i
39	29	30	0.0370 + 0.0061i	-0.0367 - 0.0054i
40	8	28	0.0327 - 0.0085i	-0.0326 - 0.0130i
41	6	28	0.1494 - 0.0396i	-0.1490 - 0.0252i

### Case Study No.3

The primary objective of *UPFC* is to control both real and reactive power independently and bus voltage. From the Table 5.3, it was found that line 10-22 is less loaded and bus voltages are shoots up. It shows that 7.749 MW and 4.46 Mvar flows in it. It has been shown in Table 6.6 that real and reactive power flow in the line has been increased to 10.83 MW and 11.1149 Mvar from the initial value after incorporating *UPFC*. The shunt converter of *UPFC* is used to control the bus voltage to which it is connected. From the table 6.5 it is clear that voltage of bus 10 is decreased to 1.023 pu from 1.04869 pu which is 2.44% drop.

*UPFC* injects a series voltage in the line. There by controlling real and reactive power independently. By absorbing or injecting shunt reactive current, it maintains the voltage of the bus to which shunt converter is connected. The magnitude and angle of series injected voltage is 0.038 pu and 3.10 radian. The shunt converter absorbs inductive current of 0.24 pu

UPFC Parameters	Values
$V_T$ (pu)	0.038
$\phi_T$ (radian)	3.10
$I_q$ (pu)	-0.24

**Table 6.5: Load Flow Results for Case III**

Bus. No	Bus Voltage (pu)	Bus phase angle (deg)	$P(P_G - P_L)$ (pu)	$Q(Q_G - Q_L)$ (pu)
1	1.0600	0	1.6759	0.0168
2	1.0430	-3.3658	0.2785	0.1828
3	1.0236	-5.2153	-0.0240	-0.0120
4	1.0149	-6.2587	-0.0760	-0.0160
5	1.0100	-9.8809	-0.7113	0.0786
6	1.0123	-7.3082	-0.0000	0.0000
7	1.0036	-8.8921	-0.2280	-0.1090
8	1.0100	-7.4125	-0.0236	-0.0744
9	1.0409	-9.3407	-0.0000	-0.0000
10	1.0232	-11.0535	0.0291	-0.0508
11	1.0820	-8.2224	0.1057	0.2148
12	1.0525	-10.4294	-0.1120	-0.0750
13	1.0710	-9.3834	0.1470	0.1425
14	1.0350	-11.3542	-0.0620	-0.0160
15	1.0277	-11.4133	-0.0820	-0.0250
16	1.0328	-10.9601	-0.0350	-0.0180
17	1.0207	-11.2359	-0.0900	-0.0580
18	1.0138	-12.0006	-0.0320	-0.0090
19	1.0087	-12.1542	-0.0950	-0.0340
20	1.0115	-11.9369	-0.0220	-0.0070
21	1.0015	-11.5272	-0.1750	-0.1120
22	0.9992	-11.5109	-0.0909	-0.2092
23	1.0111	-11.8526	-0.0320	-0.0160
24	0.9976	-12.0915	-0.0870	-0.0670
25	1.0026	-11.9902	-0.0000	0.0000
26	0.9847	-12.4225	-0.0350	-0.0230
27	1.0145	-11.6507	-0.0000	0.0000
28	1.0097	-7.8018	-0.0000	0.0000
29	0.9945	-12.9023	-0.0240	-0.0090
30	0.9829	-13.8012	-0.1060	-0.0190

Line No	From Bus	To Bus	Line flow from $i^{\text{th}}$ to $j^{\text{th}}$ Bus	Line flow from $j^{\text{th}}$ to $i^{\text{th}}$ Bus
1	1	2	1.1197 - 0.0422i	-1.0983 + 0.0772i
2	1	3	0.5562 + 0.0853i	-0.5433 - 0.0549i
3	2	4	0.3299 + 0.0580i	-0.3239 - 0.0593i
4	3	4	0.5193 + 0.0558i	-0.5159 - 0.0503i
5	2	5	0.6173 + 0.0496i	-0.6006 - 0.0015i
6	2	6	0.4296 + 0.0440i	-0.4196 - 0.0334i
7	4	6	0.4382 - 0.0594i	-0.4359 + 0.0626i
8	5	7	-0.1107 + 0.0960i	0.1117 - 0.1037i
9	6	7	0.3428 - 0.0034i	-0.3397 + 0.0042i
10	6	8	0.0556 + 0.0374i	-0.0556 - 0.0418i
11	6	9	0.1797 - 0.1360i	-0.1797 + 0.1463i
12	6	10	0.1217 - 0.0158i	-0.1217 + 0.0239i
13	9	11	-0.1057 - 0.2047i	0.1057 + 0.2148i
14	9	10	0.2894 + 0.1723i	-0.2894 - 0.1607i
15	4	12	0.3035 - 0.1380i	-0.3035 + 0.1656i
16	12	13	-0.1470 - 0.1374i	0.1470 + 0.1425i
17	12	14	0.0842 + 0.0321i	-0.0833 - 0.0302i
18	12	15	0.1945 + 0.1026i	-0.1917 - 0.0969i
19	12	16	0.0819 + 0.0657i	-0.0810 - 0.0637i
20	14	15	0.0213 + 0.0142i	-0.0211 - 0.0141i
21	16	17	0.0460 + 0.0457i	-0.0457 - 0.0450i
22	15	18	0.0654 + 0.0337i	-0.0649 - 0.0326i
23	18	19	0.0329 + 0.0236i	-0.0328 - 0.0234i
24	19	20	-0.0622 - 0.0106i	0.0623 + 0.0109i
25	10	20	0.0850 + 0.0194i	-0.0843 - 0.0179i
26	10	17	0.0444 + 0.0132i	-0.0443 - 0.0130i
27	10	21	0.2063 + 0.2006i	-0.2036 - 0.1947i
28	10	22	<b>0.1083 + 0.1111i</b>	<b>-0.1067 - 0.1077i</b>
29	21	22	0.0286 + 0.0827i	-0.0285 - 0.0825i
30	15	23	0.0653 + 0.0523i	-0.0647 - 0.0510i
31	22	24	0.0442 - 0.0190i	-0.0440 + 0.0194i
32	23	24	0.0327 + 0.0350i	-0.0324 - 0.0343i
33	24	25	-0.0107 - 0.0092i	0.0107 + 0.0093i
34	25	26	0.0355 + 0.0237i	-0.0350 - 0.0230i
35	25	27	-0.0462 - 0.0330i	0.0465 + 0.0337i
36	28	27	0.1736 - 0.0065i	-0.1736 + 0.0182i
37	27	29	0.0619 + 0.0167i	-0.0610 - 0.0151i
38	27	30	0.0710 + 0.0167i	-0.0693 - 0.0136i
39	29	30	0.0370 + 0.0061i	-0.0367 - 0.0054i
40	8	28	0.0319 - 0.0194i	-0.0319 - 0.0022i
41	6	28	0.1479 - 0.0302i	-0.1475 - 0.0349i

#### Case Study No.4

From Table 5.3, it was found that the lines 2-4 and 14-15 are less loaded. It shows that 32.66 MW and 1.75868 MW of real power flows. It is desired to increase the real power in line 2-4 and 14-15 by 20% of its initial value.

It has been shown in Table 6.6 that real power flow in the line 2-4 has been increased to 39.37 MW from 32.6 MW and power flow in 14-15 has been increased to 2.09212 MW from 1.75868 MW which is 20% increase after incorporating TCSC.

TCSC reduces line reactance there by increasing real power flow. Line reactance is reduced from 0.1737pu to 0.12366pu in line 2-4 and 0.199pu to 0.098pu in line 14-15. The above results were obtained with no variation or practically very less variation of bus voltages. The firing angles of TCSC's obtained are 2.12 radian (121.53 degree) and 1.55 radian (88.9). The TCSC is operating in the capacitive region in this case.

Parameters	TCSC I	TCSC II
Firing Angle (radian)	2.12	1.55
$X_{TCSC}$	-j0.0501	-j0.101

#### Case Study No.5

From Table 5.3, it was found that bus no.12 and 9 voltage shoots up. It shows that voltage magnitude of bus 12 is 1.061pu and 9 is 1.05405. it is desired to regulate voltage of bus 12 and 9 at 1.00pu under all conditions.

It has been shown in Table 6.7 that after incorporating SVC's, voltage of bus 12 is reduced from 1.061pu to 1.0pu, which is 5.6% drop and voltage of bus 9 is reduced from 1.05405pu to 1.0pu, which is 5.1% drop. SVC's absorbs reactive power of 49.69 Mvar and 32.23 Mvar from buses 12 and 9, there by maintaining the voltage profile.

**Table 6.6: Load Flow Results for Case IV**

Bus. No	Bus Voltage (pu)	Bus phase angle (deg)	$P(P_G - P_L)$ (pu)	$Q(Q_G - Q_L)$ (pu)
1	1.0600	0	1.6675	0.0014
2	1.0430	-3.4289	0.2785	0.1520
3	1.0262	-4.9546	-0.0240	-0.0120
4	1.0180	-5.9406	-0.0760	-0.0160
5	1.0100	-9.7786	-0.7113	0.0636
6	1.0153	-7.0993	0.0000	0.0000
7	1.0054	-8.7255	-0.2280	-0.1090
8	1.0100	-7.1494	-0.0236	-0.1649
9	1.0541	-9.1815	0.0000	-0.0000
10	1.0487	-10.8740	-0.0580	-0.0200
11	1.0820	-8.0772	0.1057	0.1461
12	1.0611	-9.9156	-0.1120	-0.0750
13	1.0710	-8.8782	0.1470	0.0768
14	1.0464	-10.8848	-0.0620	-0.0160
15	1.0416	-10.9411	-0.0820	-0.0250
16	1.0486	-10.5913	-0.0350	-0.0180
17	1.0434	-10.9947	-0.0900	-0.0580
18	1.0320	-11.6067	-0.0320	-0.0090
19	1.0294	-11.8126	-0.0950	-0.0340
20	1.0335	-11.6351	-0.0220	-0.0070
21	1.0364	-11.3242	-0.1750	-0.1120
22	1.0370	-11.3135	-0.0000	-0.0000
23	1.0312	-11.4229	-0.0320	-0.0160
24	1.0257	-11.7257	-0.0870	-0.0670
25	1.0217	-11.5461	-0.0000	-0.0000
26	1.0041	-11.9621	-0.0350	-0.0230
27	1.0279	-11.1775	0.0000	0.0000
28	1.0133	-7.5761	-0.0000	-0.0000
29	1.0081	-12.3961	-0.0240	-0.0090
30	0.9967	-13.2706	-0.1060	-0.0190

Line No	From Bus	To Bus	Line flow from $i^{th}$ to $j^{th}$ Bus	Line flow from $j^{th}$ to $i^{th}$ Bus
1	1	2	-1.1391 - 0.0474i	-1.1169 + 0.0847i
2	1	3	0.5284 + 0.0751i	-0.5169 - 0.0501i
3	2	4	<b>0.3937 + 0.0274i</b>	<b>-0.3855 - 0.0292i</b>
4	3	4	0.4929 + 0.0510i	-0.4898 - 0.0466i
5	2	5	0.6025 + 0.0514i	-0.5865 - 0.0065i
6	2	6	0.3992 + 0.0344i	-0.3906 - 0.0281i
7	4	6	0.4854 - 0.0700i	-0.4827 + 0.0750i
8	5	7	-0.1247 + 0.0860i	0.1258 - 0.0937i
9	6	7	0.3571 + 0.0074i	-0.3538 - 0.0059i
10	6	8	0.0536 + 0.1107i	-0.0534 - 0.1147i
11	6	9	0.1869 - 0.1860i	-0.1869 + 0.2000i
12	6	10	0.1261 - 0.0569i	-0.1261 + 0.0672i
13	9	11	-0.1057 - 0.1404i	0.1057 + 0.1461i
14	9	10	0.2968 + 0.0560i	-0.2968 - 0.0470i
15	4	12	0.2925 - 0.1613i	-0.2925 + 0.1889i
16	12	13	-0.1470 - 0.0734i	0.1470 + 0.0768i
17	12	14	0.0837 + 0.0215i	-0.0829 - 0.0198i
18	12	15	0.1852 + 0.0660i	-0.1829 - 0.0615i
19	12	16	0.0799 + 0.0292i	-0.0793 - 0.0279i
20	14	15	<b>0.0209 + 0.0038i</b>	<b>-0.0208 - 0.0038i</b>
21	16	17	0.0443 + 0.0099i	-0.0441 - 0.0095i
22	15	18	0.0643 + 0.0146i	-0.0639 - 0.0138i
23	18	19	0.0319 + 0.0048i	-0.0318 - 0.0046i
24	19	20	-0.0632 - 0.0294i	0.0633 + 0.0297i
25	10	20	0.0861 + 0.0384i	-0.0853 - 0.0367i
26	10	17	0.0460 + 0.0488i	-0.0459 - 0.0485i
27	10	21	0.1596 + 0.0981i	-0.1585 - 0.0957i
28	10	22	0.0773 + 0.0447i	-0.0768 - 0.0436i
29	21	22	-0.0165 - 0.0163i	0.0165 + 0.0163i
30	15	23	0.0574 + 0.0257i	-0.0571 - 0.0249i
31	22	24	0.0602 + 0.0272i	-0.0598 - 0.0265i
32	23	24	0.0251 + 0.0089i	-0.0250 - 0.0088i
33	24	25	-0.0023 + 0.0135i	0.0023 - 0.0134i
34	25	26	0.0354 + 0.0237i	-0.0350 - 0.0230i
35	25	27	-0.0377 - 0.0102i	0.0379 + 0.0105i
36	28	27	0.1652 - 0.0321i	-0.1652 + 0.0430i
37	27	29	0.0619 + 0.0167i	-0.0610 - 0.0151i
38	27	30	0.0709 + 0.0166i	-0.0693 - 0.0136i
39	29	30	0.0370 + 0.0061i	-0.0367 - 0.0054i
40	8	28	0.0298 - 0.0370i	-0.0297 + 0.0155i
41	6	28	0.1413 - 0.0392i	-0.1410 - 0.0265i



**Table 6.7: Load Flow Results for Case V**

Bus. No	Bus Voltage (pu)	Bus phase angle (deg)	$P(P_G - P_L)$ (pu)	$Q(Q_G - Q_L)$ (pu)
1	1.0600	0	1.6706	0.0675
2	1.0430	-3.3753	0.2785	0.2979
3	1.0147	-5.0558	-0.0240	-0.0120
4	1.0042	-6.0645	-0.0760	-0.0160
5	1.0100	-9.9410	-0.7113	0.1236
6	1.0037	-7.2098	0.0000	-0.0000
7	0.9984	-8.8618	-0.2280	-0.1090
8	1.0075	-7.4198	-0.0236	0.1000
9	<b>1.0000</b>	-9.4285	0.0000	<b>-0.3223</b>
10	0.9976	-11.3034	-0.0580	-0.0200
11	1.0474	-8.2261	0.1057	0.2400
12	<b>1.0000</b>	-10.1190	-0.1120	<b>-0.4536</b>
13	1.0324	-8.9768	0.1470	0.2400
14	0.9862	-11.1487	-0.0620	-0.0160
15	0.9829	-11.3268	-0.0820	-0.0250
16	0.9913	-10.9314	-0.0350	-0.0180
17	0.9900	-11.4232	-0.0900	-0.0580
18	0.9752	-12.0898	-0.0320	-0.0090
19	0.9740	-12.3302	-0.0950	-0.0340
20	0.9791	-12.1377	-0.0220	-0.0070
21	0.9853	-11.7974	-0.1750	-0.1120
22	0.9860	-11.7846	0.0000	-0.0000
23	0.9764	-11.8847	-0.0320	-0.0160
24	0.9768	-12.2436	-0.0870	-0.0670
25	0.9864	-12.1465	0.0000	-0.0000
26	0.9682	-12.5934	-0.0350	-0.0230
27	1.0014	-11.7957	-0.0000	0.0000
28	1.0017	-7.7373	0.0000	-0.0000
29	0.9811	-13.0811	-0.0240	-0.0090
30	0.9893	-14.0051	-0.1060	-0.0190

Line No	From Bus	To Bus	Line flow from $i^{th}$ to $j^{th}$ Bus	Line flow from $j^{th}$ to $i^{th}$ Bus
1	1	2	1.1226 - 0.0430i	-1.1011 + 0.0783i
2	1	3	0.5480 + 0.1367i	-0.5350 - 0.1056i
3	2	4	0.3265 + 0.1228i	-0.3200 - 0.1222i
4	3	4	0.5110 + 0.1062i	-0.5075 - 0.1005i
5	2	5	0.6218 + 0.0490i	-0.6049 + 0.0001i
6	2	6	0.4313 + 0.0937i	-0.4208 - 0.0814i
7	4	6	0.4539 - 0.1160i	-0.4513 + 0.1204i
8	5	7	-0.1064 + 0.1394i	0.1078 - 0.1460i
9	6	7	0.3389 - 0.0454i	-0.3358 + 0.0463i
10	6	8	0.0576 - 0.1096i	-0.0574 + 0.1057i
11	6	9	0.1868 + 0.0213i	-0.1868 - 0.0140i
12	6	10	0.1285 + 0.0156i	-0.1285 - 0.0064i
13	9	11	-0.1057 - 0.2270i	0.1057 + 0.2400i
14	9	10	0.2967 + 0.0271i	-0.2967 - 0.0173i
15	4	12	0.2773 + 0.0261i	-0.2773 - 0.0064i
16	12	13	-0.1470 - 0.2296i	0.1470 + 0.2400i
17	12	14	0.0776 + 0.0174i	-0.0768 - 0.0158i
18	12	15	0.1800 + 0.0416i	-0.1778 - 0.0372i
19	12	16	0.0749 + 0.0088i	-0.0744 - 0.0077i
20	14	15	0.0148 - 0.0002i	-0.0148 + 0.0003i
21	16	17	0.0394 - 0.0103i	-0.0392 + 0.0106i
22	15	18	0.0609 + 0.0050i	-0.0604 - 0.0041i
23	18	19	0.0284 - 0.0049i	-0.0284 + 0.0050i
24	19	20	-0.0666 - 0.0390i	0.0668 + 0.0394i
25	10	20	0.0898 + 0.0486i	-0.0888 - 0.0464i
26	10	17	0.0510 + 0.0693i	-0.0508 - 0.0686i
27	10	21	0.1558 + 0.0918i	-0.1546 - 0.0893i
28	10	22	0.0748 + 0.0405i	-0.0742 - 0.0395i
29	21	22	-0.0204 - 0.0227i	0.0204 + 0.0227i
30	15	23	0.0497 + 0.0069i	-0.0494 - 0.0064i
31	22	24	0.0539 + 0.0168i	-0.0535 - 0.0162i
32	23	24	0.0174 - 0.0096i	-0.0174 + 0.0097i
33	24	25	-0.0161 - 0.0195i	0.0163 + 0.0197i
34	25	26	0.0355 + 0.0237i	-0.0350 - 0.0230i
35	25	27	-0.0517 - 0.0434i	0.0522 + 0.0444i
36	28	27	0.1793 + 0.0072i	-0.1793 + 0.0055i
37	27	29	0.0620 + 0.0168i	-0.0611 - 0.0151i
38	27	30	0.0710 + 0.0168i	-0.0693 - 0.0136i
39	29	30	0.0371 + 0.0061i	-0.0367 - 0.0054i
40	8	28	0.0338 + 0.0075i	-0.0337 - 0.0288i
41	6	28	0.1519 - 0.0422i	-0.1515 - 0.0218i

## Case Study No.6

From the Table 5.3, it was found that line 10-22 and 25-26 are less loaded and bus voltages are shoots up. It shows that 7.749 MW and 4.46 Mvar flows in the line 10-22 and 3.54 MW and 2.37 Mvar flows in the line 25-26.

It has been shown in Table 6.8 that in the line 10-22 real and reactive power flow in the line has been increased to 10.83 MW and 11.1149 Mvar from the initial value after incorporating UPFC. The shunt converter of UPFC is used to control the bus voltage to which it is connected. It is clear that voltage of bus 10 is decreased to 1.0285 pu from 1.0487 pu which is 1.93% drop.

It has been shown in Table 6.8 that in the line 25-26 real and reactive power flow in the line has been increased to 10.52 MW and 3.57 Mvar from the initial value after incorporating UPFC. The shunt converter of UPFC is used to control the bus voltage to which it is connected. From the table 6.8 it is clear that voltage of bus 25 is decreased to 1.0120 pu from 1.0217 pu which is 0.95% drop.

UPFC injects a series voltage in the line. There by controlling real and reactive power independently. By absorbing or injecting shunt reactive current, it maintains the voltage of the bus to which shunt converter is connected.

UPFC Parameters	UPFC I	UPFC II
$V_T$ (pu)	0.038	0.031
$\phi_T$ (radian)	3.10	4.0
$I_q$ (pu)	-0.24	-0.11

**Table 6.8: Load Flow Results for Case VI**

Bus. No	Bus Voltage (pu)	Bus-phase angle (deg)	$P(P_G - P_L)$ (pu)	$Q(Q_G - Q_L)$ (pu)
1	1.0600	0	1.6791	0.0110
2	1.0430	-3.3720	0.2785	0.1695
3	1.0245	-5.2363	-0.0240	-0.0120
4	1.0160	-6.2842	-0.0760	-0.0160
5	1.0100	-9.8884	-0.7113	0.0721
6	1.0135	-7.3476	0.0000	0.0000
7	1.0043	-8.9180	-0.2280	-0.1090
8	1.0100	-7.4356	-0.0236	-0.1196
9	1.0438	-9.3523	0.0000	0.0000
10	<b>1.0285</b>	-11.0409	0.0291	<b>-0.0508</b>
11	1.0820	-8.2371	0.1057	0.1995
12	1.0552	-10.3894	-0.1120	-0.0750
13	1.0710	-9.3460	0.1470	0.1223
14	1.0388	-11.3180	-0.0620	-0.0160
15	1.0325	-11.4094	-0.0820	-0.0250
16	1.0366	-10.9316	-0.0350	-0.0180
17	1.0256	-11.2172	-0.0900	-0.0580
18	1.0188	-11.9867	-0.0320	-0.0090
19	1.0139	-12.1361	-0.0950	-0.0340
20	1.0168	-11.9197	-0.0220	-0.0070
21	1.0085	-11.5361	-0.1750	-0.1120
22	1.0067	-11.5294	-0.0909	-0.2092
23	1.0197	-11.9225	-0.0320	-0.0160
24	1.0112	-12.2630	-0.0870	-0.0670
25	<b>1.0120</b>	-12.5649	0.0661	<b>0.1083</b>
26	1.0031	-14.2895	-0.1023	-0.0313
27	1.0361	-11.8578	0.0000	0.0000
28	1.0127	-7.8972	0.0000	0.0000
29	1.0165	-13.0567	-0.0240	-0.0090
30	1.0052	-13.9167	-0.1060	-0.0190

Line No	From Bus	To Bus	Line flow from $i^{th}$ to $j^{th}$ Bus	Line flow from $j^{th}$ to $i^{th}$ Bus
1	1	2	1.1216 - 0.0427i	-1.1001 + 0.0779i
2	1	3	0.5575 + 0.0800i	-0.5446 - 0.0496i
3	2	4	0.3301 + 0.0515i	-0.3242 - 0.0530i
4	3	4	0.5206 + 0.0505i	-0.5172 - 0.0450i
5	2	5	0.6174 + 0.0496i	-0.6007 - 0.0014i
6	2	6	0.4311 + 0.0364i	-0.4210 - 0.0258i
7	4	6	0.4437 - 0.0646i	-0.4414 + 0.0680i
8	5	7	-0.1106 + 0.0894i	0.1115 - 0.0974i
9	6	7	0.3426 + 0.0029i	-0.3395 - 0.0022i
10	6	8	0.0572 + 0.0669i	-0.0571 - 0.0712i
11	6	9	0.1779 - 0.1445i	-0.1779 + 0.1552i
12	6	10	0.1208 - 0.0234i	-0.1208 + 0.0316i
13	9	11	-0.1057 - 0.1904i	0.1057 + 0.1995i
14	9	10	0.2876 + 0.1496i	-0.2876 - 0.1390i
15	4	12	0.2998 - 0.1446i	-0.2998 + 0.1721i
16	12	13	-0.1470 - 0.1179i	0.1470 + 0.1223i
17	12	14	0.0830 + 0.0282i	-0.0822 - 0.0265i
18	12	15	0.1929 + 0.0870i	-0.1902 - 0.0818i
19	12	16	0.0808 + 0.0603i	-0.0799 - 0.0585i
20	14	15	0.0202 + 0.0105i	-0.0200 - 0.0104i
21	16	17	0.0449 + 0.0405i	-0.0446 - 0.0398i
22	15	18	0.0647 + 0.0330i	-0.0642 - 0.0320i
23	18	19	0.0322 + 0.0230i	-0.0321 - 0.0228i
24	19	20	-0.0629 - 0.0112i	0.0630 + 0.0115i
25	10	20	0.0857 + 0.0200i	-0.0850 - 0.0185i
26	10	17	0.0455 + 0.0184i	-0.0454 - 0.0182i
27	10	21	0.2037 + 0.1808i	-0.2012 - 0.1755i
28	10	22	<b>0.1065 + 0.0982i</b>	<b>-0.1051 - 0.0952i</b>
29	21	22	0.0262 + 0.0635i	-0.0262 - 0.0634i
30	15	23	0.0636 + 0.0341i	-0.0631 - 0.0331i
31	22	24	0.0404 - 0.0505i	-0.0399 + 0.0513i
32	23	24	0.0311 + 0.0171i	-0.0309 - 0.0168i
33	24	25	-0.0162 - 0.0575i	0.0169 + 0.0586i
34	25	26	<b>0.1052 + 0.0357i</b>	<b>-0.1023 - 0.0313i</b>
35	25	27	-0.0560 + 0.0140i	0.0563 - 0.0133i
36	28	27	0.1830 - 0.0535i	-0.1830 + 0.0675i
37	27	29	0.0619 + 0.0166i	-0.0610 - 0.0150i
38	27	30	0.0709 + 0.0166i	-0.0693 - 0.0136i
39	29	30	0.0370 + 0.0060i	-0.0367 - 0.0054i
40	8	28	0.0335 - 0.0352i	-0.0334 + 0.0136i
41	6	28	0.1561 - 0.0627i	-0.1557 - 0.0025i

## Case Study No.7

From Table 5.3, it was found that the line 2-4 is less loaded. It shows that 32.66 MW of real power flows. It is desired to increase the real power in line 2-4 by 20% of its initial value. *TCSC* used had capacitive impedance and inductive impedance equal to 6.3662ohm and 0.0314ohm.

It has been shown in Table 6.9 that real power flow in the line 2-4 has been increased to 39.65 MW from 32.6 MW which is 20% increase after incorporating *TCSC*. *TCSC* reduces line reactance there by increasing real power flow. Line reactance is reduced from 0.1737pu to 0.12366pu. The above results were obtained with no variation or practically very less variation of bus voltages. The firing angle of *TCSC* obtained is 2.12 radian or 121.53 degree. The reactance offered by *TCSC* is -j0.0501. *TCSC* is operating in the capacitive region in this case.

From Table 5.3, it was found that bus no.12 voltage shoots up. It shows that voltage magnitude of bus 12 is 1.061pu. it is desired to regulate voltage of bus 12 at 1.00pu under all conditions.

It has been shown in Table 6.9 that voltage of bus 12 is reduced from 1.061pu to 1.0pu, which is 5.6% drop after incorporating *SVC*. *SVC* absorbs reactive power of 50.2 Mvar, there by maintaining the voltage profile.

**Table 6.9: Load Flow Results for Case VII**

Bus. No	Bus Voltage (pu)	Bus phase angle (deg)	$P(P_G - P_L)$ (pu)	$Q(Q_G - Q_L)$ (pu)
1	1.0600	0	1.6718	0.0421
2	1.0430	-3.4629	0.2785	0.2604
3	1.0186	-4.8263	-0.0240	-0.0120
4	1.0089	-5.7840	-0.0760	-0.0160
5	1.0100	-9.8555	-0.7113	0.0915
6	1.0099	-7.0904	-0.0000	-0.0000
7	1.0022	-8.7537	-0.2280	-0.1090
8	1.0100	-7.2348	-0.0236	-0.0080
9	1.0401	-9.3784	0.0000	0.0000
10	1.0229	-11.2260	-0.0580	-0.0200
11	1.0820	-8.2592	0.1057	0.2191
12	1.0000	-9.6072	-0.1120	-0.5770
13	1.0324	-8.4651	0.1470	0.2400
14	0.9892	-10.6531	-0.0620	-0.0160
15	0.9887	-10.9179	-0.0820	-0.0250
16	1.0020	-10.6225	-0.0350	-0.0180
17	1.0110	-11.2754	-0.0900	-0.0580
18	0.9881	-11.7813	-0.0320	-0.0090
19	0.9910	-12.0830	-0.0950	-0.0340
20	0.9982	-11.9338	-0.0220	-0.0070
21	1.0094	-11.6815	-0.1750	-0.1120
22	1.0097	-11.6639	0.0000	-0.0000
23	0.9873	-11.5424	-0.0320	-0.0160
24	0.9942	-11.9900	-0.0870	-0.0670
25	0.9998	-11.8615	0.0000	-0.0000
26	0.9818	-12.2963	-0.0350	-0.0230
27	1.0121	-11.5033	-0.0000	-0.0000
28	1.0078	-7.5978	-0.0000	0.0000
29	0.9920	-12.7610	-0.0240	-0.0090
30	0.9804	-13.6644	-0.1060	-0.0190

Line No	From Bus	To Bus	Line flow from $i^{th}$ to $j^{th}$ Bus	Line flow from $j^{th}$ to $i^{th}$ Bus
1	1	2	1.1496 - 0.0502i	-1.1270 + 0.0887i
2	1	3	0.5223 + 0.1186i	-0.5106 - 0.0929i
3	2	4	<b>0.3965 + 0.1021i</b>	<b>-0.3876 - 0.1021i</b>
4	3	4	0.4866 + 0.0937i	-0.4835 - 0.0890i
5	2	5	0.6063 + 0.0509i	-0.5902 - 0.0052i
6	2	6	0.4027 + 0.0647i	-0.3937 - 0.0572i
7	4	6	0.5131 - 0.1693i	-0.5097 + 0.1765i
8	5	7	-0.1211 + 0.1126i	0.1224 - 0.1197i
9	6	7	0.3536 - 0.0186i	-0.3504 + 0.0200i
10	6	8	0.0562 - 0.0196i	-0.0562 + 0.0152i
11	6	9	0.2016 - 0.1423i	-0.2016 + 0.1548i
12	6	10	0.1340 - 0.0187i	-0.1340 + 0.0287i
13	9	11	-0.1057 - 0.2086i	0.1057 + 0.2191i
14	9	10	0.3118 + 0.1673i	-0.3118 - 0.1546i
15	4	12	0.2628 + 0.0438i	-0.2628 - 0.0259i
16	12	13	-0.1470 - 0.2296i	0.1470 + 0.2400i
17	12	14	0.0740 + 0.0072i	-0.0734 - 0.0058i
18	12	15	0.1736 + 0.0003i	-0.1716 + 0.0037i
19	12	16	0.0693 - 0.0421i	-0.0687 + 0.0434i
20	14	15	0.0114 - 0.0102i	-0.0113 + 0.0102i
21	16	17	0.0337 - 0.0614i	-0.0333 + 0.0623i
22	15	18	0.0556 - 0.0239i	-0.0552 + 0.0248i
23	18	19	0.0232 - 0.0338i	-0.0231 + 0.0340i
24	19	20	-0.0719 - 0.0680i	0.0722 + 0.0687i
25	10	20	0.0956 + 0.0787i	-0.0942 - 0.0757i
26	10	17	0.0573 + 0.1218i	-0.0567 - 0.1203i
27	10	21	0.1610 + 0.1106i	-0.1597 - 0.1079i
28	10	22	0.0783 + 0.0528i	-0.0777 - 0.0515i
29	21	22	-0.0153 - 0.0041i	0.0153 + 0.0041i
30	15	23	0.0453 - 0.0150i	-0.0450 + 0.0154i
31	22	24	0.0624 + 0.0474i	-0.0617 - 0.0463i
32	23	24	0.0130 - 0.0314i	-0.0129 + 0.0318i
33	24	25	-0.0125 - 0.0099i	0.0125 + 0.0100i
34	25	26	0.0355 + 0.0237i	-0.0350 - 0.0230i
35	25	27	-0.0480 - 0.0337i	0.0483 + 0.0344i
36	28	27	0.1754 - 0.0051i	-0.1754 + 0.0171i
37	27	29	0.0619 + 0.0167i	-0.0610 - 0.0151i
38	27	30	0.0710 + 0.0167i	-0.0693 - 0.0136i
39	29	30	0.0370 + 0.0061i	-0.0367 - 0.0054i
40	8	28	0.0326 - 0.0099i	-0.0325 - 0.0116i
41	6	28	0.1491 - 0.0380i	-0.1487 - 0.0268i



## Case Study No.8

From Table 5.3, it was found that the line 2-4 is less loaded. It shows that 32.66 MW of real power flows. It is desired to increase the real power in line 2-4 by 20% of its initial value. TCSC used had capacitive impedance and inductive impedance equal to 6.3662ohm and 0.0314ohm.

It has been shown in Table 6.10 that real power flow in the line 2-4 has been increased to **39.88 MW** from 32.6 MW which is 20% increase after incorporating TCSC. TCSC reduces line reactance there by increasing real power flow. Line reactance is reduced from 0.1737pu to 0.12366pu. The above results were obtained with no variation or practically very less variation of bus voltages. The firing angle of TCSC obtained is **2.12 radian or 121.53 degree**. The reactance offered by TCSC is -j0.0501. TCSC is operating in the capacitive region in this case.

From the Table 5.3, it was found that line 10-22 is less loaded and bus voltages are shoots up. It shows that 7.749 MW and 4.46 Mvar flows in it.

It has been shown in Table 6.10 that real and reactive power flow in the line 10-22 has been increased to **10.82 MW** and **11.12 Mvar** from the initial value after incorporating UPFC. The shunt converter of UPFC is used to control the bus voltage to which it is connected. From the Table 6.10 it is clear that voltage of bus 10 is decreased to **1.0232 pu** from 1.04869 pu which is 2.44% drop.

UPFC injects a series voltage in the line. There by controlling real and reactive power independently. By absorbing or injecting shunt reactive current, it maintains the voltage of the bus to which shunt converter is connected. The magnitude and angle of series injected voltage is 0.038 pu and 3.10 radian. The shunt converter absorbs inductive current of 0.24 pu

UPFC Parameters	Values
$V_r$ (pu)	0.038
$\phi_r$ (radian)	3.10
$I_q$ (pu)	-0.24

**Table 6.10 Load Flow for Case VIII**

Bus. No	Bus Voltage (pu)	Bus phase angle (deg)	$P(P_G - P_L)$ (pu)	$Q(Q_G - Q_L)$ (pu)
1	1.0600	0	1.6770	0.0115
2	1.0430	-3.4527	0.2785	0.1905
3	1.0240	-4.9574	-0.0240	-0.0120
4	1.0154	-5.9441	-0.0760	-0.0160
5	1.0100	-9.8183	-0.7113	0.0781
6	1.0125	-7.0874	-0.0000	0.0000
7	1.0037	-8.7357	-0.2280	-0.1090
8	1.0100	-7.1879	-0.0236	-0.0803
9	1.0410	-9.1032	-0.0000	-0.0000
10	1.0232	-10.8072	0.0291	-0.0508
11	1.0820	-7.9850	0.1057	0.2143
12	1.0528	-10.1474	-0.1120	-0.0750
13	1.0710	-9.1017	0.1470	0.1409
14	1.0352	-11.0764	-0.0620	-0.0160
15	1.0279	-11.1400	-0.0820	-0.0250
16	1.0330	-10.6928	-0.0350	-0.0180
17	1.0208	-10.9832	-0.0900	-0.0580
18	1.0139	-11.7365	-0.0320	-0.0090
19	1.0088	-11.8957	-0.0950	-0.0340
20	1.0117	-11.6814	-0.0220	-0.0070
21	1.0016	-11.2800	-0.1750	-0.1120
22	0.9993	-11.2635	-0.0909	-0.2092
23	1.0113	-11.5887	-0.0320	-0.0160
24	0.9977	-11.8406	-0.0870	-0.0670
25	1.0027	-11.7500	-0.0000	0.0000
26	0.9848	-12.1822	-0.0350	-0.0230
27	1.0146	-11.4170	-0.0000	0.0000
28	1.0099	-7.5788	-0.0000	0.0000
29	0.9946	-12.6684	-0.0240	-0.0090
30	0.9830	-13.5671	-0.1060	-0.0190

Line No	From Bus	To Bus	Line flow from $i^{\text{th}}$ to $j^{\text{th}}$ Bus	Line flow from $j^{\text{th}}$ to $i^{\text{th}}$ Bus
1	1	2	1.1464 - 0.0494i	-1.1240 + 0.0875i
2	1	3	0.5305 + 0.0871i	-0.5188 - 0.0613i
3	2	4	<b>0.3988 + 0.0472i</b>	<b>-0.3903 - 0.0483i</b>
4	3	4	0.4948 + 0.0622i	-0.4917 - 0.0575i
5	2	5	0.6039 + 0.0512i	-0.5879 - 0.0061i
6	2	6	0.3997 + 0.0505i	-0.3910 - 0.0438i
7	4	6	0.4776 - 0.0645i	-0.4749 + 0.0692i
8	5	7	-0.1234 + 0.1001i	0.1246 - 0.1074i
9	6	7	0.3559 - 0.0063i	-0.3526 + 0.0078i
10	6	8	0.0555 + 0.0426i	-0.0555 - 0.0469i
11	6	9	0.1783 - 0.1355i	-0.1783 + 0.1457i
12	6	10	0.1209 - 0.0156i	-0.1209 + 0.0237i
13	9	11	-0.1057 - 0.2041i	0.1057 + 0.2143i
14	9	10	0.2879 + 0.1724i	-0.2879 - 0.1609i
15	4	12	0.3061 - 0.1370i	-0.3061 + 0.1649i
16	12	13	-0.1470 - 0.1359i	0.1470 + 0.1409i
17	12	14	0.0844 + 0.0320i	-0.0835 - 0.0301i
18	12	15	0.1957 + 0.1024i	-0.1928 - 0.0966i
19	12	16	0.0832 + 0.0654i	-0.0823 - 0.0634i
20	14	15	0.0215 + 0.0141i	-0.0214 - 0.0140i
21	16	17	0.0473 + 0.0454i	-0.0469 - 0.0447i
22	15	18	0.0661 + 0.0336i	-0.0656 - 0.0324i
23	18	19	0.0336 + 0.0234i	-0.0335 - 0.0232i
24	19	20	-0.0615 - 0.0108i	0.0617 + 0.0111i
25	10	20	0.0843 + 0.0196i	-0.0837 - 0.0181i
26	10	17	0.0431 + 0.0135i	-0.0431 - 0.0133i
27	10	21	0.2061 + 0.2007i	-0.2034 - 0.1947i
28	10	22	<b>0.1082 + 0.1112i</b>	<b>-0.1066 - 0.1077i</b>
29	21	22	0.0284 + 0.0827i	-0.0283 - 0.0826i
30	15	23	0.0661 + 0.0520i	-0.0654 - 0.0507i
31	22	24	0.0439 - 0.0189i	-0.0437 + 0.0193i
32	23	24	0.0334 + 0.0347i	-0.0331 - 0.0341i
33	24	25	-0.0102 - 0.0094i	0.0103 + 0.0095i
34	25	26	0.0355 + 0.0237i	-0.0350 - 0.0230i
35	25	27	-0.0457 - 0.0332i	0.0461 + 0.0339i
36	28	27	0.1732 - 0.0064i	-0.1732 + 0.0181i
37	27	29	0.0619 + 0.0167i	-0.0610 - 0.0151i
38	27	30	0.0709 + 0.0167i	-0.0693 - 0.0136i
39	29	30	0.0370 + 0.0061i	-0.0367 - 0.0054i
40	8	28	0.0318 - 0.0202i	-0.0318 - 0.0014i
41	6	28	0.1475 - 0.0293i	-0.1472 - 0.0359i

## Case Study No.9

From Table 5.3, it was found that bus no.30 voltage drops. It shows that voltage magnitude of bus 30 is 0.9967pu. it is desired to regulate voltage of bus 30 at 1.00pu under all conditions.

It has been shown in Table 6.11 that voltage of bus 30 is increased from 0.9967pu to 1.0pu, which is 0.3% increase after incorporating SVC. SVC generates reactive power of 2.5 Mvar, there by maintaining the voltage profile.

From the Table 5.3, it was found that line 10-22 is less loaded and bus voltages are shoots up. It shows that 7.749 MW and 4.46 Mvar flows in it.

It has been shown in Table 6.11 that real and reactive power flow in the line 10-22 has been increased to 10.75 MW and 10.89 Mvar from the initial value after incorporating UPFC. The shunt converter of UPFC is used to control the bus voltage to which it is connected. From the Table 6.11 it is clear that voltage of bus 10 is decreased to 1.0242 pu from 1.04869 pu which is 2.33% drop.

The magnitude and angle of series injected voltage is 0.038 pu and 3.10 radian. The shunt converter absorbs inductive current of 0.24 pu

UPFC Parameters	Values
$V_T$ (pu)	0.038
$\phi_T$ (radian)	3.10
$I_q$ (pu)	-0.24

**Table 6.11 Load Flow Results for Case IX**

Bus. No	Bus Voltage (pu)	Bus phase angle (deg)	$P(P_G - P_L)$ (pu)	$Q(Q_G - Q_L)$ (pu)
1	1.0600	0	1.6755	0.0155
2	1.0430	-3.3648	0.2785	0.1789
3	1.0239	-5.2165	-0.0240	-0.0120
4	1.0152	-6.2601	-0.0760	-0.0160
5	1.0100	-9.8784	-0.7113	0.0767
6	1.0127	-7.3131	-0.0000	0.0000
7	1.0038	-8.8938	-0.2280	-0.1090
8	1.0100	-7.4125	-0.0236	-0.0886
9	1.0415	-9.3315	-0.0000	-0.0000
10	1.0242	-11.0352	0.0291	-0.0508
11	1.0820	-8.2139	0.1057	0.2117
12	1.0531	-10.4087	-0.1120	-0.0750
13	1.0710	-9.3632	0.1470	0.1386
14	1.0358	-11.3321	-0.0620	-0.0160
15	1.0287	-11.3953	-0.0820	-0.0250
16	1.0336	-10.9404	-0.0350	-0.0180
17	1.0216	-11.2169	-0.0900	-0.0580
18	1.0148	-11.9811	-0.0320	-0.0090
19	1.0097	-12.1342	-0.0950	-0.0340
20	1.0126	-11.9172	-0.0220	-0.0070
21	1.0028	-11.5091	-0.1750	-0.1120
22	1.0006	-11.4934	-0.0909	-0.2092
23	1.0128	-11.8401	-0.0320	-0.0160
24	1.0002	-12.0867	-0.0870	-0.0670
25	1.0085	-12.0200	0.0000	-0.0000
26	0.9906	-12.4472	-0.0350	-0.0230
27	1.0224	-11.7013	0.0000	0.0000
28	1.0107	-7.8256	-0.0000	0.0000
29	1.0068	-13.0530	-0.0240	-0.0090
30	1.0000	-14.0650	-0.1060	0.0060

Line No	From Bus	To Bus	Line flow from $i^{th}$ to $j^{th}$ Bus	Line flow from $j^{th}$ to $i^{th}$ Bus
1	1	2	1.1194 - 0.0421i	-1.0980 + 0.0771i
2	1	3	0.5561 + 0.0839i	-0.5433 - 0.0536i
3	2	4	0.3297 + 0.0563i	-0.3237 - 0.0577i
4	3	4	0.5193 + 0.0545i	-0.5158 - 0.0490i
5	2	5	0.6171 + 0.0496i	-0.6005 - 0.0015i
6	2	6	0.4297 + 0.0419i	-0.4197 - 0.0313i
7	4	6	0.4394 - 0.0614i	-0.4371 + 0.0646i
8	5	7	-0.1108 + 0.0941i	0.1118 - 0.1019i
9	6	7	0.3429 - 0.0016i	-0.3398 + 0.0023i
10	6	8	0.0561 + 0.0462i	-0.0560 - 0.0505i
11	6	9	0.1786 - 0.1372i	-0.1786 + 0.1475i
12	6	10	0.1211 - 0.0170i	-0.1211 + 0.0252i
13	9	11	-0.1057 - 0.2017i	0.1057 + 0.2117i
14	9	10	0.2883 + 0.1682i	-0.2883 - 0.1569i
15	4	12	0.3021 - 0.1390i	-0.3021 + 0.1665i
16	12	13	-0.1470 - 0.1336i	0.1470 + 0.1386i
17	12	14	0.0838 + 0.0314i	-0.0829 - 0.0296i
18	12	15	0.1937 + 0.0998i	-0.1909 - 0.0942i
19	12	16	0.0816 + 0.0647i	-0.0807 - 0.0628i
20	14	15	0.0209 + 0.0136i	-0.0208 - 0.0135i
21	16	17	0.0457 + 0.0448i	-0.0454 - 0.0440i
22	15	18	0.0653 + 0.0336i	-0.0648 - 0.0325i
23	18	19	0.0328 + 0.0235i	-0.0327 - 0.0233i
24	19	20	-0.0623 - 0.0107i	0.0624 + 0.0110i
25	10	20	0.0851 + 0.0195i	-0.0844 - 0.0180i
26	10	17	0.0447 + 0.0141i	-0.0446 - 0.0140i
27	10	21	0.2051 + 0.1972i	-0.2024 - 0.1914i
28	10	22	<b>0.1075 + 0.1089i</b>	<b>-0.1059 - 0.1056i</b>
29	21	22	0.0274 + 0.0794i	-0.0273 - 0.0793i
30	15	23	0.0643 + 0.0491i	-0.0637 - 0.0479i
31	22	24	0.0423 - 0.0243i	-0.0420 + 0.0247i
32	23	24	0.0317 + 0.0319i	-0.0315 - 0.0313i
33	24	25	-0.0135 - 0.0174i	0.0136 + 0.0176i
34	25	26	0.0355 + 0.0237i	-0.0350 - 0.0230i
35	25	27	-0.0491 - 0.0413i	0.0495 + 0.0421i
36	28	27	0.1764 - 0.0237i	-0.1764 + 0.0359i
37	27	29	0.0618 + 0.0063i	-0.0610 - 0.0048i
38	27	30	0.0709 + 0.0017i	-0.0693 + 0.0012i
39	29	30	0.0370 - 0.0042i	-0.0367 + 0.0048i
40	8	28	0.0324 - 0.0248i	-0.0323 + 0.0032i
41	6	28	0.1503 - 0.0424i	-0.1499 - 0.0228i

### Case Study No.10

From Table 5.3, it was found that the line 2-4 is less loaded. It shows that 32.66 MW of real power flows. It is desired to increase the real power in line 2-4 by 20% of its initial value.

It has been shown in Table 6.12 that real power flow in the line 2-4 has been increased to 39.85 MW from 32.6 MW which is 20% increase after incorporating TCSC. TCSC reduces line reactance there by increasing real power flow. Line reactance is reduced from 0.1737pu to 0.12366pu.. The firing angle of TCSC obtained is 2.12 radian or 121.53 degree. The reactance offered by TCSC is -j0.0501. TCSC is operating in the capacitive region in this case.

From Table 5.3, it was found that bus no.30 voltage drops. It shows that voltage magnitude of bus 30 is 0.9967pu. it is desired to regulate voltage of bus 30 at 1.00pu under all conditions.

It has been shown in Table 6.12 that voltage of bus 30 is increased from 0.9967pu to 1.0pu, which is 0.3% increase after incorporating SVC. SVC generates reactive power of 2.49 Mvar, there by maintaining the voltage profile.

From the Table 5.3, it was found that line 10-22 is less loaded and bus voltages are shoots up. It shows that 7.749 MW and 4.46 Mvar flows in it.

It has been shown in Table 6.12 that real and reactive power flow in the line 10-22 has been increased to 10.74 MW and 10.90 Mvar from the initial value after incorporating UPFC. It is clear that voltage of bus 10 is decreased to 1.0243 pu from 1.04869 pu which is 2.33% drop.

UPFC Parameters	Values
$V_T$ (pu)	0.038
$\phi_r$ (radian)	3.10
$I_q$ (pu)	-0.24

**Table 6.12: Load Flow Results for Case X**

Bus. No	Bus Voltage (pu)	Bus phase angle (deg)	$P(P_G - P_L)$ (pu)	$Q(Q_G - Q_L)$ (pu)
1	1.0600	0	1.6766	0.0103
2	1.0430	-3.4515	0.2785	-0.1862
3	1.0242	-4.9591	-0.0240	-0.0120
4	1.0157	-5.9461	-0.0760	-0.0160
5	1.0100	-9.8160	-0.7113	0.0763
6	1.0129	-7.0928	-0.0000	0.0000
7	1.0039	-8.7378	-0.2280	-0.1090
8	1.0100	-7.1886	-0.0236	-0.0942
9	1.0416	-9.0948	-0.0000	-0.0000
10	1.0243	-10.7896	0.0291	-0.0508
11	1.0820	-7.9772	0.1057	0.2112
12	1.0533	-10.1275	-0.1120	-0.0750
13	1.0710	-9.0823	0.1470	0.1370
14	1.0360	-11.0552	-0.0620	-0.0160
15	1.0288	-11.1229	-0.0820	-0.0250
16	1.0337	-10.6738	-0.0350	-0.0180
17	1.0217	-10.9649	-0.0900	-0.0580
18	1.0149	-11.7179	-0.0320	-0.0090
19	1.0098	-11.8765	-0.0950	-0.0340
20	1.0127	-11.6626	-0.0220	-0.0070
21	1.0029	-11.2627	-0.1750	-0.1120
22	1.0007	-11.2467	-0.0909	-0.2092
23	1.0129	-11.5770	-0.0320	-0.0160
24	1.0003	-11.8366	-0.0870	-0.0670
25	1.0085	-11.7803	0.0000	-0.0000
26	0.9907	-12.2075	-0.0350	-0.0230
27	1.0224	-11.4680	0.0000	0.0000
28	1.0109	-7.6030	-0.0000	0.0000
29	1.0068	-12.8188	-0.0240	-0.0090
30	1.0000	-13.8299	-0.1060	0.0059



Line No	From Bus	To Bus	Line flow from $i^{th}$ to $j^{th}$ Bus	Line flow from $j^{th}$ to $i^{th}$ Bus
1	1	2	1.1461 - 0.0493i	-1.1236 + 0.0873i
2	1	3	0.5305 + 0.0858i	-0.5188 - 0.0600i
3	2	4	<b>0.3985 + 0.0451i</b>	<b>-0.3900 - 0.0462i</b>
4	3	4	0.4948 + 0.0609i	-0.4917 - 0.0563i
5	2	5	0.6038 + 0.0512i	-0.5878 - 0.0061i
6	2	6	0.3999 + 0.0484i	-0.3911 - 0.0417i
7	4	6	0.4787 - 0.0668i	-0.4760 + 0.0715i
8	5	7	-0.1235 + 0.0982i	0.1246 - 0.1056i
9	6	7	0.3559 - 0.0046i	-0.3526 + 0.0060i
10	6	8	0.0560 + 0.0511i	-0.0559 - 0.0554i
11	6	9	0.1772 - 0.1368i	-0.1772 + 0.1470i
12	6	10	0.1203 - 0.0169i	-0.1203 + 0.0249i
13	9	11	-0.1057 - 0.2013i	0.1057 + 0.2112i
14	9	10	0.2869 + 0.1684i	-0.2869 - 0.1571i
15	4	12	0.3047 - 0.1381i	-0.3047 + 0.1658i
16	12	13	-0.1470 - 0.1321i	0.1470 + 0.1370i
17	12	14	0.0841 + 0.0313i	-0.0832 - 0.0295i
18	12	15	0.1949 + 0.0996i	-0.1920 - 0.0939i
19	12	16	0.0829 + 0.0644i	-0.0820 - 0.0625i
20	14	15	0.0212 + 0.0135i	-0.0211 - 0.0133i
21	16	17	0.0470 + 0.0445i	-0.0466 - 0.0437i
22	15	18	0.0660 + 0.0334i	-0.0655 - 0.0323i
23	18	19	0.0335 + 0.0233i	-0.0334 - 0.0231i
24	19	20	-0.0616 - 0.0109i	0.0618 + 0.0112i
25	10	20	0.0844 + 0.0197i	-0.0838 - 0.0182i
26	10	17	0.0434 + 0.0145i	-0.0434 - 0.0143i
27	10	21	0.2049 + 0.1973i	-0.2022 - 0.1915i
28	10	22	<b>0.1074 + 0.1090i</b>	<b>-0.1058 - 0.1056i</b>
29	21	22	0.0272 + 0.0795i	-0.0271 - 0.0793i
30	15	23	0.0651 + 0.0489i	-0.0645 - 0.0476i
31	22	24	0.0420 - 0.0243i	-0.0417 + 0.0247i
32	23	24	0.0325 + 0.0316i	-0.0322 - 0.0311i
33	24	25	-0.0131 - 0.0176i	0.0132 + 0.0177i
34	25	26	0.0355 + 0.0237i	-0.0350 - 0.0230i
35	25	27	-0.0486 - 0.0414i	0.0491 + 0.0423i
36	28	27	0.1759 - 0.0234i	-0.1759 + 0.0356i
37	27	29	0.0618 + 0.0064i	-0.0610 - 0.0049i
38	27	30	0.0709 + 0.0018i	-0.0693 + 0.0011i
39	29	30	0.0370 - 0.0041i	-0.0367 + 0.0048i
40	8	28	0.0323 - 0.0256i	-0.0322 + 0.0040i
41	6	28	0.1499 - 0.0415i	-0.1496 - 0.0237i

### Case Study No.11

From Table 5.3, it was found that the lines 2-4 and 14-15 are less loaded. It shows that 32.66 MW and 1.75868 MW of real power flows. It is desired to increase the real power in line 2-4 and 14-15 by 20% of its initial value.

It has been shown in Table 6.13 that real power flow in the line 2-4 has been increased to 40.36 MW from 32.6 MW and power flow in 14-15 has been increased to 2.83 MW from 1.75868 MW which is 20% increase after incorporating TCSC.

TCSC reduces line reactance there by increasing real power flow. Line reactance is reduced from 0.1737pu to 0.12366pu in line 2-4 and 0.199pu to 0.098pu in line 14-15. The firing angles of TCSC's obtained are 2.12 radian (121.53 degree) and 1.55 radian (88.9). The TCSC is operating in the capacitive region in this case.

Parameters	TCSC I	TCSC II
Firing Angle (radian)	2.12	1.55
$X_{TCSC}$	-j0.0501	-j0.101

From Table 5.3, it was found that bus no.30 and 9 voltage shoots up. It shows that voltage magnitude of bus 30 is 0.9967 pu and 9 is 1.05405 pu. it is desired to regulate voltage of bus 30 and 9 at 1.00pu under all conditions.

It has been shown in Table 6.13 that after incorporating SVC's, voltage of bus 30 is increased from 0.9967 pu to 1.0 pu, which is 0.3% increase and voltage of bus 9 is reduced from 1.05405pu to 1.0pu, which is 5.1% drop. SVC generates reactive power of 2.49 Mvar from buses 30 and absorbs 32.23 Mvar from 9, there by maintaining the voltage profile.

From the Table 5.3, it was found that line 10-22 and 25-26 are less loaded and bus voltages are shoots up. It shows that 7.749 MW and 4.46 Mvar flows in the line 10-22 and 3.54 MW and 2.37 Mvar flows in the line 25-26.

It has been shown in table 6.13 that in the line 10-22 real and reactive power flow in the line has been increased to 10.83 MW and 11.1149 Mvar from the initial value after incorporating UPFC. The shunt converter of UPFC is used to control the bus voltage to which it is connected. From the Table 6.13 it is clear that voltage of bus 10 is decreased to 1.0285 pu from 1.0487 pu which is 1.93% drop.

It has been shown in Table 6.13 that in the line 25-26 real and reactive power flow in the line has been increased to 10.52 MW and 3.57 Mvar from the initial value after incorporating UPFC. The shunt converter of UPFC is used to control the bus voltage to which it is connected. From the Table 6.13 it is clear that voltage of bus 25 is decreased to 1.0120 pu from 1.0217 pu which is 0.95% drop.

UPFC Parameters	UPFC I	UPFC II
$V_r$ (pu)	0.038	0.031
$\phi_r$ (radian)	3.10	4.0
$I_q$ (pu)	-0.24	-0.11

**Table 6.13: Load Flow Results for Case XI**

Bus. No	Bus Voltage (pu)	Bus phase angle (deg)	$P(P_G - P_L)$ (pu)	$Q(Q_G - Q_L)$ (pu)
1	1.0600	0	1.6850	0.0249
2	1.0430	-3.4754	0.2785	0.2435
3	1.0212	-4.9441	-0.0240	-0.0120
4	1.0121	-5.9278	-0.0760	-0.0160
5	1.0100	-9.8617	-0.7113	0.1005
6	1.0082	-7.0470	-0.0000	0.0000
7	1.0011	-8.7314	-0.2280	-0.1090
8	1.0100	-7.2271	-0.0236	0.0322
9	1.0000	-8.9650	0.0000	-0.3532
10	1.0285	-10.6798	0.0291	-0.0508
11	1.0474	-7.7626	0.1057	0.2400
12	1.0461	-10.3276	-0.1120	-0.0750
13	1.0710	-9.2751	0.1470	0.1920
14	1.0267	-11.3386	-0.0620	-0.0160
15	1.0189	-11.2762	-0.0820	-0.0250
16	1.0185	-10.7399	-0.0350	-0.0180
17	0.9989	-10.9134	-0.0900	-0.0580
18	0.9991	-11.8026	-0.0320	-0.0090
19	0.9906	-11.9153	-0.0950	-0.0340
20	0.9917	-11.6647	-0.0220	-0.0070
21	0.9793	-11.2160	-0.1750	-0.1120
22	0.9780	-11.2132	-0.0909	-0.2092
23	1.0025	-11.7732	-0.0320	-0.0160
24	0.9894	-12.0848	-0.0870	-0.0670
25	1.0120	-12.4799	0.0661	0.1083
26	1.0029	-14.2533	-0.1023	-0.0313
27	1.0273	-11.7961	0.0000	0.0000
28	1.0080	-7.6305	-0.0000	0.0000
29	1.0094	-13.0674	-0.0240	-0.0090
30	1.0000	-13.9979	-0.1060	-0.0082

Line No	From Bus	To Bus	Line flow from $i^{\text{th}}$ to $j^{\text{th}}$ Bus	Line flow from $j^{\text{th}}$ to $i^{\text{th}}$ Bus
1	1	2	1.1534 - 0.0512i	-1.1307 + 0.0902i
2	1	3	0.5315 + 0.1024i	-0.5197 - 0.0758i
3	2	4	<b>0.4036 + 0.0728i</b>	<b>-0.3947 - 0.0730i</b>
4	3	4	0.4957 + 0.0766i	-0.4925 - 0.0718i
5	2	5	0.6057 + 0.0510i	-0.5897 - 0.0054i
6	2	6	0.3998 + 0.0754i	-0.3909 - 0.0680i
7	4	6	0.4708 - 0.0393i	-0.4682 + 0.0437i
8	5	7	-0.1216 + 0.1218i	0.1230 - 0.1286i
9	6	7	0.3543 - 0.0274i	-0.3510 + 0.0290i
10	6	8	0.0592 - 0.0617i	-0.0591 + 0.0574i
11	6	9	0.1622 + 0.0426i	-0.1622 - 0.0368i
12	6	10	0.1147 + 0.0216i	-0.1147 - 0.0142i
13	9	11	-0.1057 - 0.2270i	0.1057 + 0.2400i
14	9	10	0.2716 + 0.0195i	-0.2716 - 0.0114i
15	4	12	0.3173 - 0.1223i	-0.3173 + 0.1512i
16	12	13	-0.1470 - 0.1848i	0.1470 + 0.1920i
17	12	14	0.0914 + 0.0361i	-0.0903 - 0.0338i
18	12	15	0.1962 + 0.1199i	-0.1930 - 0.1136i
19	12	16	0.0878 + 0.1034i	-0.0862 - 0.1001i
20	14	15	<b>0.0283 + 0.0178i</b>	<b>-0.0281 - 0.0177i</b>
21	16	17	0.0512 + 0.0821i	-0.0504 - 0.0804i
22	15	18	0.0710 + 0.0575i	-0.0702 - 0.0557i
23	18	19	0.0382 + 0.0467i	-0.0379 - 0.0463i
24	19	20	-0.0571 + 0.0123i	0.0572 - 0.0120i
25	10	20	0.0798 - 0.0037i	-0.0792 + 0.0050i
26	10	17	0.0396 - 0.0222i	-0.0396 + 0.0224i
27	10	21	0.1974 + 0.1619i	-0.1951 - 0.1570i
28	10	22	<b>0.1083 + 0.1111i</b>	<b>-0.1051 - 0.0952i</b>
29	21	22	0.0201 + 0.0450i	-0.0201 - 0.0449i
30	15	23	0.0681 + 0.0489i	-0.0674 - 0.0475i
31	22	24	0.0301 - 0.0811i	-0.0292 + 0.0825i
32	23	24	0.0354 + 0.0315i	-0.0351 - 0.0309i
33	24	25	-0.0227 - 0.0765i	0.0239 + 0.0786i
34	25	26	<b>0.1053 + 0.0358i</b>	<b>-0.1023 - 0.0313i</b>
35	25	27	-0.0631 - 0.0061i	0.0635 + 0.0070i
36	28	27	0.1899 - 0.0422i	-0.1899 + 0.0570i
37	27	29	0.0618 + 0.0122i	-0.0610 - 0.0106i
38	27	30	0.0709 + 0.0101i	-0.0693 - 0.0072i
39	29	30	0.0370 + 0.0016i	-0.0367 - 0.0010i
40	8	28	0.0355 - 0.0120i	-0.0354 - 0.0096i
41	6	28	0.1613 - 0.0739i	-0.1608 + 0.0094i

## 6.4 CONCLUSION

In this chapter, an application of Evolutionary Programming to Optimal Power Flow incorporating Multi-Type FACTS Devices has been developed. It has been observed that objective attained (to minimize the Cost of generation) by EP-OPF incorporating Multi type FACTS devices is very Close to that obtained by EP-OPF and gives better control over the power flow and the voltage.. To validate the performance of the proposed algorithm, IEEE 30 bus system with multiple devices has been used. The algorithm is found to be robust and independent of number and type of devices.

## CONCLUSIONS

---

The algorithm for optimal power flow incorporating Multi type FACTS devices has been proposed in this thesis. The proposed model used non classical techniques for better results. Decision for optimal placement and selection of control parameter of FACTS devices has been carried out using evolutionary programming. The following conclusions have been derived from the proposed model,

- With the above proposal it is possible for utility to place multiple FACTS devices in the transmission line such that optimal power flow can be achieved with minimum total cost of generation.
- OPF without FACTS devices reduces the cost of generation. By including FACTS devices in the complete OPF problem, additional reduction in the total cost of generation have been achieved as compared to the OPF without FACTS devices.
- It has also been observed that proposed algorithm is also suitable for large systems with multiple FACTS devices, and the results so obtained are found to be encouraging.

## FUTURE SCOPE OF WORK

---

Research and development is a continuous process. Each end of a research project opens many avenues for further work. As a consequences of the investigations carried out in this thesis on location of FACTS devices, power flow, optimization of total cost of generation with and without FACTS devices, following aspects are identified for future research work in this area.

- Present study has considered the placement of FACTS devices from static point of view. Dynamic consideration of these devices can also be explored.
- In regulated market, FACTS devices are mainly used to improve the dynamic performance of the system. Some of the series devices are also used to control the power in the transmission lines. In on-going deregulation of electric supply industries, due to the unplanned exchanges/transactions, lines located on

particular paths may become overloaded (known as congestion) and control of the power flows by reallocating production seems not to be possible any more. FACTS devices can play an important role in mitigating the congestion along with the dynamic performances. This may be another area of study.

- The objective functions considered in this model include minimization of cost of generation considering FACTS devices. It can be further extended by considering other criteria such as costs of installation, real and reactive power losses and maintaining devices
- The work presented in this thesis has been restricted to AC systems. The studies may be extended to HVDC systems as well, considering the detailed models of the converters and HVDC line operation with FACTS equipped deregulated power system



## REFERENCES

---

1. J.Yuryevich and K.P.Wong, "Evolutionary Programming Based Optimal Power Flow Algorithm", IEEE Transaction on Power Systems, Vol.14, No.4, November 1999,pp.1245-1250.
2. A.G.Bakirtzis, Pandel N.Biskas, Christoforous E. Zoumas and Vasilios Petridis, "Optimal Power Flow by Genetic Algorithm",IEEE Transaction on Power Systems, Vol.17, NO.2, May 2002,pp.229-236.
3. J.A.Momoh, M.E.El-Hawary and Ramababu Adapa, "A Review of selected Optimal Power Flow Literature to 1993 Part-I", IEEE Transaction on Power System, Vol.14, No.1, February 1999,pp 105-111.
4. H.C.Leung and T.S.Chung, "Optimal Power Flow With a Versatile FACTS Controller by Genetic Algorithm Approach", Power engineering society winter meeting, 2000; IEEE, Vol:4, Jan 2000, pp 2806-2811.
5. T.S.Chung and Y.Z.Li, "A Hybrid GA Approach for OPF with consideration of FACTS Devices", IEEE Power Engineering Review, February 2001,pp 47-50.
6. P.Bhasaputra and W.Ongsakul, "Optimal Power flow with Multi-type of FACTS Devices by Hybrid TS/SA Approach", IEEE ICIT 2002,Bangkok, Thailand, pp 285-288.
7. H.Ambriz-Perez, E.Acha, and C.R.Fuerte-Esquivel, "Advanced svc models for Newton Raphson load flow and Newton optimal power flow studies",IEEE Transaction on power systems, vol.15, no.1,feb 2000,pp 129-136.
8. Stephane Gerbex, Rachid Cherkaoui and Alain J. Germond, "Optimal Location of Multi type FACTS Devices in a Power System by means of Genetic Algorithms", IEEE Transactions of power system, Vol. 16, No.3, Aug-2001, pp:537-544
9. C.R. Fuerte-Esquivel, E. Acha, "A Newton-Type Algorithm for the control of Power Flow in electrical power network", IEEE Transactions on power systems, Vol.12, No.4, Jan-1997, pp:1474-1480

10. Y.H.Song, J.Y.Liu and P.A.Mehta, "Power injection modeling and optimal multiplier power flow algorithm for steady-state studies of unified power flow controllers", *Electric Power Systems Research*, Vol.52, No.3, September 1999, p.p.51-59.
11. L.Gyugyi, C.D.Schauder and S.L.Williams, "The Unified Power Flow Controller: A New Approach to Power Transmission Control", *IEEE Transaction on Power Delivery*, Vol.10, No.2, April 1995, p.p.1085-1097
12. Ying Xiao, Y.H.Song and Y.Z.Sun, "Power Flow Control Approach to Power Systems With Embedded FACTS Devices", *IEEE Transaction on Power Systems*, Vol.17, No.4, November 2002, p.p.943-949
13. M.H.Haque and C.M.Yam, "A simple method of solving the controlled load flow problem of a power system in the presence of UPFC", *Electric Power Systems Research*, Vol.65, No.3, September 2003, p.p.55-62.
14. L.L.Lai and J.T.Ma, "Power flow control in FACTS using Evolutionary Programming", *IEEE Power Engineering Review*, February 1995, pp 109-113
15. H.Ambriz-Perez, E.Acha, and C.R.Fuerte-Esquivel, "Advanced SVC models for Newton Raphson load flow and Newton optimal power flow studies", *IEEE Transaction on power systems*, Vol.15, No.1, feb 2000, pp 129-136.
16. H.W.Dommel and W.F.Tinney., "Optimal Power Flow Solution", *IEEE Transaction on Power Apparatus and Systems*, Vol.PAS-87, No.10, October 1968, pp:1866-1876.
17. O.Alsac and B.Stott., "Optimal load flow with steady state security", *IEEE Transactions on Power Apparatus and Systems*, Vol.PAS-93, No.3, May/June 197, pp.745-751
18. D.B.Fogel., "An Introduction to Simulated evolutionary optimization", *IEEE Transaction on Neural Networks*, Vol.5, No.1, January 1994, pp.3-14.
19. Yong Hua Song, A.T.Johns, Editor, "Flexible AC Transmission Systems", IEE, London, U.K.

20. Elgerd.O.L. "Electric Energy System Theory-an Introduction", McGraw-Hill, New York, 1971.
21. Hadi Saadat, "Power System Analysis", Tata McGraw-Hill, New Delhi, 2002.
22. D.E.Goldberg, "Genetic Algorithms in search Optimization and Machine Learning" Addison-Wesley Publishing Company, Inc.,1989
23. R.Mohan Mathur and Rajiv.k.Varma, "Thyristor based FACTS controllers for electrical transmission systems", IEEE Press, John Wiley and Sons, INC, Publication 2002.
24. N.G.Hingorani and L.Gyugi, "Understanding FACTS", IEEE Press, New Delhi,2001
25. C.R. Fuerte-Esquivel, E.Acha, and H.Ambriz-perez, "A Comprehensive Newton-Raphson UPFC Model for the Quadratic Power Flow Solution of Practical Power Networks", IEEE Transactions on Power System, Vol.15, No.1, Feb 2000, pp 102-109.
26. P.Venkatesh, R.Gnanadass and Narayana Prased Padhy, "Comparison and Application of Evolutionary Programming Techniques to Combined Economic Emission Dispatch with Line Flow Constraints", " IEEE Transactions on Power System, Vol.18, No.2, May 2003, pp 688-697
27. K.S.Verma, S.N.Singh and H.O.Gupta, "Location of unified power flow controller for congestion management", Electric Power Systems Research, Vol.58, No.2, July 2001, pp.89-96.
28. I.J.Nagrath and D.P.Kothari, "Power System Engineering", Tata McGraw-Hill Publishing Company Limited, New Delhi, 1996.
29. C.R. Fuerte-Esquivel, E.Acha, and H.Ambriz-perez, "A Thyristorised Controlled Series Compensator Model for Power Flow Solution of Practical Network", IEEE Transactions on Power Systems, Vol.15, No.1, Feb-2002, pp:58-63
30. IEEE test data, taken from <http://www.ee.washington.edu/research/pstca>.

## APPENDIX A

### DATA FOR IEEE-30 BUS SYSTEM (AT 100 MVA BASE)

The IEEE 30-bus system data is taken from the reference 30. The relevant data are provided in the following tables

Table A.1

Generator Power Data

Bus no.	Real Power Generation		Reactive Power limits		Specified Voltage (p.u.)
	Max (MW)	Min (MW)	Max (MVAR)	Min (MAR)	
1	50	200	-20	250	1.060
2	20	80	-20	100	1.043
5	15	50	-15	80	1.010
8	10	35	-15	60	1.010
11	10	30	-10	50	1.082
13	12	40	-15	60	1.071

Table A.2

Reactor / Capacitor data

Bus No.	Impedance(pu)	
	Resistance	Reactance
10	0.00	-0.019
24	0.00	-0.43

Table A.3

Load bus data

Bus No.	Load	
	Real(MW)	Reactive(MVAR)
3	2.4	1.2
4	7.6	1.6
6	0.0	0.0
7	22.8	10.9
9	0.0	0.0
10	5.8	2.0
12	11.2	7.5
14	6.2	1.6
15	8.2	2.5
16	3.5	1.8
17	9.0	5.8
18	3.2	0.9
19	9.5	3.4
20	2.2	0.7
21	17.5	11.2
22	0.0	0.0
23	3.2	1.6
24	8.7	6.7
25	0.0	0.0
26	3.5	2.3
27	0.0	0.0
28	0.0	0.0
29	2.4	0.9
30	10.6	1.9

Table A.4

Transformer data

Line No.	From Bus	To Bus	Series Impedance(p.u.)		Taps
			Resistance	Reactance	
11	6	9	0.0	0.2080	0.978
12	6	10	0	0.5560	0.969
15	4	12	0	0.2560	0.932
36	28	27	0	0.3960	0.968

Table A.5

## Line Data

Line no	Bus nl	Bus Nr	R p.u.	X p.u.	1/2 B p.u.
1	1	2	0.0192	0.0575	0.02640
2	1	3	0.0452	0.1852	0.02040
3	2	4	0.0570	0.1737	0.01840
4	3	4	0.0132	0.0379	0.00420
5	2	5	0.0472	0.1983	0.02090
6	2	6	0.0581	0.1763	0.01870
7	4	6	0.0119	0.0414	0.00450
8	5	7	0.0460	0.1160	0.01020
9	6	7	0.0267	0.0820	0.00850
10	6	8	0.0120	0.0420	0.00450
13	9	11	0	0.2080	0
14	9	10	0	0.1100	0
16	12	13	0	0.1400	0
17	12	14	0.1231	0.2559	0
18	12	15	0.0662	0.1304	0
19	12	16	0.0945	0.1987	0
20	14	15	0.2210	0.1997	0
21	16	17	0.0824	0.1923	0
22	15	18	0.1073	0.2185	0
23	18	19	0.0639	0.1292	0
24	19	20	0.0340	0.0680	0
25	10	20	0.0936	0.2090	0
26	10	17	0.0324	0.0845	0
27	10	21	0.0348	0.0749	0
28	10	22	0.0727	0.1499	0
29	21	22	0.0116	0.0236	0
30	15	23	0.1000	0.2020	0
31	22	24	0.1150	0.1790	0
32	23	24	0.1320	0.2700	0
33	24	25	0.1885	0.3292	0
34	25	26	0.2544	0.3800	0
35	25	27	0.1093	0.2087	0
37	27	29	0.2198	0.4153	0
38	27	30	0.3202	0.6027	0
39	29	30	0.2399	0.4533	0
40	8	28	0.0636	0.2000	0.0214
41	6	28	0.0169	0.599	0.065

Table A.6  
Generator Cost Characteristics

Bus. No	Cost Coefficients		
	a	b	c
1	0.0	2.00	0.00375
2	0.0	1.75	0.01750
5	0.0	1.00	0.06250
8	0.0	3.25	0.00834
11	0.0	3.00	0.02500
13	0.0	3.00	0.02500

Generator input/output function  $C_i = a_i + b_i P_i + C_i P_i^2$